



CONTRACT NO. 94-320  
FINAL REPORT  
March 1997

# **Aircraft Measurements in Support of the NOAA 2-D Lidar Demonstration**

**CALIFORNIA ENVIRONMENTAL PROTECTION AGENCY**



**AIR RESOURCES BOARD  
Research Division**



# **AIRCRAFT MEASUREMENTS IN SUPPORT OF THE NOAA 2-D LIDAR DEMONSTRATION**

Final Report  
Contract No. 94-320

Prepared for:

California Air Resources Board  
Research Division  
2020 L Street  
Sacramento, CA 95814

Prepared by:

John J. Carroll and Alan J. Dixon  
Department of Land, Air and Water Resources  
University of California  
Davis, California 95616

March, 1997



For more information about the ARB's Research Division,  
its research and activities, please visit our Web site:

<http://www.arb.ca.gov/rd/rd.htm>



## DISCLAIMER

The statements and conclusions in this report are those of the contractor and not necessarily those of the California Air Resources Board. The mention of commercial products, their source or their use in connection with material reported herein is not to be construed as actual or implied endorsement of such products.

## ACKNOWLEDGMENTS

University of California, Davis, student, Ms. Cheuk Yi Kong, assisted in the instrument calibrations, flight preparation, data reduction and data management during the project. Her valued assistance is gratefully acknowledged. This report was submitted in fulfillment of interagency agreement #94-320, Aircraft Measurements in Support of the NOAA 2D Lidar Demonstration, by the University of California, Davis, under the sponsorship of the California Air Resources Board. Work was completed as of March 31, 1997.



## TABLE OF CONTENTS

DISCLAIMER .....	i
ACKNOWLEDGMENTS.....	ii
TABLE OF CONTENTS.....	iii
LIST OF FIGURES.....	v
LIST OF TABLES .....	vii
ABSTRACT .....	ix
EXECUTIVE SUMMARY .....	xi
BODY OF REPORT .....	1
INTRODUCTION.....	1
AIRCRAFT INSTRUMENTATION .....	1
AIRCRAFT OPERATION AND DATA ACQUISITION .....	2
DATA REDUCTION .....	3
DATA MANAGEMENT.....	4
DATA ANALYSIS .....	4
RESULTS AND CONCLUSIONS .....	4
REFERENCES.....	7
TABLES .....	8
FIGURES.....	23



## LIST OF FIGURES

- Figure 1. UCD aircraft data acquisition and reduction software flowcharts.
- Figure 2. UCD aircraft data management software flowchart.
- Figure 3. Plot of aircraft ozone data and lidar ozone data versus altitude AGL for 08-03-95 from 17:20 to 17:41 UTC (09:20 to 09:41 PST).
- Figure 4. Same as Figure 3 but for 08-03-95 from 17:45 to 18:04 UTC (09:45 to 10:04 PST).
- Figure 5. Same as Figure 3 but for 08-04-95 from 00:58 to 01:22 UTC (08-03-95, 16:58 to 17:22 PST).
- Figure 6. Same as Figure 3 but for 08-04-95 from 01:25 to 01:49 UTC (08-03-95, 17:25 to 17:49 PST).
- Figure 7. Same as Figure 3 but for 08-04-95 from 18:01 to 18:24 UTC (10:01 to 10:24 PST).
- Figure 8. Same as Figure 3 but for 08-08-95 from 17:59 to 18:20 UTC (09:59 to 10:20 PST).
- Figure 9. Same as Figure 3 but for 08-08-95 from 22:35 to 22:58 UTC (14:35 to 14:58 PST).
- Figure 10. Same as Figure 3 but for 08-09-95 from 01:58 to 02:23 UTC (08-08-95, 17:58 to 18:23 PST).
- Figure 11. Same as Figure 3 but for 08-10-95 from 02:00 to 02:20 UTC (08-09-95, 18:00 to 18:20 PST).
- Figure 12. Same as Figure 3 but for 08-10-95 from 14:01 to 14:21 UTC (06:01 to 06:21 PST).
- Figure 13. Same as Figure 3 but for 08-10-95 from 14:25 to 14:46 UTC (06:25 to 06:46 PST).
- Figure 14. Same as Figure 3 but for 08-12-95 from 01:57 to 02:17 UTC (08-11-95, 17:57 to 18:17 PST).
- Figure 15. Plot of the number of records of both aircraft and lidar ozone data available at each altitude within 7 nm of the lidar site.
- Figure 16. Plot of the RMS difference between the lidar and aircraft ozone concentrations within 7 nm of the lidar site.
- Figure 17. Plot of the mean bias between the lidar and aircraft ozone concentrations and of average aircraft ozone concentrations at a given altitude for aircraft flight within 7 nm of the lidar site.
- Figure 18. Lidar - aircraft ozone differences by altitude range for data within 7 nm of the lidar site.
- Figure 19. Same as Figure 15 but for data within 0.75 nm of the lidar site.
- Figure 20. Same as Figure 16 but for data within 0.75 nm of the lidar site.
- Figure 21. Same as Figure 17 but for data within 0.75 nm of the lidar site.
- Figure 22. Same as Figure 18 but for data within 0.75 nm of the lidar site.
- Figure 23. Plot of aircraft observed ozone concentrations during an ascent and descent on 08-03-95 from 17:20 to 18:04 UTC (09:20 to 10:04 PST).

### LIST OF FIGURES (Continued)

- Figure 24. Plot of aircraft observed ozone concentrations during an ascent and descent on 08-04-95 from 18:01 to 18:48 UTC (10:01 to 10:48 PST).
- Figure 25. Plot of aircraft observed ozone concentrations during a box pattern ascent and a descending spiral on 08-08-95 from 22:08 to 22:58 UTC (14:08 to 14:58 PST).
- Figure 26. Same as Figure 25 but for 08-10-95 from 14:01 to 14:46 UTC (06:01 to 06:46 PST).
- Figure 27. Same as Figure 25 but for 08-11-95 from 13:59 to 14:43 UTC (05:59 to 06:43 PST).
- Figure 28. Same as Figure 25 but for 08-12-95 from 01:57 to 02:42 UTC (08-11-95, 17:57 to 18:42 PST).
- Figure 29. Same as Figure 17 but for data between 13:00 and 16:00 UTC (05:00 and 08:00 PST).
- Figure 30. Same as Figure 17 but for data between 17:00 and 20:00 UTC (09:00 and 12:00 PST).
- Figure 31. Same as Figure 17 but for data between 21:00 and 23:59 UTC (13:00 and 15:59 PST).
- Figure 32. Same as Figure 17 but for data between 01:00 and 04:00 UTC (17:00 and 20:00 PST).
- Figure 33. Same as Figure 16 but for data between 13:00 and 16:00 UTC (05:00 and 08:00 PST).
- Figure 34. Same as Figure 18 but for 13:00 to 16:00 UTC (05:00 to 08:00 PST).
- Figure 35. Same as Figure 16 but for data between 21:00 and 23:59 UTC (13:00 and 15:59 PST).
- Figure 36. Same as Figure 18 but for 21:00 to 23:59 UTC (13:00 to 15:59 PST).
- Figure 37. Plot of the mean bias between the lidar and aircraft ozone concentrations (ppbv) and of average temperature (degrees C) at a given altitude within 7 nm of the lidar site.
- Figure 38. Plot of the mean bias between the lidar and aircraft ozone concentrations (ppbv) and of average relative humidity (percent) at a given altitude within 7 nm of the lidar site.
- Figure 39. Plot of the mean bias between the lidar and aircraft ozone concentrations (ppbv) and of particle count (millions) greater than 0.3 microns at a given altitude within 7 nm of the lidar site.
- Figure 40. Plot of the mean bias between the lidar and aircraft ozone concentrations (ppbv) and of particle count (thousands) greater than 3.0 microns at a given altitude within 7 nm of the lidar site.
- Figure 41. Same as Figure 37 but for data between 13:00 and 16:00 UTC (05:00 and 08:00 PST).
- Figure 42. Same as Figure 38 but for data between 13:00 and 16:00 UTC (05:00 and 08:00 PST).
- Figure 43. Same as Figure 39 but for data between 13:00 and 16:00 UTC (05:00 and 08:00 PST).
- Figure 44. Same as Figure 40 but for data between 13:00 and 16:00 UTC (05:00 and 08:00 PST).
- Figure 45. Same as Figure 37 but for data between 21:00 and 23:59 UTC (13:00 and 15:59 PST).
- Figure 46. Same as Figure 38 but for data between 21:00 and 23:59 UTC (13:00 and 15:59 PST).
- Figure 47. Same as Figure 39 but for data between 21:00 and 23:59 UTC (13:00 and 15:59 PST).
- Figure 48. Same as Figure 40 but for data between 21:00 and 23:59 UTC (13:00 and 15:59 PST).

## LIST OF TABLES

Table 1.	UCD aircraft instrumentation system.
Table 2.	Ozone calibrations.
Table 3.	Temperature calibrations.
Table 4.	Relative humidity calibrations.
Table 5.	Aircraft data processing programs and data files.
Table 6.	Aircraft data file variable list for mm-dd-nn.DAS.
Table 7.	Aircraft data file variable list for mm-dd-nn.NAV.
Table 8.	Data conversion.
Table 9.	Aircraft data file variable list for mm-dd-nn.DAT.
Table 10.	Aircraft data file variable list for mm-dd-nn.NAT.
Table 11.	Aircraft data file variable list for mm-dd-nn.DAC.
Table 12.	Aircraft data files for lidar comparison and El Mirage flights.



## ABSTRACT

The measurement of ozone concentrations by ground-based instruments using light detecting and ranging (lidar) systems needs to be verified by reliable observations. A light aircraft, equipped with meteorological and air quality measuring instruments, was flown in conjunction with lidar operations near Victorville, California during the period from August 3 to 11, 1995. Vertical soundings were made by the aircraft to compare the lidar results to traditional aircraft measurements. The results from this project show that the two methods do not agree when measuring the same vertical profiles and that further refinement of the lidar system or its data processing algorithms are needed prior to independent operations.





## EXECUTIVE SUMMARY

The purpose of this project was to use an instrument-equipped aircraft to verify the results of ozone measurements obtained using a ground-based lidar system that had been configured to sample in a two-dimensional, vertical plane. A Cessna 182 aircraft operated by the University of California, Davis (UCD) was equipped with an ozone analyzer for verification of the lidar along with a nitrogen oxides analyzer and meteorological instruments for additional information. During the period August 3 to 11, 1995, air sampling flights were conducted at the Southern California International (VCV) airport near Victorville, California coincident with the National Oceanic and Atmospheric Administration's (NOAA) differential absorption lidar measurements.

On August 3 and 4 and 8 through 11, four flights per day were flown in conjunction with the operation of the NOAA lidar system. The flight times were chosen to sample during different meteorological conditions: prior to surface heating, during late morning boundary layer mixing, after the boundary layer is well mixed and early evening when surface heating has stopped. Each flight consisted of two vertical soundings from the surface (875 meters above sea level) to approximately 3000 meters above ground level (AGL). In addition to these flights, on August 7, three flights were flown consisting of a vertical sounding to 2200 meters AGL followed by 5 to 10 nautical mile (nm) horizontal transects along a roughly east-west line at 300 meter descending intervals. The vertical sounding and horizontal transects were then repeated with the transects flown along a north-south line. These data were to be compared with the lidar system when using a non-vertical beam. Two additional flights were made on the afternoons of August 10 and 11. Each flight consisted of an ascent to 2200 meters while transiting to El Mirage Dry Lake, about 12 nm west of VCV, followed by a descending sounding over the dry lake.

The data from the flights were reduced and quality controlled by UCD personnel and then compared to the NOAA lidar ozone data. The results of the analysis show that less than 25 percent of the comparison readings are within  $\pm 5$  parts per billion by volume (ppbv) and about 50 percent are within  $\pm 15$  ppbv. The lidar-derived concentrations tend to be higher than the aircraft at low altitudes and in the morning hours and lower than the aircraft at high altitudes and during the afternoon, although there are considerable fluctuations around individual profiles. Thus, the data show that the ozone data from the aircraft and lidar do not agree when measuring vertical profiles.

Since there is disagreement between the lidar and aircraft measured ozone concentrations, continued refinement of the lidar system and its data processing algorithms should be pursued. Aircraft or other reliable measuring systems should continue to be used to verify lidar-derived ozone concentrations prior to independent operation of the lidar systems.



## INTRODUCTION

The purpose of this project was to use an instrument-equipped aircraft to verify the results of ozone measurements obtained using a ground-based lidar system that had been configured to sample in a two-dimensional, vertical plane. A Cessna 182 aircraft operated by the University of California, Davis (UCD) was equipped with an ozone analyzer for verification of the lidar along with a nitrogen oxides analyzer and meteorological instruments for additional information. During the period August 3 to 11, 1995, air sampling flights were conducted at the Southern California International (VCV) airport near Victorville, California coincident with the National Oceanic and Atmospheric Administration's (NOAA) differential absorption lidar measurements.

On August 3 and 4 and 8 through 11, four flights per day were flown in conjunction with the operation of the NOAA lidar system. The flight times were chosen to sample during different meteorological conditions: prior to surface heating, during late morning boundary layer mixing, after the boundary layer is well mixed and early evening when surface heating has stopped. Each flight consisted of two vertical soundings from the surface (875 meters above sea level) to approximately 3000 meters above ground level (AGL). In addition to these flights, on August 7, three flights were flown consisting of a vertical sounding to 2200 meters AGL followed by 5 to 10 nautical mile (nm) horizontal transects along a roughly east-west line at 300 meter descending intervals. The vertical sounding and horizontal transects were then repeated with the transects flown along a north-south line. These data were to be compared with the lidar system when using a non-vertical beam. Two additional flights were made on the afternoons of August 10 and 11. Each flight consisted of an ascent to 2200 meters while transiting to El Mirage Dry Lake, about 12 nm west of VCV, followed by a descending sounding over the dry lake. All aircraft flights, except the El Mirage flights, were done in close communication with the NOAA group in order to have concurrent data from both systems.

## AIRCRAFT INSTRUMENTATION

In order to accurately measure atmospheric variables, a compact high-quality instrumentation system has been developed for light aircraft. For the study, a Cessna 182 was outfitted with the instrumentation package consisting of the instruments listed in Table 1. The temperature, relative humidity and airspeed sensors are mounted on the right-hand strut of the aircraft. A 1.27 cm diameter Teflon tube enters the aircraft through the cabin ventilating system and supplies the ambient gas sample to the analyzers. A 1.2 mm diameter metal tube draws air directly into the particle sampler, providing isokinetic sampling at airspeeds of  $50 \text{ ms}^{-1}$ . The strut-mounted instruments and both sampling tube inlets are configured in such a way as to be well outside of the propeller slipstream. The pressure transducer and global positioning system (GPS) are mounted to the data acquisition system located in the cabin. Data acquisition is accomplished by using a small personal computer (486DX, 33 Hz) and an analog to digital converter.

Since the primary variable of concern for this project was ozone, the ozone analyzer was calibrated before, during and after the project by a Dasibi 1008 PC transfer standard. The calibrations, shown in Table 2, indicate that the ozone analyzer was within about 6 percent of the

calibrator for the ozone concentrations most frequently observed (70 to 150 ppbv). The ozone analyzer recorded ozone concentrations 9 ppbv higher than actual due to an intentional 9 ppbv offset used to observe negative values. Any negative values that occurred would not be recorded in the data acquisition system unless an offset was used (Dasibi, 1990, Section 6.6.4). This offset is removed during data processing. All of the instruments operated without problems throughout the study. However, due to an electrical switch problem in the aircraft that surfaced during the third flight on August 9, 1995, the nitrogen oxides instrument was disconnected for the remainder of the flights.

Temperature and relative humidity instruments were also calibrated throughout the project using portable transfer standards. These calibrations are shown in Tables 3 and 4. The position information was determined using the GPS instrument's output in latitude and longitude and then converting this information to nautical miles from the reference point at the center of the airport. This reference point is approximately one nautical mile southwest of the lidar site.

## AIRCRAFT OPERATION AND DATA ACQUISITION

Prior to each flight, the sampling instruments are turned on and warmed up. The ozone instrument requires approximately fifteen minutes and the nitrogen oxides analyzer requires about 45 minutes of warm up before the first flight of the day. These instruments are powered by an external power source during the warm-up period. During this warm up, the aircraft is prepared for the flight. The time, date, location and flight information are recorded on a cassette tape. The instruments are checked by running AC-TEST which displays the current values to the screen every few seconds.

During flight, power to the instruments is supplied by an inverter which is run by a 28 volt battery mounted on the aircraft instrument rack. This battery can be switched to and charged by the aircraft alternator during a flight. When the aircraft engine is shut down, the battery continues to run the instruments for 30 minutes or more.

When the aircraft is ready for take off, the sampling instruments are again checked using AC-TEST and then the data logging program, AC-DATA, is run. A flow chart for data acquisition is shown in Figure 1 and a summary of programs used with aircraft flights is shown in Table 5. To simplify this task during aircraft operation, the operator runs A.BAT: a batch file which automatically runs AC-TEST and then AC-DATA. The operator enters the file number, sample period (usually three seconds), the navigation data sample period (30 seconds) and the number of data channels to sample (usually 11).

Just prior to departure, data logging is begun and the operator records the time, file number, altitude and the current location on the audio tape. Periodic recording of pertinent in-flight information is also recorded on the audio tape. At the end of a flight segment, the data logging is interrupted by the operator and the time, altitude, file number and location are again noted on the audio tape. This sequence of starting and ending data logging and audio tape notations is repeated for each flight segment as determined by the operator. Each file can last up to approximately 30

minutes. All times are Universal Coordinated Time (UTC) unless otherwise noted. The data stream includes time as seconds from midnight on the day identified in UTC for each scan. (Pacific Standard Time (PST) = UTC - 8 hours).

At the flight's conclusion, the aircraft is secured and the sampling instruments are shut down, if no further flights are planned. The data files, mm-dd-nn.DAS and mm-dd-nn.NAV, are copied from the computer to a floppy disk using program MILK.BAT. The naming convention uses month (mm), date (dd) and file number (nn). Data variables for these files are shown in Tables 6 and 7. The audio tape is also removed for transcription.

## DATA REDUCTION

The audio tapes are transcribed into text files for each flight. Hard copies of these logs are printed and contain the time, altitude and file number for each pertinent comment during a flight. Interactive programs for data reduction shown in Figure 1 are run to remove errors, convert the voltage data to scientific units and combine decoded navigation data with the atmospheric data.

Radiated energy associated with radio transmissions from the aircraft puts small spikes into some of the data. These erroneous readings are corrected by interpolating between the closest valid data. Any of the 16 channels may be corrected, but primarily the errors affect channels one through five which record fast and very fast response temperatures, airspeed, relative humidity and pressure. When one of these five channels is corrected so are the other four. A file mm-dd-nn.LOG automatically records all changes made to the original mm-dd-nn.DAS file.

Voltages recorded in the mm-dd-nn.DAS files are converted to scientific units using AC-CNVRT. Supplied with the initial altitude from the voice transcriptions, AC-CNVRT calculates altitude from the recorded pressure for the entire file. If the initial altitude for a file is unavailable, then an altitude from a corresponding pressure in a contiguous file is used. The data are converted to scientific units using the equations in Table 8. Output is to files mm-dd-nn.DAT and mm-dd-nn.NAT in the formats shown in Tables 9 and 10.

AC-CVRT2 makes the final data files, mm-dd-nn.DAC, by incorporating information from both the mm-dd-nn.DAT and mm-dd-nn.NAT files. The program applies calibration corrections, flags erroneous or missing data, calculates  $\text{NO}_2$  from  $\text{NO}_x$  and NO data and combines the navigation data with the atmospheric data. Navigation data are presented as nautical miles from a reference position. The reference position is the airport center from which the flight originated. Table 11 shows the file format. AC-CVRT2 is run in batch mode, processing all pairs of mm-dd-nn.DAT and mm-dd-nn.NAT files for a given flight date unless the position information for the beginning of a file is missing. In this case the data processor manually inputs the initial latitude and longitude for each file. The remainder of the position information is then estimated from the heading and airspeed values. If valid GPS values occur later, those are used from that point in the record onward. The mm-dd-nn.DAC files are the primary archived data files.

## DATA MANAGEMENT

Figure 2 shows the data management programs. For easy reference, ACDACLST creates a catalogue of all the mm-dd-nn.DAC files stored in file DAC-LIST.TXT. The programs AC-LOOK, AC-LOOK2 and AC-LOOK3 are used to view the data and can provide printed outputs of variables in selected increments. AC-SCAL2 plots the main variables (Ta, RH, O<sub>3</sub>, PC1, PC2, NO, NO<sub>2</sub> and turbulence variables) versus altitude. This program uses DOS commands to run a graphics program (GRAPHER) which plots the data. These plots are filed with the voice logs for each flight.

## DATA ANALYSIS

Lidar ozone data are analyzed by creating a catalogue of the lidar data, using AC-VICTO. The NOAA data are averaged over approximately 150 meter vertical ranges centered every 15 meters in the vertical. On the other hand, the aircraft measurements are made every three seconds giving a vertical resolution of about ten meters. In addition, the lidar files average an entire profile for a period 7.5 minutes long; whereas the aircraft files are for a given ascent or descent and cover 20 to 30 minutes. Therefore, three or four lidar files usually exist for each aircraft sounding. Program AC-LIDAR averages the aircraft data over the same range bin depths as the lidar uses and compares only data with overlapping times. Hence, the comparisons are made, as closely as possible, in the same air. Three additional programs, AC-VICDF, AC-DIFF and AC-DIFF1, use these data to create histograms of the differences between the lidar ozone and the aircraft ozone at four different altitude ranges and to calculate the average ozone bias, aircraft ozone, temperature, relative humidity, particle count and root mean square (RMS) for the ozone differences for each range bin. The program AC-OZTME creates similar data files but for the four different time periods during the day which correspond to the four intercomparison flight periods. In order to determine the effects of spatial variability on the comparison results, two horizontal criteria are used. Histograms and averages are calculated for valid data within about 7 nm and 0.75 nm of the lidar site. The 7 nm range includes both the ascents and descents, but excludes the El Mirage flights; whereas the 0.75 nm range contains data primarily from the descending spirals.

## RESULTS AND CONCLUSIONS

Table 12 lists the aircraft data files made during the project. These data were analyzed according to the procedures outlined above. A comparison of the lidar and aircraft ozone data shows that the two methods do not agree when measuring the same vertical profiles. Figures 3 to 14 show various soundings over the course of the study. Each figure displays the date, time (UTC) and file number of the aircraft sounding. Figures 6, 7 and 8 show some of the profiles for which the methods have better than average agreement, especially, for Figures 7 and 8 in the altitude range above 1000 meters. In this better agreement range, the difference between the lidar and aircraft measurements is often less than 10 ppbv. Yet, below 1000 meters in Figures 7 and 8 and throughout Figure 6, the ozone difference is usually greater than 10 ppbv and as high as 60 ppbv.

Figures 3, 4, 5, 11, 12 and 14 show more average degrees of agreement. Figure 3 generally has agreement within 10 ppbv between 700 and 2400 meters, but diverges in the lowest and highest 600 to 700 meters of the sounding. Consistent with many of the sounding comparisons, the lidar indicates substantially higher ozone values near the surface but lower ozone values aloft. Figure 4 shows agreement similar to Figure 3 except that the range within 10 ppbv is smaller, between 700 and 1700 meters. Figure 5 has only a few altitudes where the agreement is within 10 ppbv, but over the entire sounding, the agreement is almost always within 25 ppbv. The data in Figure 11 is similar to Figure 5 except that average difference is greater. Figure 12 shows the better agreement only in the altitude range above 1500 meters with lidar to aircraft differences fluctuating between -50 and 70 ppbv below 1500 meters. Figure 14 shows good agreement below 700 meters and above 1600 meters, but it generally differs by more than 20 ppbv in the intermediate altitudes.

Figures 9, 10, and 13 show some of the soundings with large differences between the lidar and aircraft ozone values. The only close agreement in Figure 9 occurs below 400 meters while differences greater than 50 ppbv exist throughout most of the sounding. Figure 10 shows average agreement below 1300 meters, but substantially high differences as altitude increases. Figure 13 shows high differences especially in the 500 to 1400 meter range.

Data from the full intercomparison period is summarized in Figures 15 through 22. Figure 15 is a plot of the number of times concurrent samples are available versus altitude, i.e. about 45 concurrent samples for altitudes between 100 and 2900 meters AGL. Figure 16 shows the vertical profile of the RMS difference between lidar and aircraft measured ozone concentrations, which vary between 15 and 50 ppbv. Figure 17 shows the average bias (lidar - aircraft) in the ozone measurements. Note that differences expressed as both RMS and bias are smaller between 1100 and 1500 meters AGL and that below about 700 meters AGL the lidar concentrations exceed the aircraft values. Between 1400 and 2900 meters, the average lidar values are typically 15 to 20 ppbv smaller than the average aircraft ozone values. Above 3000 meters AGL, too few data were available for the results there to be significant.

The histograms in Figure 18 show the frequency of occurrence of various difference ranges by altitude. Note that the difference range of -5 to 5 ppbv occurs for 17 to 25 percent of the observations, while differences of greater than 25 ppbv occur for more than 25 percent of the observations at and above 2000 meters and below 500 meters. At low altitudes, the lidar values are generally higher than the aircraft, but are lower than the aircraft values at the higher altitudes, reinforcing the results shown in Figure 17.

For most of the sounding flights, the aircraft was flown upward in a box pattern, three to four miles per side, whereas the descent was made in a tight spiral directly over the lidar site. To examine the possible role of spatial variability in the lack of agreement, data were analyzed for the two different types of flights: those with data within about 7 nm of the lidar site and those with data within about 0.75 nm. Figures 19 through 22 show the same information as Figures 15 through 18, respectively, but for data within 0.75 nm of the site. We find no significant difference existed between the spirals and box patterns, i.e. the spatial and temporal variabilities on the scale of 7 nm and 30 to 50 minutes are small on average.

An additional concern is that the lag time in the response of the ozone analyzer on the aircraft could create an altitude difference between the lidar and aircraft measurements. This would be seen if the ozone values between the ascending and descending soundings by the aircraft were similar, but staggered by altitude. Figures 17 and 21 show very similar biases for a given altitude. Since the majority of values in Figure 21 are from the descents while Figure 17 is both ascents and descents, we can conclude that any vertical variation is negligible. Figures 23 through 28 show the ascending and descending soundings for five flights. While there is some variation, it does not appear to be caused by the vertical lag time, but more likely from temporal or horizontal deviations. Since the Victorville site is removed from the primary pollutant source, these variations could be due to slight changes in wind direction causing significant concentration changes. This would be especially true in the afternoon when wind direction changes most. (Wolfe et al., 1997).

NOAA concerns regarding variations in accuracy of the lidar due to different atmospheric conditions prompted an analysis of the comparison data by period of day. The mean biases for the four periods are shown in Figures 29 through 32. The biases show large variations in the morning (Figures 29 and 30) between 500 and 1500 meters, but have better agreement above 1500 meters. The afternoon (Figures 31 and 32) shows variations smaller than in the morning below 1500 meters but larger differences above. While there is some difference between the morning and afternoon biases, less difference exists between the early and late morning flights or the mid-afternoon and early evening flights.

Histograms displaying frequency of occurrence of the lidar and aircraft ozone differences and vertical profiles of the RMS difference for the early morning flights and the mid-afternoon flights are shown in Figures 33 through 36. During the early morning flights (Figures 33 and 34), the lidar measured ozone concentrations are closest to the aircraft measured ozone concentrations at and above 1000 meters. The frequency of occurrence of the lidar measured ozone concentrations being within 5 ppbv of the aircraft ozone concentrations is around 35 percent. The lidar tends to significantly overestimate ozone concentrations below 1000 meters during this time period. The histogram for this time period shows that a difference of greater than 25 ppbv occurs over 35 percent of the time. In the mid-afternoon (Figures 35 and 36), lidar measured ozone concentrations are closest to the aircraft measured ozone values in the 500 to 1000 meter altitude range. Also, in this time period, the lidar generally underestimates the ozone concentrations at and above 1000 meters. Above 1000 meters, the lidar measured ozone concentrations differ by more than 25 ppbv from the aircraft measured ozone concentrations over 35 percent of the time.

Since the NOAA mirror was not re-calibrated until August 7, an analysis of the data by period of day was performed using only the data from after the re-calibration. This consisted of data from August 8 through August 11. However, no significant differences were found between the smaller data set and the overall data set. Therefore, all the data from August 3 to August 11 were included in the period-of-day analysis discussed above.

Figures 37 to 48 show vertical profiles of mean atmospheric temperature, relative humidity and particle counts of greater than 0.3 and 3.0 microns along with the mean ozone bias for the entire data set (Figures 37 to 40), for the early morning flights (Figures 41 to 44) and for the



mid-afternoon flights (Figures 45 to 48). There seems to be no correlation between the ozone bias and temperature, relative humidity or 0.3 micron particle concentrations, at least below 2900 meters AGL. During the morning flights, the 3.0 micron particle concentrations show a change in concentration at about the same altitude as a significant variation in the mean ozone bias. Also, some changes in the particle and ozone concentrations during the afternoon appear coincident. Thus, there may be a possible correlation between the large particle concentrations and the ozone bias. Other than this possibility, it does not appear that the differences between the lidar and aircraft measured ozone concentrations are related to variations in ambient meteorological conditions. Assuming that the aircraft monitoring measurements are the more accurate, the measured ozone discrepancies appear to lie with the lidar system or its data processing algorithms. We conclude that this lidar system is not yet operational and its future use should be considered experimental until more consistently accurate results are achieved.

## REFERENCES

- Dasibi Environmental Corp., 1990. Series 1008 U.V. Photometric Ozone Analyzer Operating And Maintenance Manual. Dasibi Environmental Corp., Glendale, CA.
- Wolfe, D.E., Weber, B.L., Wuertz, D.B. and Moran, K.P., 1997. 449-MHz Profiler/RASS: Meteorological Support for the California Air Resources Board 1995 Mojave Desert Ozone Experiment. NOAA Technical Memorandum ERL ETL-273.

TABLE 1 UCD AIRCRAFT INSTRUMENTATION SYSTEM				
VARIABLE	SENSOR TYPE	MANUFACTURER	USEFUL RANGE	ACCURACY
Pressure (Altitude)	Capacitive	Setra	- 30 to 3650 meters	$\pm 0.3$ mb $\pm 3$ meters
Temperature	Platinum RTD	Omega Engineers	- 20 to 50 °C	$\pm 0.5$ °C
Relative Humidity	Capacitive	Met One	0 to 100%	$\pm 3\%$ between 20 and 85%
Air Speed	Thermal Anemometer	T. S. I.	15 to 77 ms <sup>-1</sup>	$\pm 0.4$ ms <sup>-1</sup>
Heading	Heading Sensor / Electric Compass	Precision Navigation	0 to 360 °	$\pm 2$ °
Position	Global Position- ing System (GPS)	Garmin 10-05 Board Set	$\pm 90$ ° Latitude $\pm 180$ ° Longitude	Position = 15 m (100 m with Se- lective Availabil- ity) Veloc. = 0.2 ms <sup>-1</sup>
Particle Concentration	Optical counter	Climet CI-3100-0112	d > 0.3 $\mu$ m d > 3.0 $\mu$ m	$\pm 2\%$ of count
Ozone Concentration	U. V. absorption	Dasibi 1008 AH	0 to 999 ppbv	3 ppbv
Nitrogen Oxides Concentration	Gas-phase chemi- luminescence	Monitor Labs ML 9841A	0 to 500 ppbv	0.5 ppbv or 1% of reading

**TABLE 2**  
**OZONE CALIBRATIONS**

Date	Calibrator Value (ppbv)	Data Acquisition Value (ppbv)	Percent Difference (%)
07/27/95	192.7	193.3	0.3
	142.7	140.7	-1.4
	90.7	88.0	-3.0
	40.3	38.0	-5.7
	-0.3	0.3	-200.0
08/08/95	190.2	190.0	-0.1
	138.3	138.0	-0.2
	88.7	84.7	-4.5
	40.0	37.0	-7.5
	1.0	-3.7	-470.0
08/11/95	192.0	190.0	-1.0
	140.3	138.7	-1.1
	90.0	85.3	-5.2
	39.3	34.7	-11.7
	1.7	-0.7	-141.2
09/07/95	190.7	186.0	-2.5
	140.3	135.0	-3.8
	90.3	85.0	-5.9
	41.0	37.3	-9.0
	0.7	-3.3	-571.4

**TABLE 3**  
**TEMPERATURE CALIBRATIONS**

Date	<sup>1</sup> Temperature (Ta) (°C)	<sup>2</sup> Temperature (T') (°C)	Calibration Tem- perature (°C)	Ta Percent Differ- ence (%)	T' Percent Differ- ence (%)
07/27/95	35.4	34.1	33.4	6.0	2.1
	35.2	34.5	34.0	3.5	1.5
	35.6	34.8	34.3	3.8	1.5
08/08/95	37.2	36.5	37.1	0.3	-1.6
	37.0	36.4	36.7	0.8	-0.8
	36.7	36.4	36.5	0.5	-0.3
	36.9	36.6	36.5	1.1	.3
	38.7	37.5	37.4	3.5	.3
	38.9	38.2	37.9	2.6	0.8
	39.4	38.6	38.4	2.6	0.5
	39.4	38.2	38.6	2.1	-1.0
	38.9	38.5	38.8	0.3	-0.8
	39.6	38.6	38.9	1.8	-0.8
	39.5	38.6	38.7	2.1	-0.3
08/10/95	26.1	25.7	26.1	0.0	-1.5
	26.0	25.9	26.1	-0.4	-0.8
	26.1	26.0	26.1	0.0	-0.4
	26.4	26.2	26.1	1.1	0.4
08/11/95	37.9	37.8	37.2	1.9	1.6
	38.7	38.3	37.3	3.8	2.7
	38.6	38.8	37.6	2.7	3.2
	39.0	38.5	38.0	2.6	1.3
	38.6	38.2	37.9	1.8	0.8
	38.9	38.9	37.9	2.6	2.6
	38.3	37.7	37.3	2.7	2.7

<sup>1</sup> Ta is the primary temperature probe (fast response).

<sup>2</sup> T' is the secondary temperature probe (very fast response).

**TABLE 4**  
**RELATIVE HUMIDITY CALIBRATIONS**

[illegible]

**TABLE 5**  
**AIRCRAFT DATA PROCESSING PROGRAMS AND DATA FILES**

	PROGRAM	INPUT FILES	OUTPUT FILES	COMMENTS
	AC-TEST	N/A	N/A	Prints the data to the screen at approximately five second intervals to verify data logging.
1	AC-DATA	N/A	mm-dd-nn.DAS mm-dd-nn.NAV	Aircraft data logging program (*.DAS is the primary data. *.NAV is navigation data).
2	AC-CRRCT	mm-dd-nn.DAS	mm-dd-nn.DAS mm-dd-nn.LOG	Corrects radio transmission data spikes.
	AC-CRRCF	mm-dd-nn.DAS	mm-dd-nn.DAS	Corrects format of files not formatted efficiently by AC-CRRCT.
	AC-CRRT2	mm-dd-nn.DAC	mm-dd-nn.DAC	Similar to AC-CRRCT but uses *.DAC files.
3	AC-CNVRT	mm-dd-nn.DAS mm-dd-nn.NAV	mm-dd-nn.DAT mm-dd-nn.NAT	Converts voltages to scientific units and decodes GPS nav data. Requires initial altitude of file.
4	AC-CVRT2	mm-dd-nn.DAT mm-dd-nn.NAT	mm-dd-nn.DAC	Makes calibration corrections, flags erroneous data and combines navigation data with other variables. *.DAC files are main working files.
5	ACDACLST	mm-dd-nn.DAC	DAC-LIST.TXT	Makes list of all *.DAC files.
6	AC-SCAL2	mm-dd-nn.DAC	mm-dd-nn.SCL	Plots vertical soundings of aircraft data using GRAPHER. Requires GRAPHER files for operation.
	AC-LOOK	mm-dd-nn.DAC	N/A	User selected screen plots and print summaries of data.
	AC-LOOK2	mm-dd-nn.DAC	N/A	AC-LOOK plus additional plot of aircraft heading and direction.
	AC-LOOK3	mm-dd-nn.DAC	N/A	AC-LOOK plus shows airspace boundaries used in AC-SURF2 to separate data into transects.
	AC-WIND	mm-dd-nn.DAC	N/A	Shows wind speed and direction data calculated from aircraft heading, airspeed and track info.
7	AC-WIND2	mm-dd-nn.DAC	mm-dd-nn.WND AIRHDCOR.DAT	Minimizes RMS of calculated wind to find airspeed and heading corrections for more accurate wind calculations. Edit AIRHDCOR.DAT to include only useful files (those with multiple track directions).
8	AC-WIND4	mm-dd-nn.DAC	mm-dd-nn.W10 mm-dd-nn.W20 AIRCORA1.DAT AIRCORA2.DAT	Same as AC-WIND2 except that it is done for two different altitude ranges: < 7000 feet msl and >= 7000 feet msl. Valid (useful) files are calculated automatically.
9	AC-ASHDG	AIRHDCOR.DAT AIRCORA1.DAT AIRCORA2.DAT	N/A	Calculates average airspeed and heading correction values to use for entire data set. Output is to screen only.
10	AC-WIND3	mm-dd-nn.DAC	mm-dd-nn.WN2 TOTWN2.DAT	Applies airspeed and heading correction values to wind calculations as f(alt). Input corr't values from AIR*.DAT. Output is for each valid GPS leg.

TABLE 5 (CONTINUED) AIRCRAFT DATA PROCESSING PROGRAMS AND DATA FILES				
	PROGRAM	INPUT FILES	OUTPUT FILES	COMMENTS
11	AC-NOAA	VICyyjjj.W23 VICyyjjj.T23 DAC-LIST.TXT	mm-dd-nn.NWN mm-dd-nn.NTP	Takes pertinent wind and temp information from NOAA files.
12	AC-NOAAW	mm-dd-nn.NWN mm-dd-nn.WN2	mm-dd-nn.WN3 SURFWIND.DAT SURFWABS.DAT	Compares NOAA & A/C computed winds. WN3 => beginning time of 30 sec GPS leg, ave alt and A/C and NOAA ave alt and A/C and NOAA FF/DIR.
13	AC-NOAAT	mm-dd-nn.NTP mm-dd-nn.DAC	mm-dd-nn.TP1 SFHIGHTA.DAT SFLOWTA.DAT SFTAIR.DAT	Compares NOAA & A/C temperatures at various altitudes. A/C data is averaged within 60 m of NOAA data.
	AC-SURF	mm-dd-nn.EWT mm-dd-nn.NS*	mmdd-xyz.DAT	Creates input file for SURFER program to plot 2D cross sections.
	AC-SURF2	mm-dd-nn.DAC	mmdd-xyz.DAT	Creates input file for SURFER program to plot 2D cross sections. Separates data by transects using boundaries shown in AC-LOOK3.
14	AC-HISTO	SURFWIND.DAT SFTAIR.DAT	ACHISTO.DAT	Creates a histogram of aircraft versus NOAA data for temperature, wind direction and wind speed.
15	AC-VICTO	OZmmddnn.VTw	VICLIST.TXT	Creates catalogue of Victorville lidar data.
16	AC-LIDAR	OZmmddnn.VTw VICLIST.TXT mm-dd-nn.DAC	mm-dd-nn.LID VICTOR.DIF VICTOR1.DIF	Creates lidar and aircraft comparison data.
17	AC-VICDF	VICTOR.DIF VICTOR1.DIF	VICPER.DAT VICPER1.DAT	Creates histogram at four altitudes of lidar -aircraft differences.
18	AC-DIFF	VICTOR.DIF REFALT.LID	VICDIFF.DAT	Calculates ave. error and RMS error for lidar - aircraft ozone differences, ave. aircraft ozone, temperature, relative humidity and particle counts within 7 nm of site.
19	AC-DIFF1	VICTOR1.DIF REFALT.LID	VICDIFF1.DAT	Same as AC-DIFF except uses data within 0.75 nm of the site.
20	AC-OZTME	mm-dd-nn.LID REFALT.LID	VICDIFn.DAT VICPERn.DAT	Creates files similar to VICDIFF.DAT and VICPER.DAT but for four different time periods: n = A to D where A = 1300 to 1600, B = 1700 to 2000, C = 2100 to 2359, D = 0100 to 0400 UTC.

1 to 10 mandatory for complete data processing. If Victorville lidar comparison data, then 1 to 20.

**TABLE 6**  
**AIRCRAFT DATA FILE VARIABLE LIST**  
**FOR**  
**mm-dd-yy.DAS**

**HEADER VARIABLES**  
MONTH, DAY, YEAR, FILE NUMBER, NUMBER OF  
CHANNELS, DATA SAMPLE PERIOD, NAV SAMPLE PE-  
RIOD, SCAN NUMBER

INDEX	VARIABLE	UNITS
1	TIME <sup>1</sup>	SECONDS
2	TURBULENCE 1	MILLIVOLTS
3	TURBULENCE 2	MILLIVOLTS
4	TURBULENCE 3	MILLIVOLTS
5	AVE. TEMP. (T')	MILLIVOLTS
6	AIRSPPEED	MILLIVOLTS
7	REL. HUMIDITY	MILLIVOLTS
8	PRESSURE	MILLIVOLTS
9	AVE. TEMP. (Ta)	MILLIVOLTS
10	NO	MILLIVOLTS
11	NOx	MILLIVOLTS
12	OZONE	MILLIVOLTS
13	PARTICLES > 0.3	MILLIVOLTS
14	PARTICLES > 3.0	MILLIVOLTS
15	HEADING	MILLIVOLTS
16	EVENT MARKER	MILLIVOLTS

<sup>1</sup> Seconds since midnight in UTC.



**TABLE 7**  
**AIRCRAFT DATA FILE VARIABLE LIST**  
**FOR**  
**mm-dd-nn.NAV**

**HEADER VARIABLES**

MONTH, DAY, YEAR, HOUR, MINUTES, SECONDS (GMT), FILE NUMBER

**REPEATING VARIABLES**

TIME, PRESSURE 1, PRESSURE 2, TEMPERATURE (Ta or T'), V-COMPONENT OF AIRSPEED, U-COMPONENT OF AIRSPEED

GPS WORD 1

GPS WORD 2: TIME (HR, MN, SEC), LATITUDE, LONGITUDE, GROUND SPEED, TRUE TRACK, MAGNETIC VARIATION

COMPASS WORD: MAGNETIC HEADING, PITCH, ROLL<sup>1</sup>

<sup>1</sup> While data called "roll" is recorded, it is not a valid indicator of aircraft bank angle.

TABLE 8 DATA CONVERSION		
VARIABLE	EQUATION	SCIENTIFIC UNITS
Pressure	$P = \text{millivolts} * 0.09997 + 600$	millibars
Altitude	$Z = - (0.96 * P + 7470) * \ln(P/1013.25) / 0.3048 + Z_{\text{corr}}$ Where $Z_{\text{corr}} = Z_{\text{initial}}$ (for the first altitude)	feet
Temperature 1	$T_a = \text{millivolts} * 0.172 - 18.5$	° C
Temperature 2	$T' = \text{millivolts} * 0.1423 - 19.15$	° C
Relative Humidity	$RH = \text{millivolts} / 10$	%
Airspeed	$V = \text{millivolts} * 0.01524 * 1013 / P * (T_a + 273.15) / 295.25$	$\text{ms}^{-1}$
Heading	$HDG = \text{millivolts} * 0.072$	deg. magnetic
Nitric Oxide	$NO = \text{millivolts} * 0.05$	ppbv
Oxides of Nitrogen	$NO_x = \text{millivolts} * 0.05$	ppbv
Ozone	$O_3 = \text{millivolts} - 9$	ppbv
Particles $\geq 0.3$	$PC1 = \text{millivolts} * 11307 / 1000000$	$\# * 10^6 / \text{m}^3$
Particles $\geq 3.0$	$PC2 = \text{millivolts} * 113.1 / 1000$	$\# * 10^3 / \text{m}^3$

**TABLE 9**  
**AIRCRAFT DATA FILE VARIABLE LIST**  
**FOR**  
**mm-dd-nn.DAT**

**HEADER VARIABLES**  
MONTH, DAY, YEAR, FILE NUMBER, NUMBER OF  
SCANS

INDEX	VARIABLE	UNITS
1	TIME <sup>1</sup>	SECONDS
2	AVE. TEMP. (Ta)	° C
3	AVE. TEMP. (T')	° C
4	AIRSPPEED	ms <sup>-1</sup>
5	PRESSURE	mb
6	ALTITUDE	FEET MSL
7	REL. HUMIDITY	%
8	SPEC. HUMIDITY	g/Kg
9	NO	ppbv
10	NO <sub>x</sub>	ppbv
11	OZONE	ppbv
12	HEADING	DEGREES (MAG)
13	PARTICLES > 0.3	Nx10 <sup>6</sup> /m <sup>3</sup>
14	PARTICLES > 3.0	Nx10 <sup>3</sup> /m <sup>3</sup>
15	rmsT (.1 sec)	° C
16	rmsV (.1 sec)	ms <sup>-1</sup>
17	rmsRH (.1 sec)	%
18	EVENT MARKER	MILLIVOLTS

<sup>1</sup> Seconds since midnight in UTC.

**TABLE 10**  
**AIRCRAFT DATA FILE VARIABLE LIST**  
**FOR**  
**mm-dd-mm.NAT**

**HEADER VARIABLES**  
MONTH, DAY, YEAR, HOUR, MINUTES, SECONDS (GMT), FILE NUMBER

INDEX	VARIABLE	UNITS
1	TIME	SECONDS
2	GMT	HR, MIN, SEC
3	GPS ALTITUDE	METERS
4	AVE PRESS ALT	METERS
5	INST PRESS ALT	METERS
6	LATITUDE DEG	DEGREES
7	LATITUDE MIN	MINUTES
8	LONGITUDE DEG	DEGREES
9	LONGITUDE MIN	MINUTES
10	GROUND SPEED	ms <sup>-1</sup>
11	TRUE TRACK	DEGREES TRUE
12	TRUE HEADING	DEGREES TRUE
13	V-AIRSPEED	ms <sup>-1</sup>
14	U-AIRSPEED	ms <sup>-1</sup>
15	PITCH	DEGREES
16	ROLL <sup>1</sup>	DEGREES

<sup>1</sup> While data called "roll" is recorded, it is not a valid indicator of aircraft bank angle.

**TABLE 11**  
**AIRCRAFT DATA FILE VARIABLE LIST**  
**FOR**  
**mm-dd-nn.DAC**  
**HEADER VARIABLES**  
 MONTH, DAY, YEAR, FILE NUMBER, SCAN NUMBER,  
 SITE NUMBER, SCALE VALUE

INDEX	VARIABLE	UNITS
1	TIME	SECONDS
2	AVE. TEMP. (Ta)	° C
3	AVE. TEMP. (T'')	° C
4	AIRSPEED	ms <sup>-1</sup>
5	PRESSURE	mb
6	ALTITUDE	FEET MSL
7	REL. HUMIDITY	%
8	SPEC. HUMIDITY	g/Kg
9	NO	ppbv
10	NO <sub>2</sub>	ppbv
11	OZONE	ppbv
12	HEADING	DEGREES (MAG)
13	PARTICLES > 0.3	Nx10 <sup>6</sup> /m <sup>3</sup>
14	PARTICLES > 3.0	Nx10 <sup>3</sup> /m <sup>3</sup>
15	rmsT (.1 sec)	° C
16	rmsV (.1 sec)	ms <sup>-1</sup>
17	rmsRH (.1 sec)	%
18	rmsT (3 sec)	° C
19	rmsV (3 sec)	ms <sup>-1</sup>
20	rmsRH (3 sec)	%
21	X - POSITION <sup>1</sup>	NAUTICAL MILES
22	Y - POSITION <sup>1</sup>	NAUTICAL MILES
23	EVENT MARKER	—
24	GPS INDEX	—

<sup>1</sup> Relative to reference location.

**TABLE 12**  
**AIRCRAFT DATA FILES FOR LIDAR COMPARISON AND EL MIRAGE FLIGHTS**

DATE	FILE	TIME (UTC)		ALT (FEET MSL)		EASTING		NORTHING	
		START	STOP	INITIAL	FINAL	START	STOP	START	STOP
8/ 3/95	1	17:20	to 17:41	2875	12103	1	6	1	1
8/ 3/95	2	17:45	to 18: 4	12000	3126	2	-0	4	0
8/ 3/95	3	20: 3	to 20:30	3000	12072	0	0	0	-1
8/ 3/95	4	20:32	to 20:59	11900	2769	3	0	0	0
8/ 3/95	5	23: 1	to 23:24	2875	12150	1	-0	1	2
8/ 3/95	6	23:25	to 23:46	11960	2746	-2	-0	-0	1
8/ 4/95	1	0:58	to 1:22	2875	12216	1	0	1	-2
8/ 4/95	2	1:25	to 1:49	12150	2710	3	-0	-3	1
8/ 4/95	11	14: 7	to 14:29	2875	12155	1	2	1	-3
8/ 4/95	12	14:31	to 14:51	12050	2901	4	0	-3	0
8/ 4/95	13	18: 1	to 18:24	2875	12139	1	-1	1	-1
8/ 4/95	14	18:26	to 18:48	12000	2766	3	1	-1	1
8/ 4/95	15	22: 0	to 22:27	2875	12640	1	2	1	0
8/ 4/95	16	22:28	to 22:54	12500	2749	3	-0	2	1
8/ 5/95	1	2: 0	to 2:23	2875	12138	1	2	1	3
8/ 5/95	2	2:25	to 2:45	12000	3801	-1	1	3	-1
8/ 5/95	3	2:56	to 2:57	2875	2877	1	1	0	0
8/ 7/95	1	14: 7	to 14:26	3250	10336	-0	4	0	-0
8/ 7/95	2	14:26	to 14:30	10300	10397	3	-3	0	4
8/ 7/95	3	14:32	to 14:37	9000	9004	-3	4	4	-2
8/ 7/95	4	14:40	to 14:45	8900	9006	5	-2	-3	2
8/ 7/95	5	14:48	to 14:51	7930	7939	-2	4	3	-2
8/ 7/95	6	14:55	to 14:59	5900	6007	4	-2	-1	2
8/ 7/95	7	15: 1	to 15: 5	5100	5085	-2	5	2	-2
8/ 7/95	8	15: 9	to 15:13	3950	4117	5	-2	-1	1
8/ 7/95	9	15:14	to 15:14	4160	4651	-3	-3	1	1
8/ 7/95	10	15:15	to 15:19	4350	6591	-2	4	1	-1
8/ 7/95	11	15:58	to 16:14	3900	10102	2	5	-1	7
8/ 7/95	12	16:16	to 16:20	10040	10168	5	1	8	2
8/ 7/95	13	16:22	to 16:27	9980	10146	1	5	-0	8
8/ 7/95	14	16:29	to 16:35	7950	7990	5	1	11	1
8/ 7/95	15	16:37	to 16:42	7000	7057	1	5	-1	9
8/ 7/95	16	16:45	to 16:51	6100	5735	5	1	11	1
8/ 7/95	17	16:53	to 16:57	5100	5029	1	4	-0	8
8/ 7/95	18	17: 0	to 17: 6	4130	2906	5	1	10	1
8/ 7/95	21	19: 4	to 19:21	2875	10098	1	2	1	-4
8/ 7/95	22	19:24	to 19:30	9980	9968	7	-2	-3	2
8/ 7/95	23	19:33	to 19:37	8960	9006	-4	4	4	-1
8/ 7/95	24	19:40	to 19:44	8000	8146	4	-2	-2	1
8/ 7/95	25	19:46	to 19:51	6950	7043	-3	4	3	-1
8/ 7/95	26	19:53	to 19:57	6000	6015	5	-2	-2	1
8/ 7/95	27	19:59	to 20: 2	4950	5084	-2	4	2	-1
8/ 7/95	28	20: 4	to 20: 8	4080	4034	4	-1	-1	2
8/ 7/95	29	20: 9	to 20:22	4430	10163	-3	-2	2	-1
8/ 7/95	30	20:25	to 20:29	9940	9940	-0	2	-4	4
8/ 7/95	31	20:32	to 20:37	9020	9125	2	-0	6	-2
8/ 7/95	32	20:41	to 20:44	8250	8090	-0	2	-3	3
8/ 7/95	33	20:47	to 20:51	7150	7029	2	-0	5	-2
8/ 7/95	34	20:54	to 20:58	6080	6138	-0	2	-4	4

**TABLE 12 (CONTINUED)**  
**AIRCRAFT DATA FILES FOR LIDAR COMPARISON AND EL MIRAGE FLIGHTS**

DATE	FILE	TIME (UTC)		ALT (FEET MSL)		EASTING		NORTHING	
		START	STOP	INITIAL	FINAL	START	STOP	START	STOP
8/ 7/95	35	21: 0 to	21: 5	5000	5276	2	-0	5	-3
8/ 7/95	36	21: 8 to	21:14	4230	4174	-0	2	-5	4
8/ 8/95	1	0: 8 to	0:22	4200	9979	3	6	-0	-3
8/ 8/95	2	0:23 to	0:27	9930	10068	5	-1	-2	2
8/ 8/95	3	0:30 to	0:34	9200	9129	-2	5	3	-2
8/ 8/95	4	0:36 to	0:41	8000	8005	6	-2	-3	3
8/ 8/95	5	0:43 to	0:47	7000	7270	-2	5	3	-1
8/ 8/95	6	0:50 to	0:55	5900	5905	6	-1	-2	1
8/ 8/95	7	0:58 to	1: 1	5000	5077	-2	4	2	-2
8/ 8/95	8	1: 4 to	1: 7	5000	5097	5	-0	-2	1
8/ 8/95	9	1: 8 to	1:20	4100	9977	-1	1	2	-1
8/ 8/95	10	1:21 to	1:25	10050	9964	0	4	0	8
8/ 8/95	11	1:28 to	1:34	9000	8862	5	2	11	1
8/ 8/95	12	1:36 to	1:40	7950	8317	1	5	1	9
8/ 8/95	13	1:43 to	1:49	7010	6975	6	2	11	2
8/ 8/95	14	1:51 to	1:55	5950	6025	1	3	1	7
8/ 8/95	15	1:57 to	2: 2	5050	5026	4	1	9	1
8/ 8/95	16	2: 4 to	2: 8	4100	4087	1	4	0	8
8/ 8/95	17	2: 8 to	2:18	4020	2857	4	0	9	1
8/ 8/95	21	14: 1 to	14:22	2875	12120	1	2	1	2
8/ 8/95	22	14:24 to	14:47	12000	2750	0	1	2	1
8/ 8/95	23	17:59 to	18:20	2875	12148	1	2	1	-2
8/ 8/95	24	18:28 to	18:52	12250	3964	1	0	1	-1
8/ 8/95	25	18:53 to	18:56	4085	2893	0	0	-1	0
8/ 8/95	41	22: 8 to	22:31	2875	12099	1	-3	1	-3
8/ 8/95	42	22:35 to	22:58	12000	2776	0	-0	-1	1
8/ 9/95	1	1:58 to	2:23	2875	12279	1	-1	1	1
8/ 9/95	2	2:24 to	2:48	12200	2748	0	-0	-0	1
8/ 9/95	11	13:59 to	14:22	2875	12132	1	1	1	3
8/ 9/95	12	14:24 to	14:48	12060	2725	-0	1	3	1
8/ 9/95	13	17:58 to	18:26	2875	12140	0	2	0	-3
8/ 9/95	14	18:29 to	18:50	12000	2774	1	1	-0	1
8/ 9/95	15	22:14 to	22:20	3028	4569	10	3	0	-1
8/ 9/95	16	22:53 to	23:17	2950	12033	-0	2	1	0
8/ 9/95	17	23:20 to	23:43	12100	2792	1	-0	2	1
8/10/95	1	2: 0 to	2:20	2875	12140	1	0	1	3
8/10/95	2	2:26 to	2:47	12030	2746	1	-0	-0	1
8/10/95	11	14: 1 to	14:21	2875	12117	1	3	1	3
8/10/95	12	14:25 to	14:46	12020	2815	0	0	1	1
8/10/95	13	18: 3 to	18: 6	2875	4661	1	-1	1	-2
8/10/95	14	18:11 to	18:31	4000	12123	0	0	3	3
8/10/95	15	18:33 to	18:56	12010	2754	-1	1	0	1
8/10/95	16	21:57 to	22:17	2875	12133	1	2	1	0
8/10/95	17	22:20 to	22:41	11950	2879	1	0	-1	1
8/10/95	18	22:41 to	22:57	3300	10172	0	-12	0	1
8/10/95	19	22:57 to	23:12	10100	3090	-11	-10	1	4
8/10/95	20	23:13 to	23:33	3700	2833	-11	1	4	1
8/11/95	1	1:56 to	2:18	2875	13066	1	1	1	1
8/11/95	2	2:22 to	2:48	13000	2725	-0	1	0	1

TABLE 12 (CONTINUED)  
AIRCRAFT DATA FILES FOR LIDAR COMPARISON AND EL MIRAGE FLIGHTS

DATE	FILE	TIME (UTC)		ALT (FEET MSL)		EASTING		NORTHING	
		START	STOP	INITIAL	FINAL	START	STOP	START	STOP
8/11/95	11	13:59	to 14:20	2875	12113	1	1	1	-1
8/11/95	12	14:24	to 14:43	12160	3418	2	1	-0	1
8/11/95	13	17:57	to 18:21	2875	13157	1	-3	1	0
8/11/95	14	18:25	to 18:26	12120	12056	1	1	0	0
8/11/95	15	18:26	to 18:47	11950	2721	2	-0	0	1
8/11/95	16	22: 1	to 22:23	2875	13026	1	3	1	-1
8/11/95	17	22:26	to 22:47	12560	2904	2	0	0	1
8/11/95	18	22:47	to 23: 1	3300	10141	-0	-13	-0	1
8/11/95	19	23: 4	to 23:17	9900	3616	-15	-11	2	4
8/11/95	20	23:18	to 23:32	3850	2865	-12	0	4	1
8/12/95	1	1:57	to 2:17	2875	12151	1	3	1	-1
8/12/95	2	2:20	to 2:42	12020	2744	0	-0	1	1



FIGURE 1  
UCD AIRCRAFT DATA ACQUISITION SOFTWARE

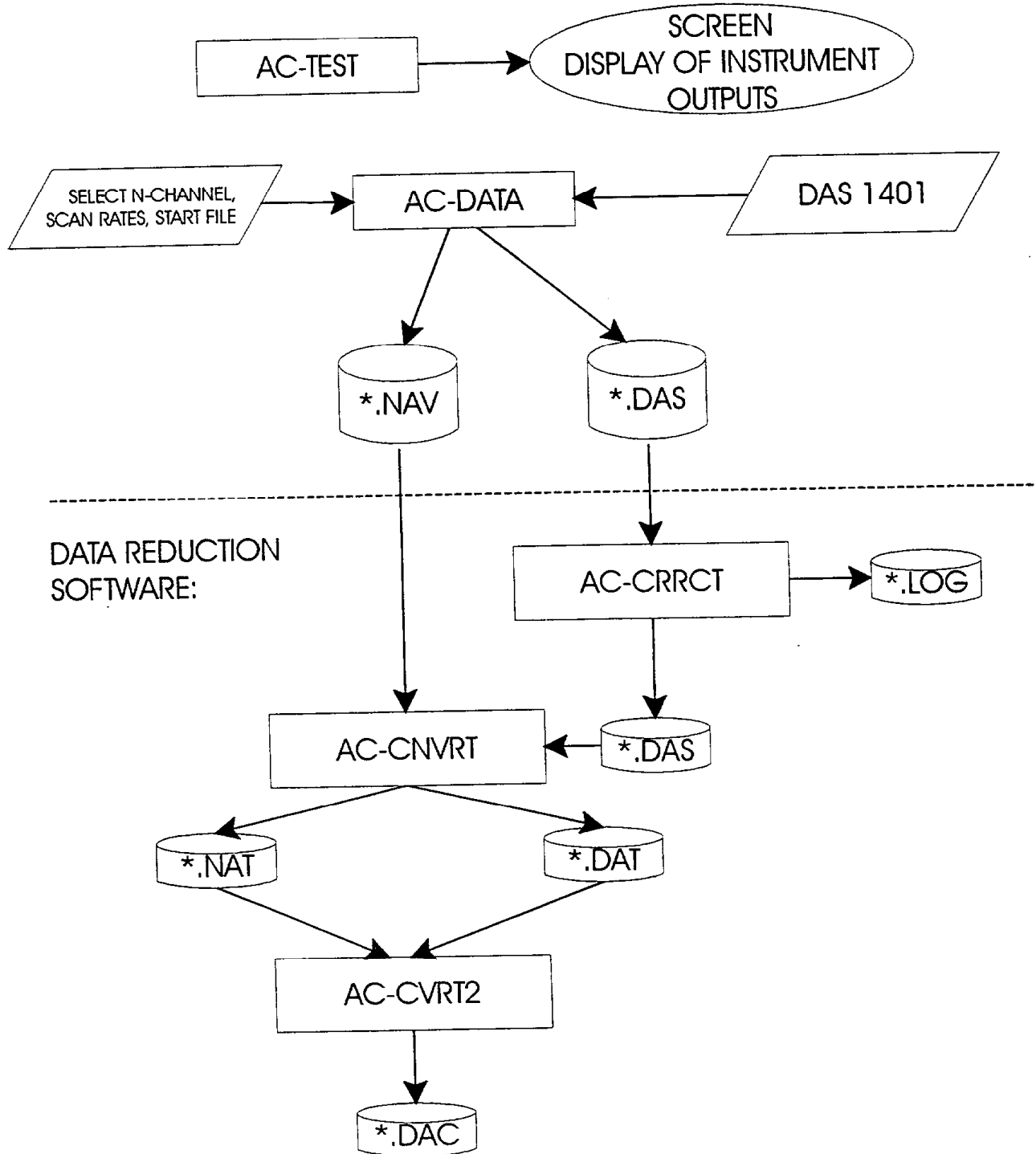
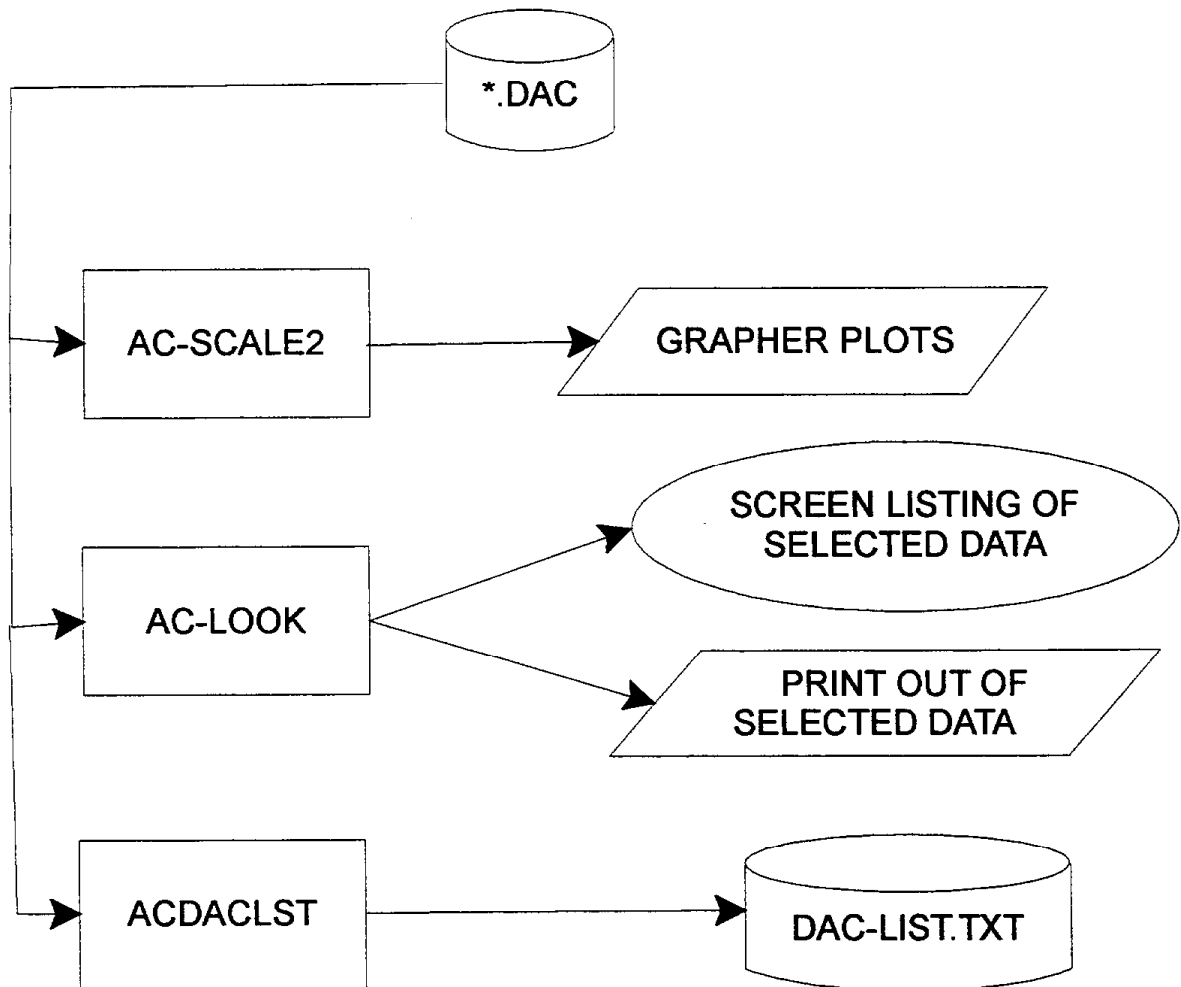


FIGURE 2

## Aircraft Data Management



DATE: 08-03-95 TIME: 17:20 - 17:41 FILE # 01

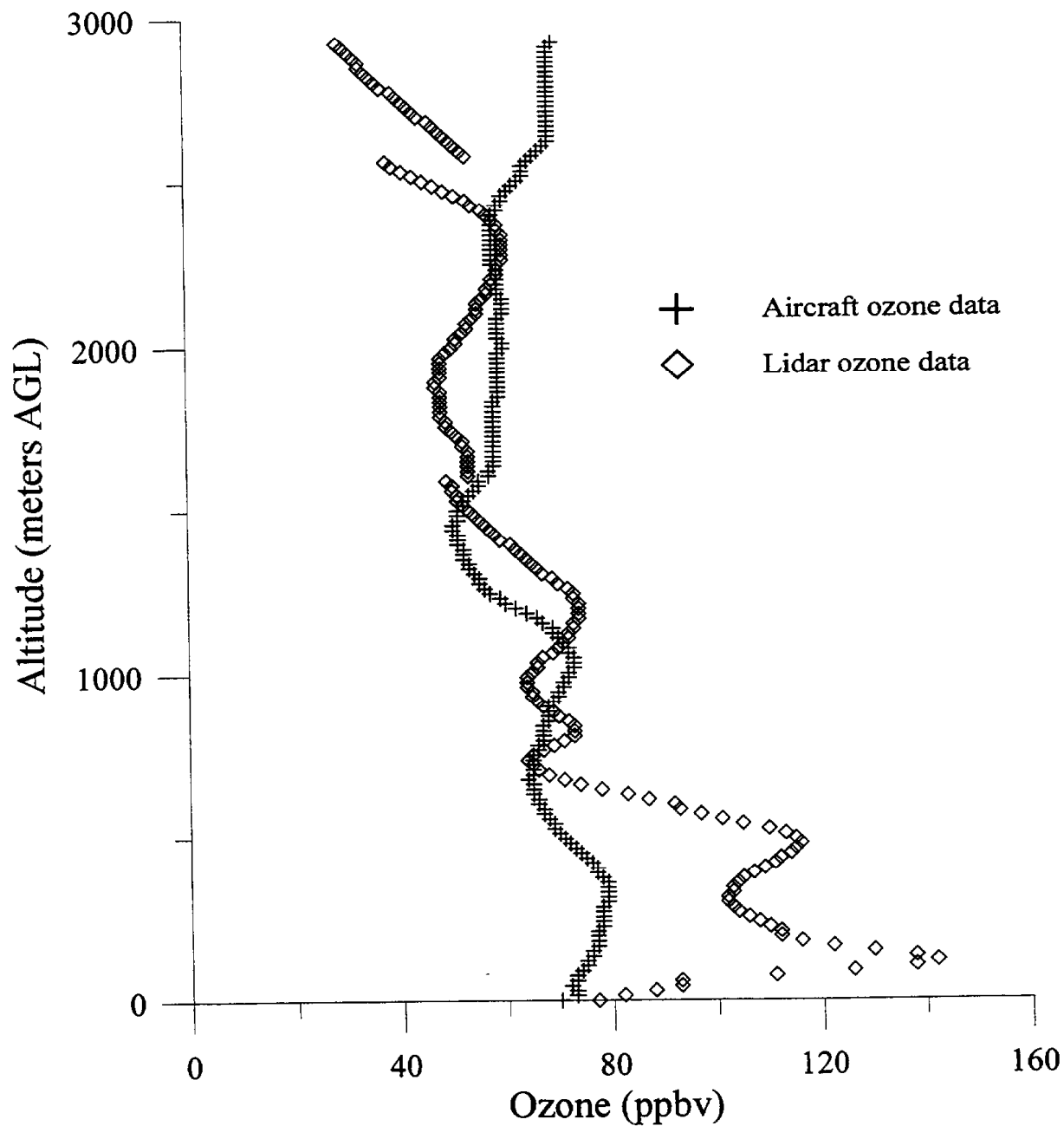


Figure 3: Plot of aircraft ozone data and lidar ozone data versus altitude AGL for 08-03-95 from 17:20 to 17:41 UTC (09:20 to 09:41 PST).

DATE: 08-03-95 TIME: 17:45 to 18:04 FILE # 02

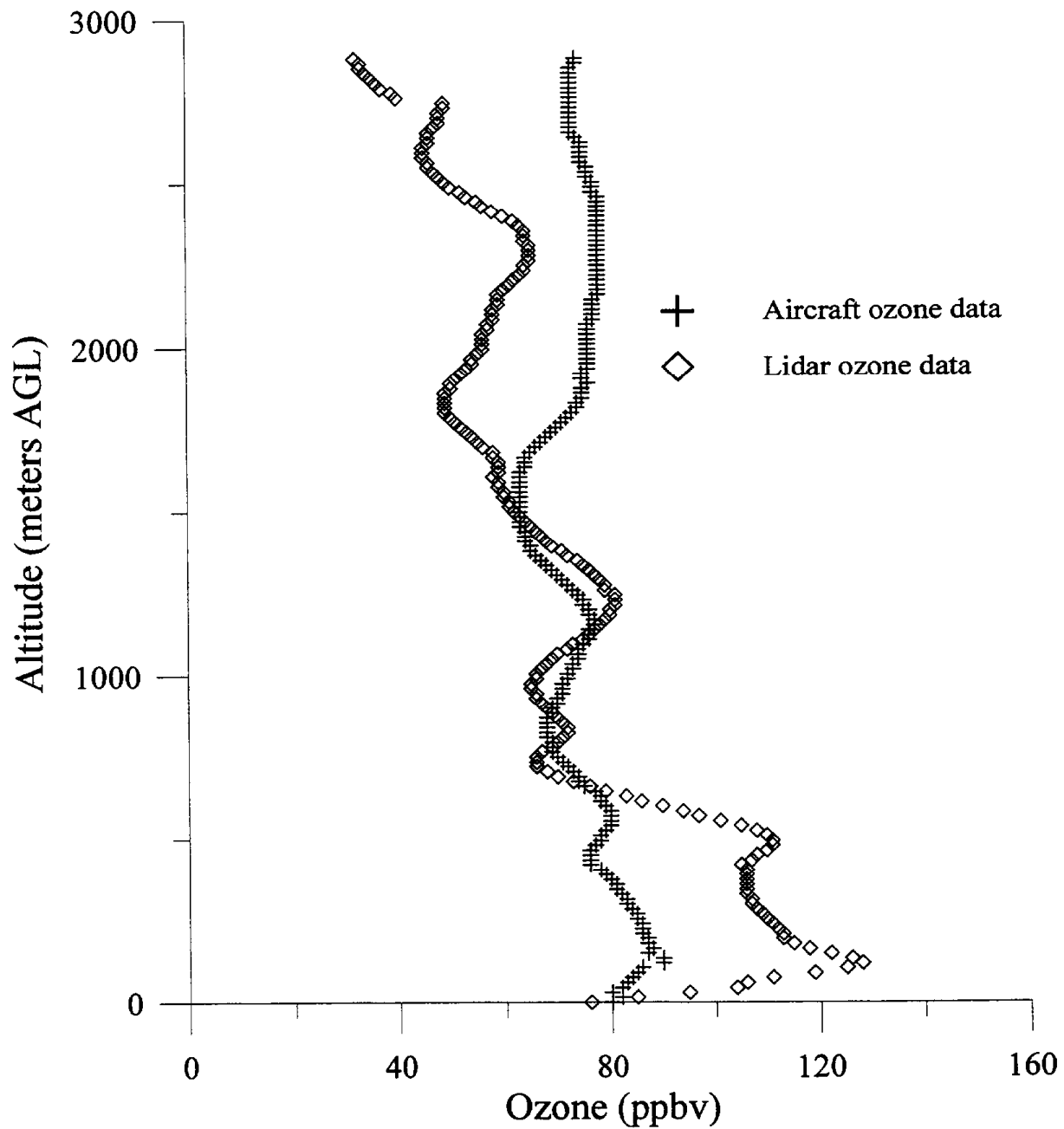


Figure 4: Plot of aircraft ozone data and lidar ozone data versus altitude AGL for 08-03-95 from 17:45 to 18:04 UTC (09:45 to 10:04 PST).

DATE: 08-04-95 TIME: 00:58 - 01:22 FILE # 01

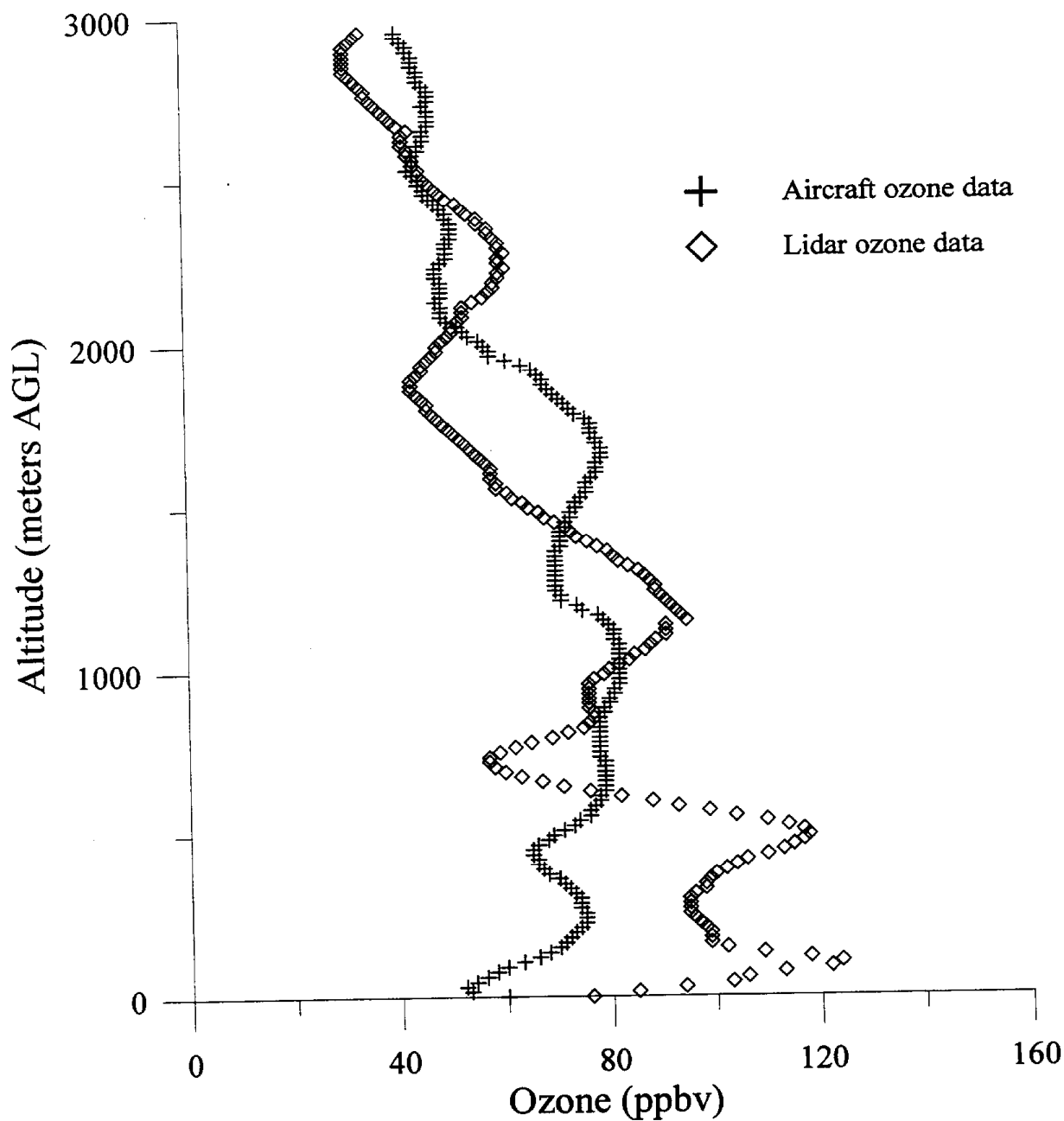


Figure 5: Plot of aircraft ozone data and lidar ozone data versus altitude AGL for 08-04-95 from 00:58 to 01:22 UTC (08-03-95, 16:58 to 17:22 PST).

DATE: 08-04-95 TIME: 01:25 - 01:49 FILE # 02

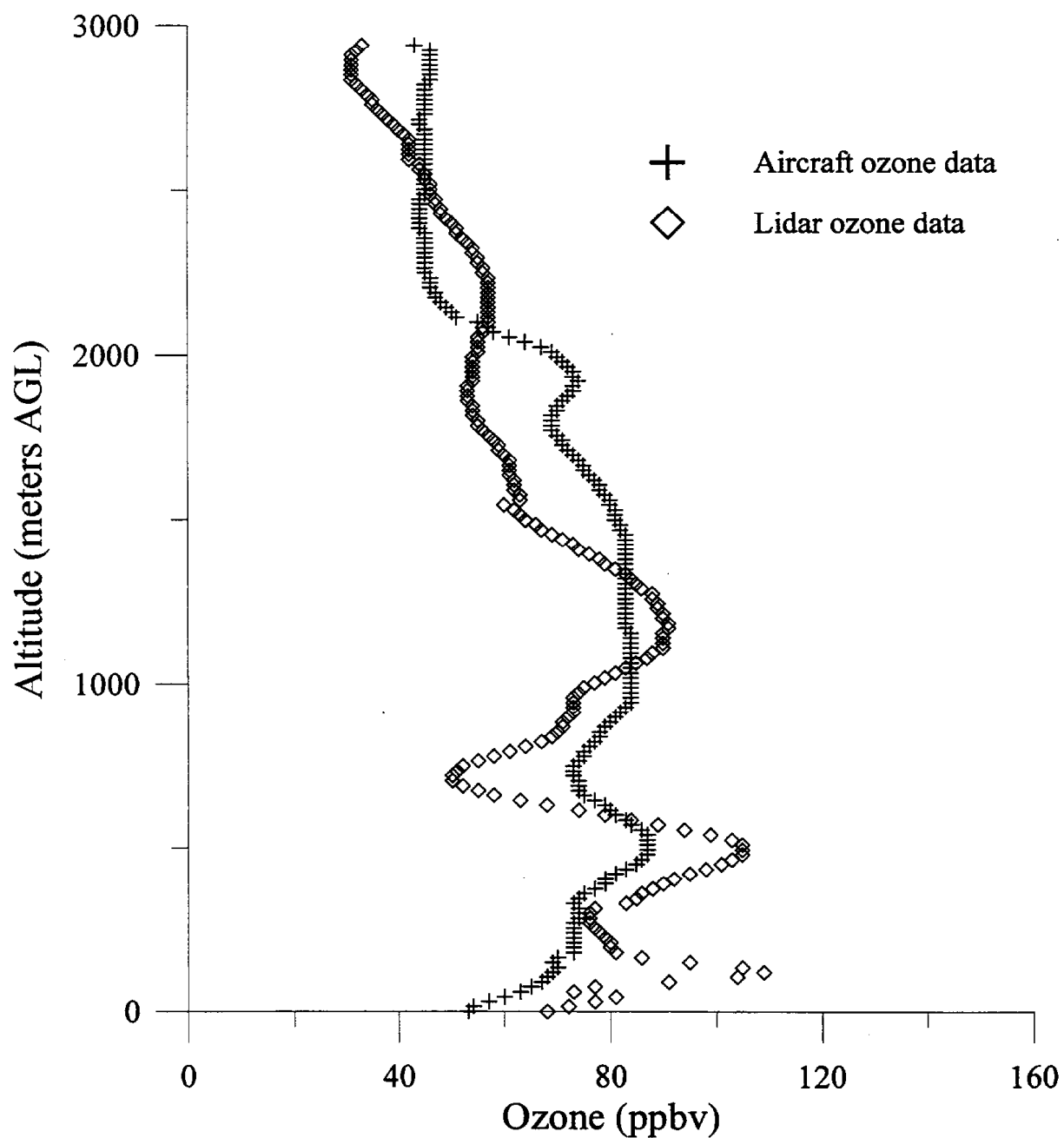


Figure 6: Plot of aircraft ozone data and lidar ozone data versus altitude AGL for 08-04-95 from 01:25 to 01:49 UTC (08-03-95, 17:25 to 17:49).

DATE: 08-04-95    TIME: 18:01 to 18:24    FILE # 13

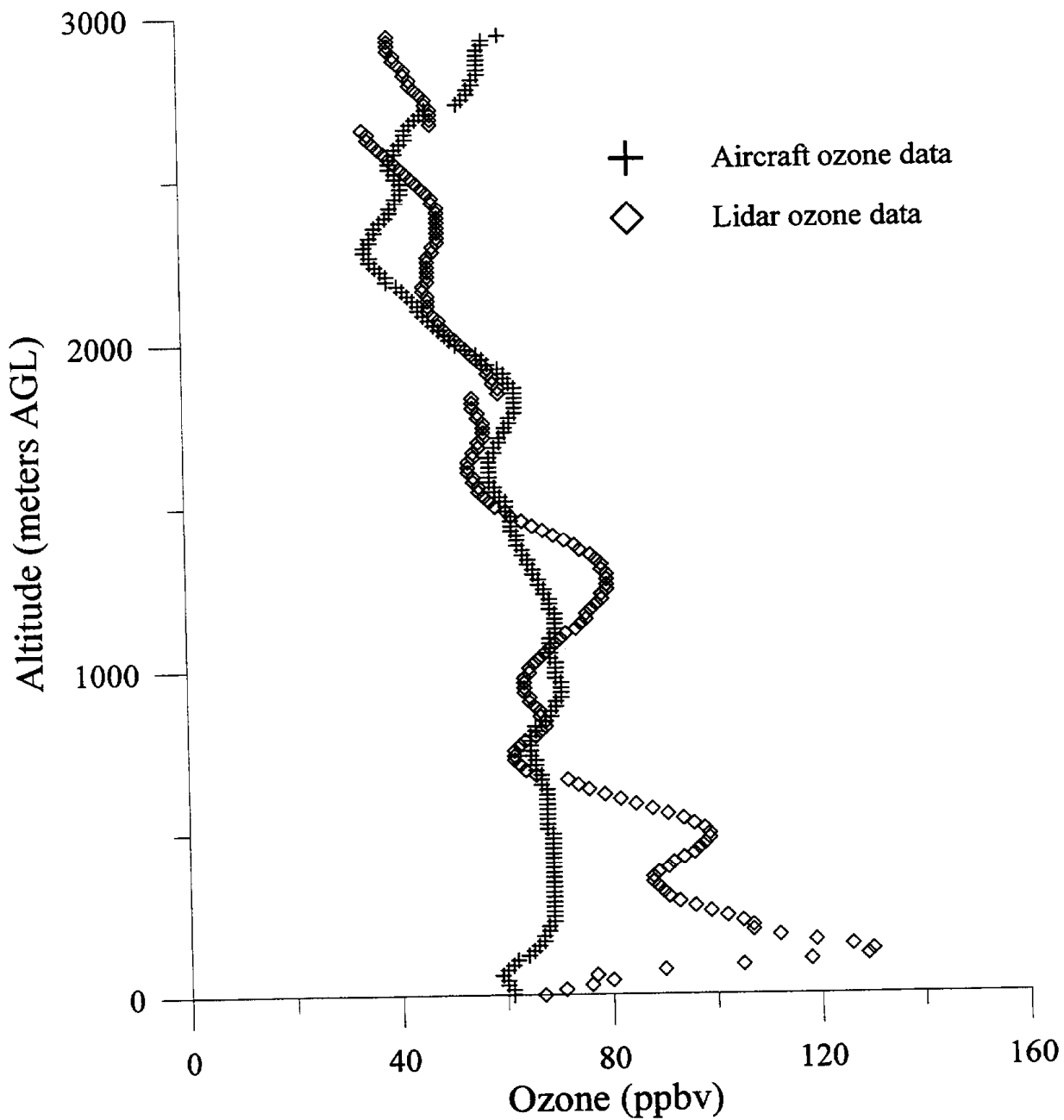


Figure 7: Plot of aircraft ozone data and lidar ozone data versus altitude AGL for 08-04-95 from 18:01 to 18:24 UTC (10:01 to 10:24 PST).

DATE: 08-08-95    TIME: 17:59 to 18:20    FILE # 23

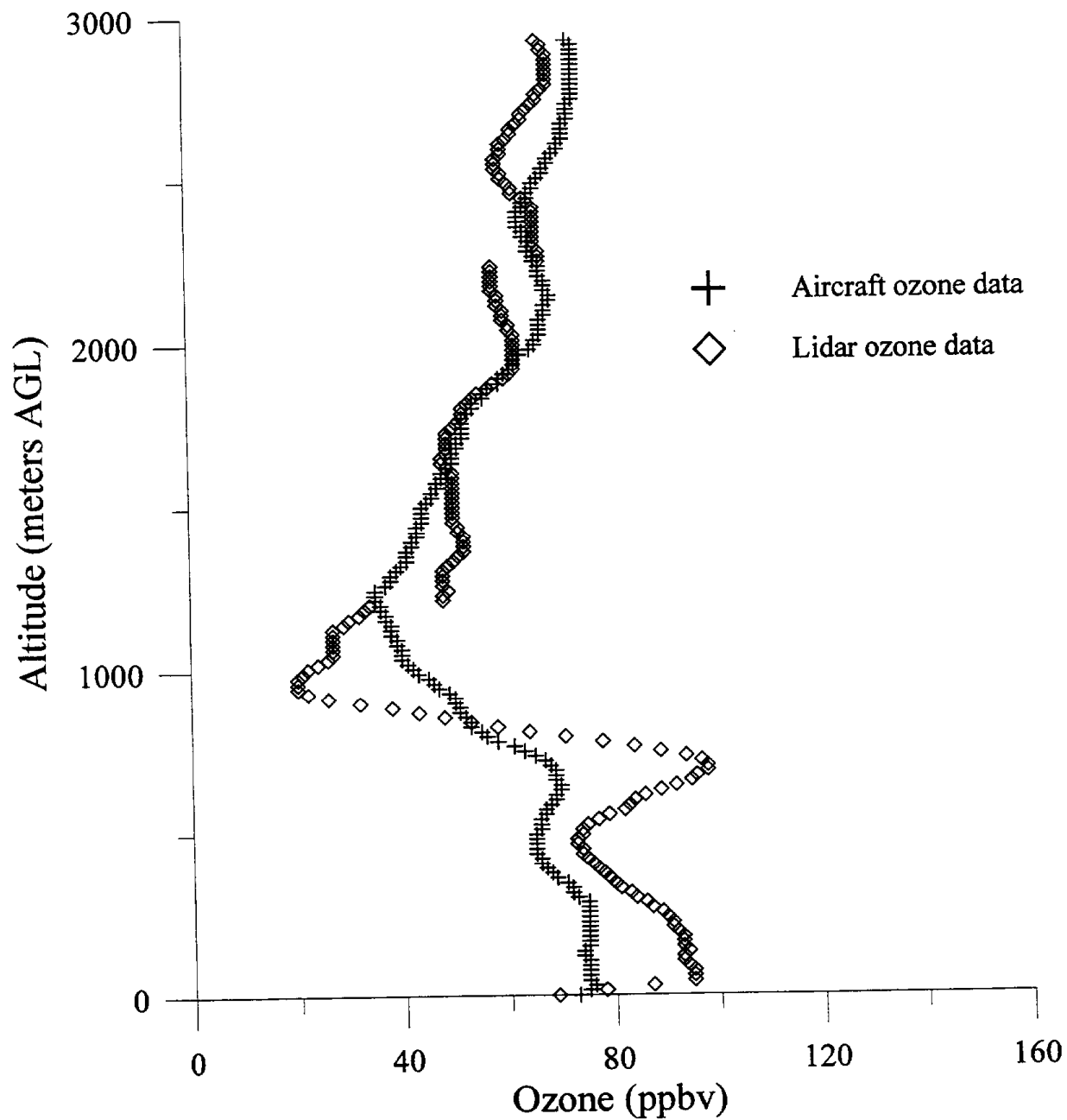


Figure 8: Plot of aircraft ozone data and lidar ozone data versus altitude AGL for 08-08-95 from 17:59 to 18:20 UTC (09:59 to 10:20 PST).



DATE: 08-08-95 TIME: 22:35 to 22:58 FILE # 42

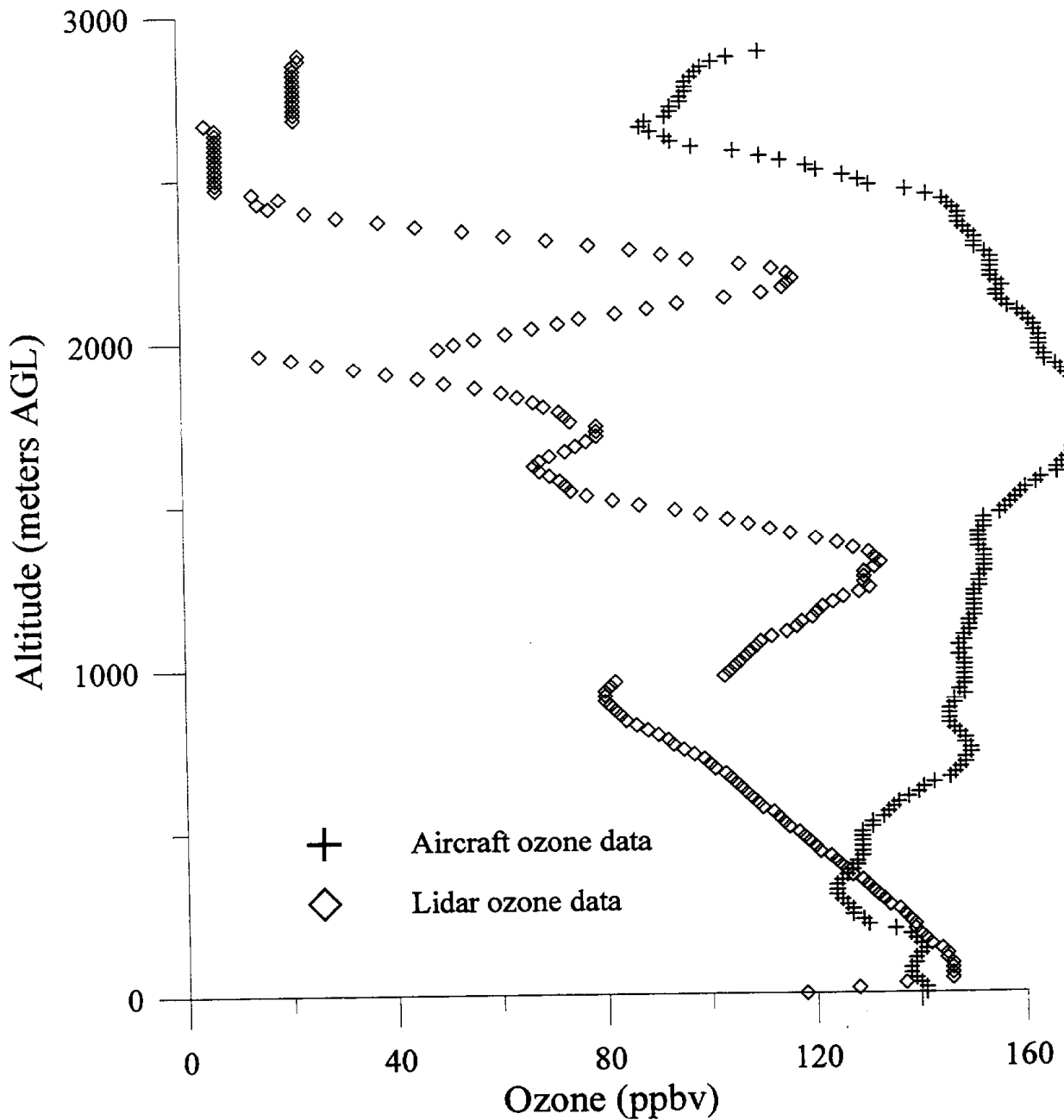


Figure 9: Plot of aircraft ozone data and lidar ozone data versus altitude AGL for 08-08-95 from 22:35 to 22:58 UTC (14:35 to 14:58 PST).

DATE: 08-09-95    TIME: 01:58 to 02:23    FILE # 01

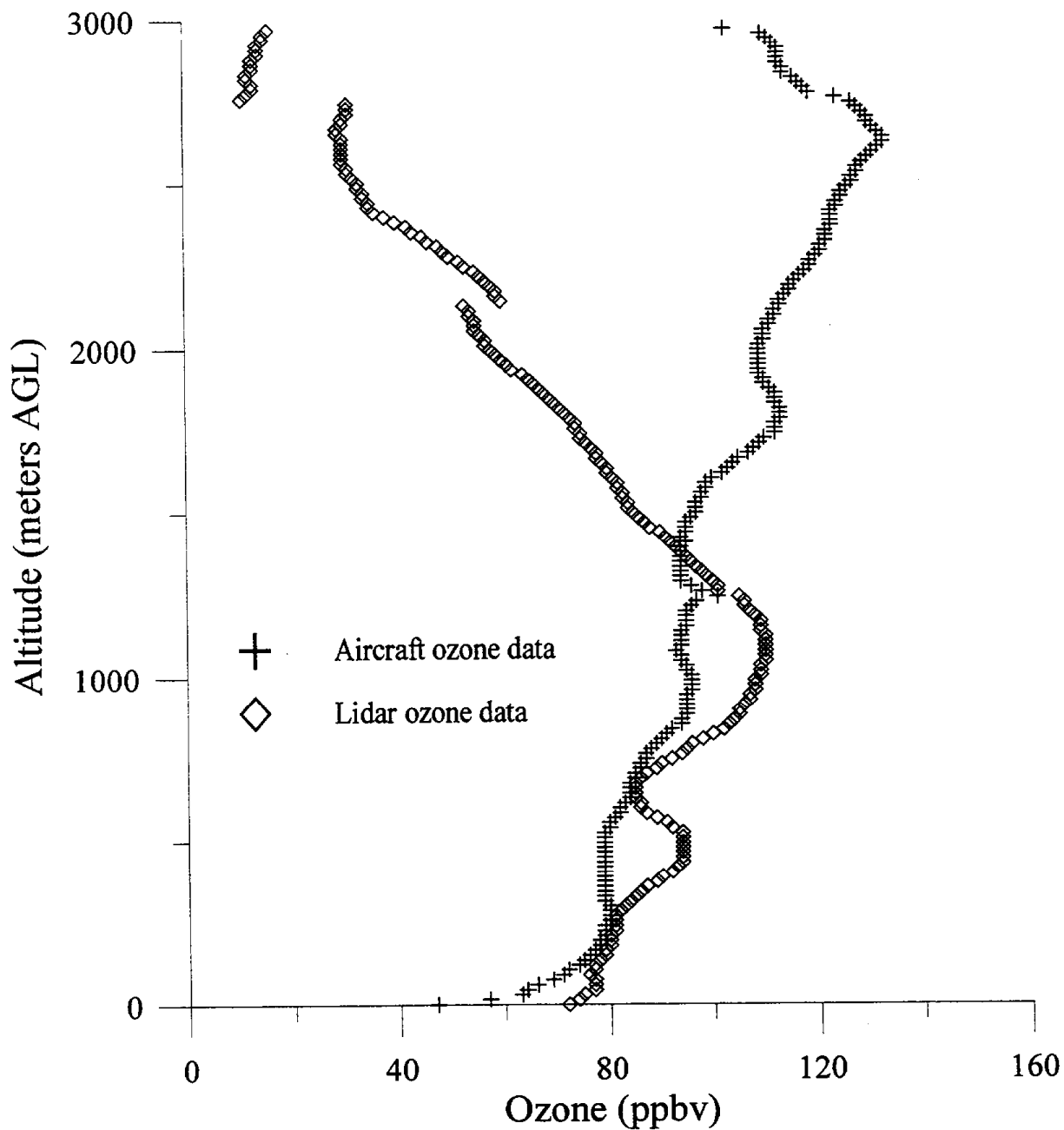


Figure 10: Plot of aircraft ozone data and lidar ozone data versus altitude AGL for 08-09-95 from 01:58 to 02:23 UTC (08-08-95, 17:58 to 18:23 PST).

DATE: 08-10-95 TIME: 02:00 to 02:20 FILE # 01

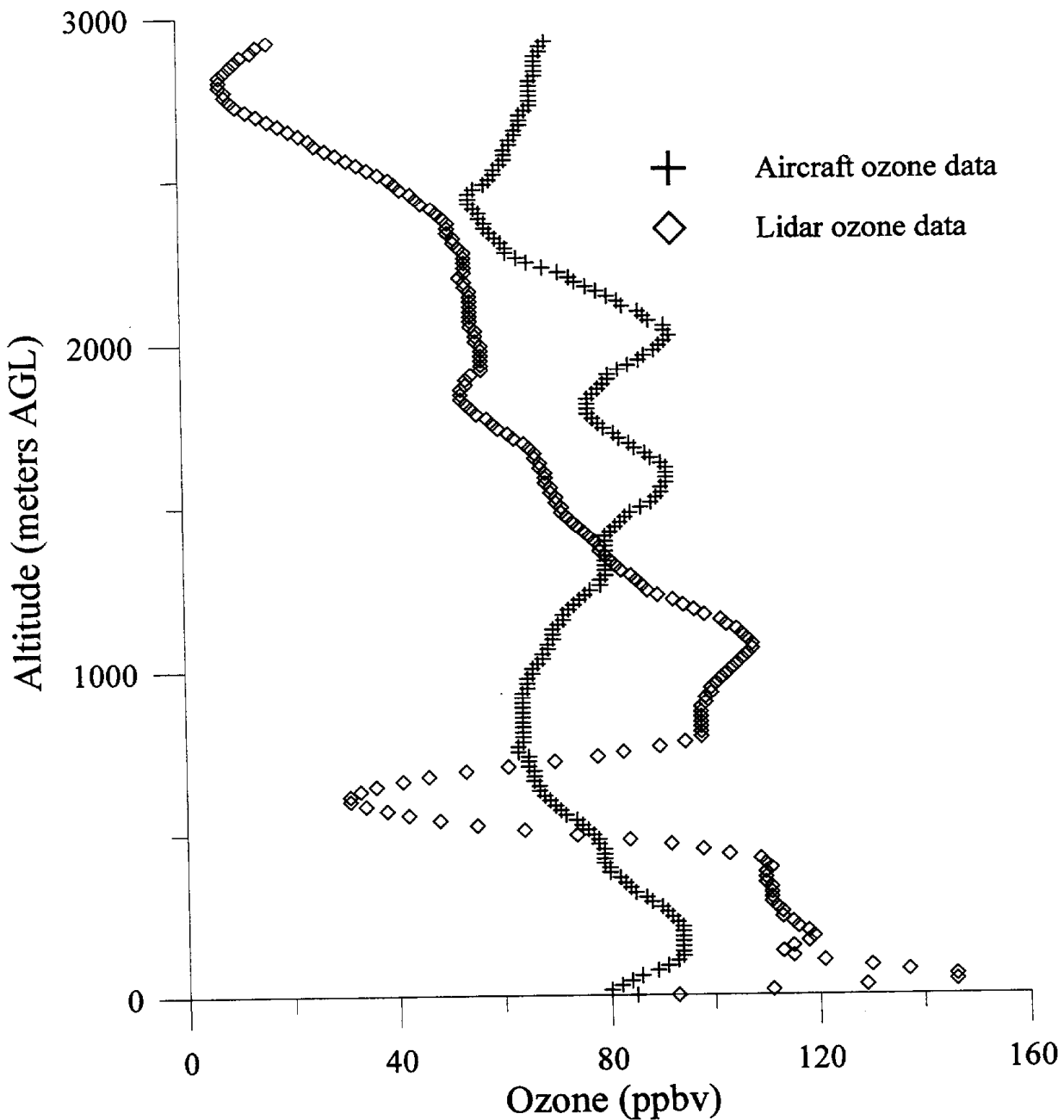


Figure 11: Plot of aircraft ozone data and lidar ozone data versus altitude AGL for 08-10-95 from 02:00 to 02:20 UTC (08-09-95, 18:00 to 18:20 PST).

DATE: 08-10-95 TIME: 14:01 to 14:21 FILE # 11

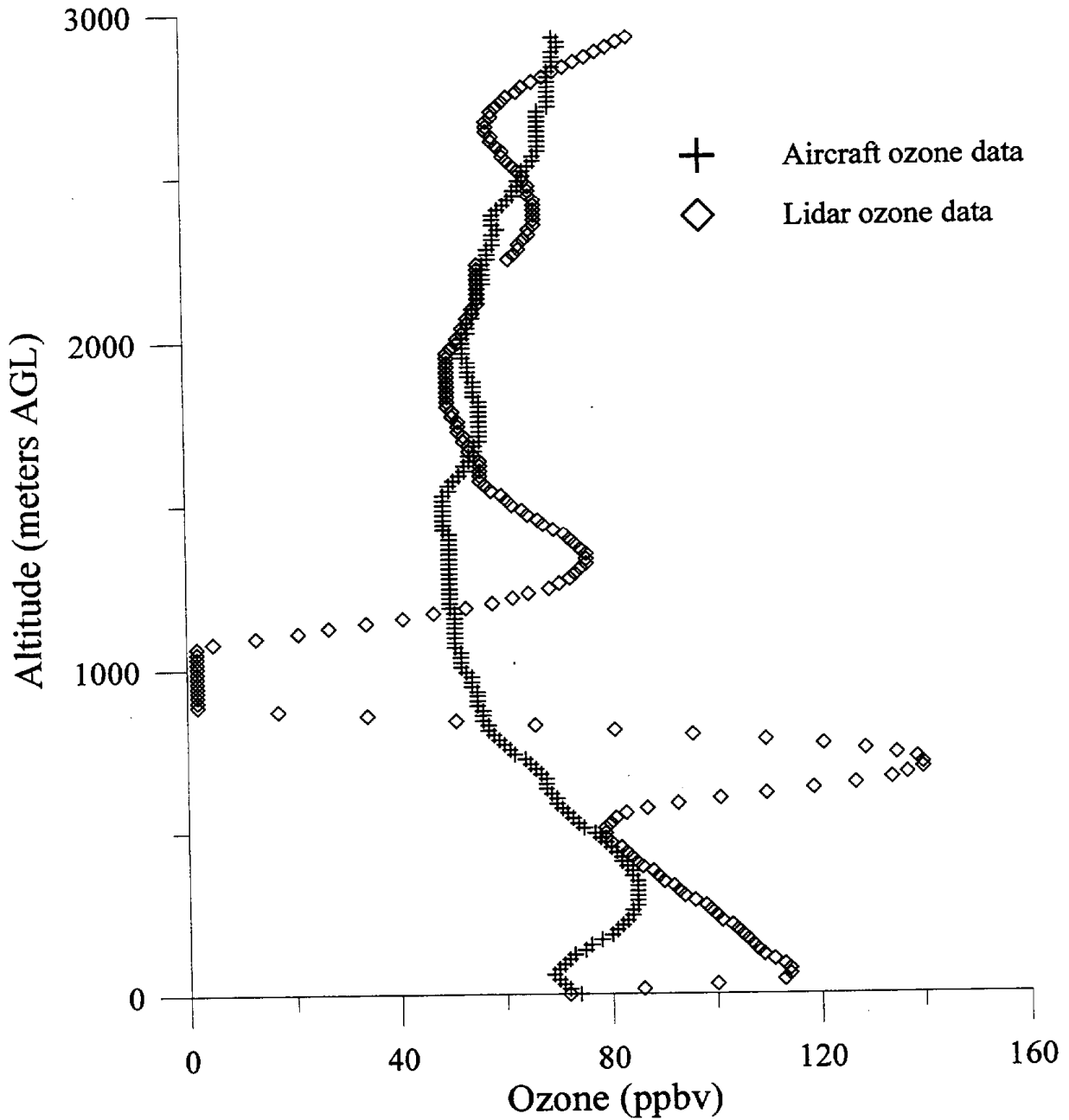


Figure 12: Plot of aircraft ozone data and lidar ozone data versus altitude AGL for 08-10-95 from 14:01 to 14:21 UTC (06:01 to 06:21 PST).

DATE: 08-10-95 TIME: 14:25 to 14:46 FILE # 12

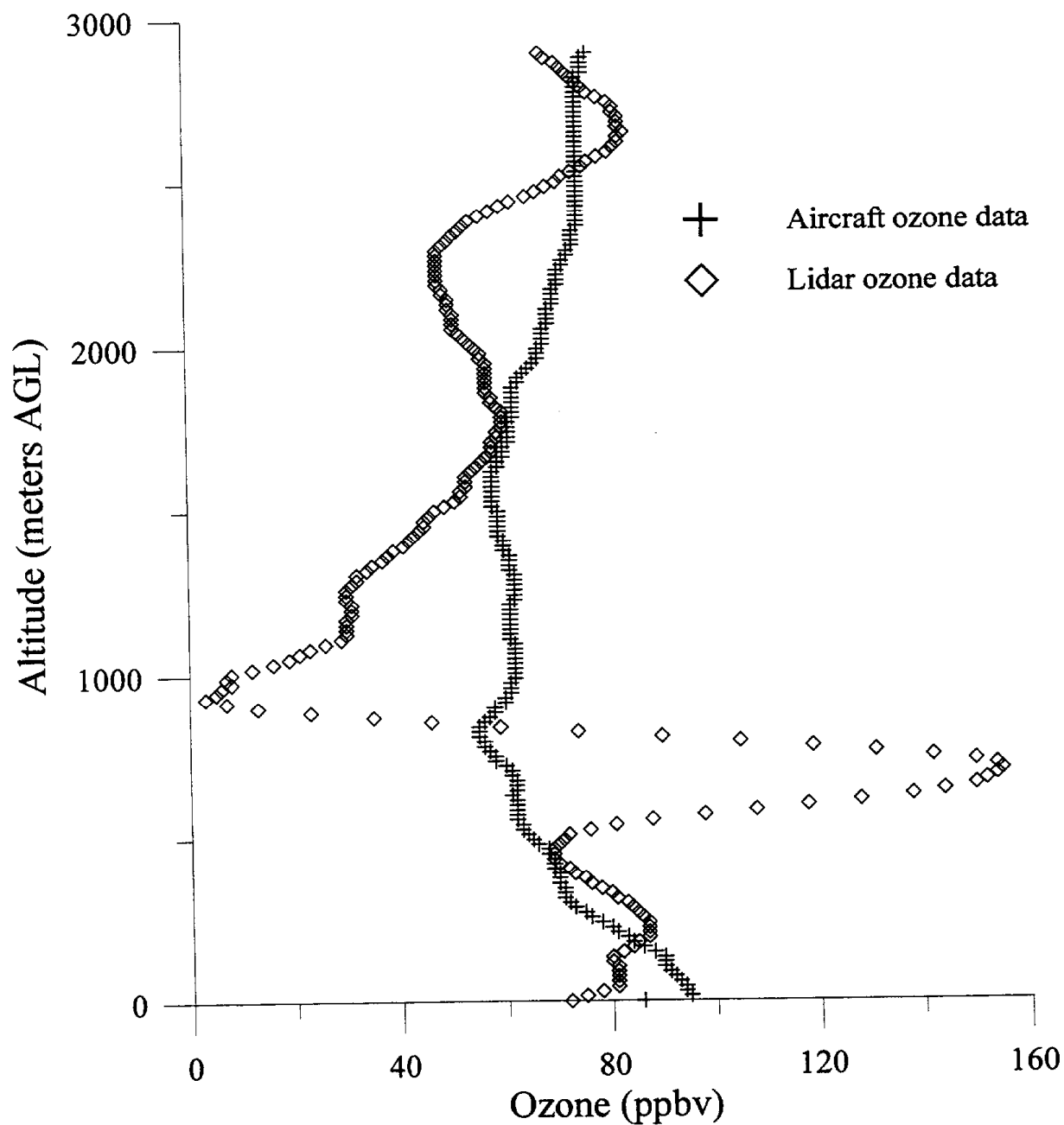


Figure 13: Plot of aircraft ozone data and lidar ozone data versus altitude AGL for 08-10-95 from 14:25 to 14:46 UTC (06:25 to 06:46 PST).

DATE: 08-12-95 TIME: 01:57 to 02:17 FILE # 01

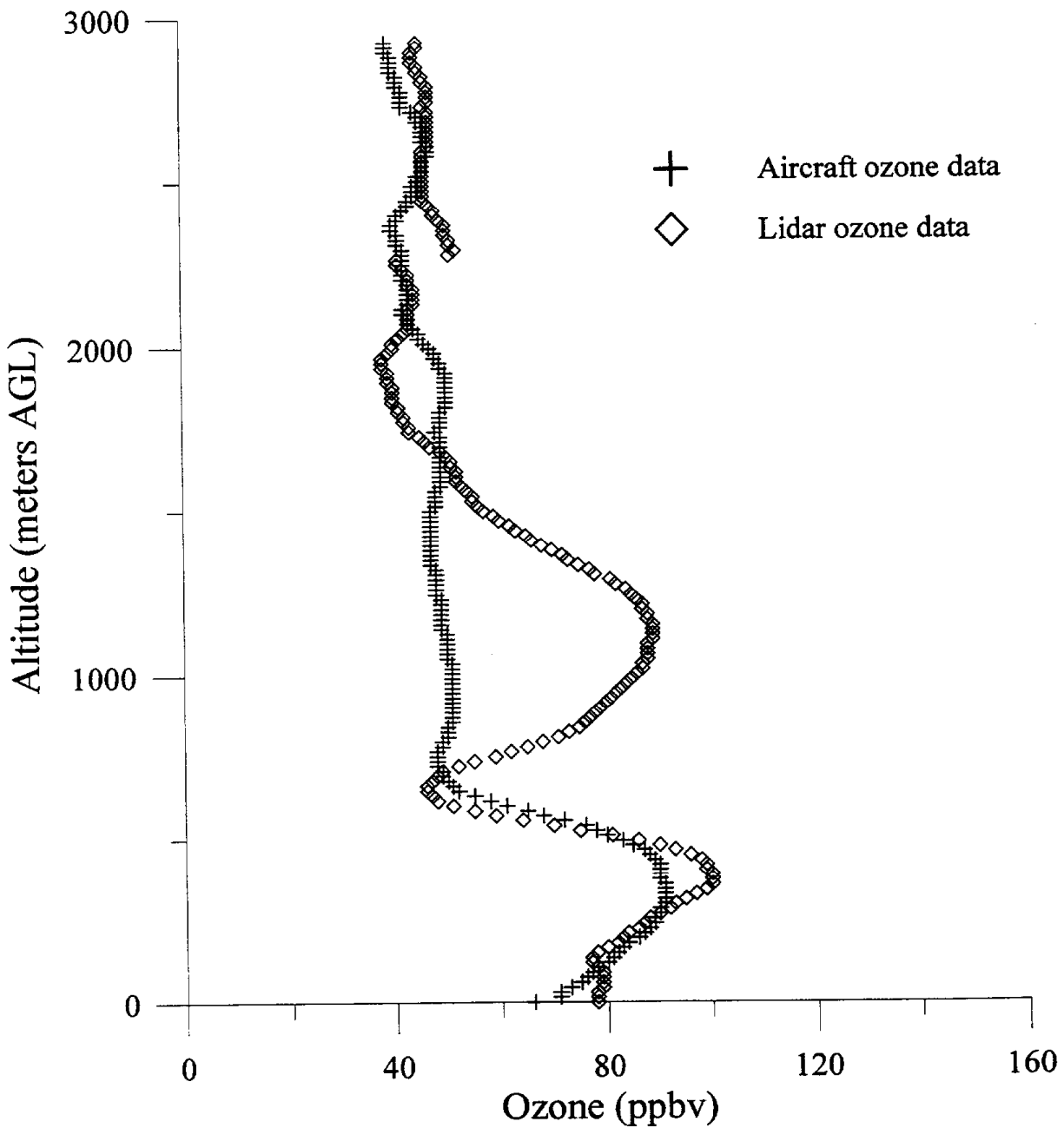


Figure 14: Plot of aircraft ozone data and lidar ozone data versus altitude AGL for 08-12-95 from 01:57 to 02:17 UTC (08-11-95, 17:57 to 18:17 PST).

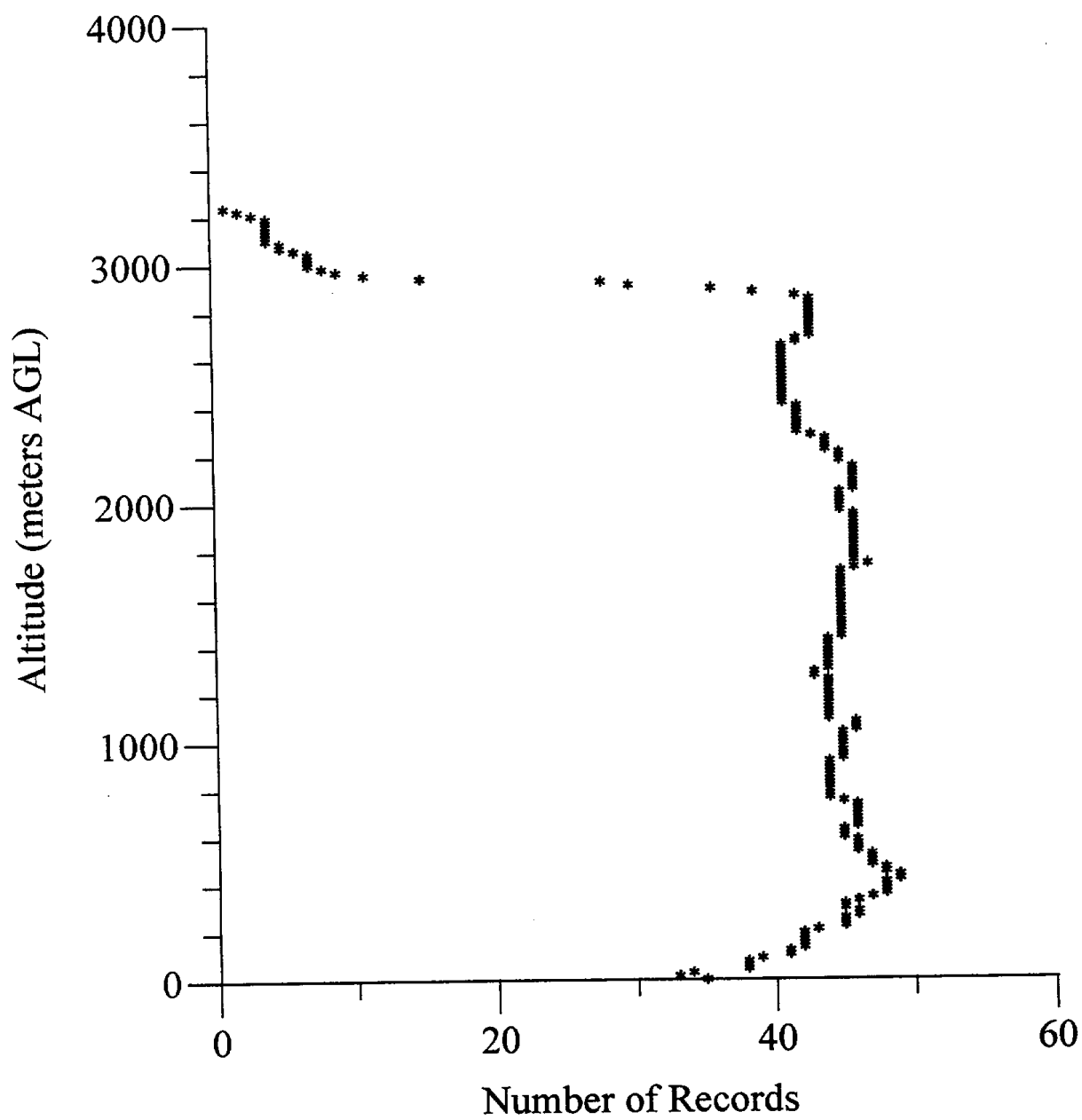


Figure 15: Plot of the number of records of both aircraft and lidar ozone data available at each altitude within 7 nm of the lidar site.

## Lidar - Aircraft Ozone RMS Difference

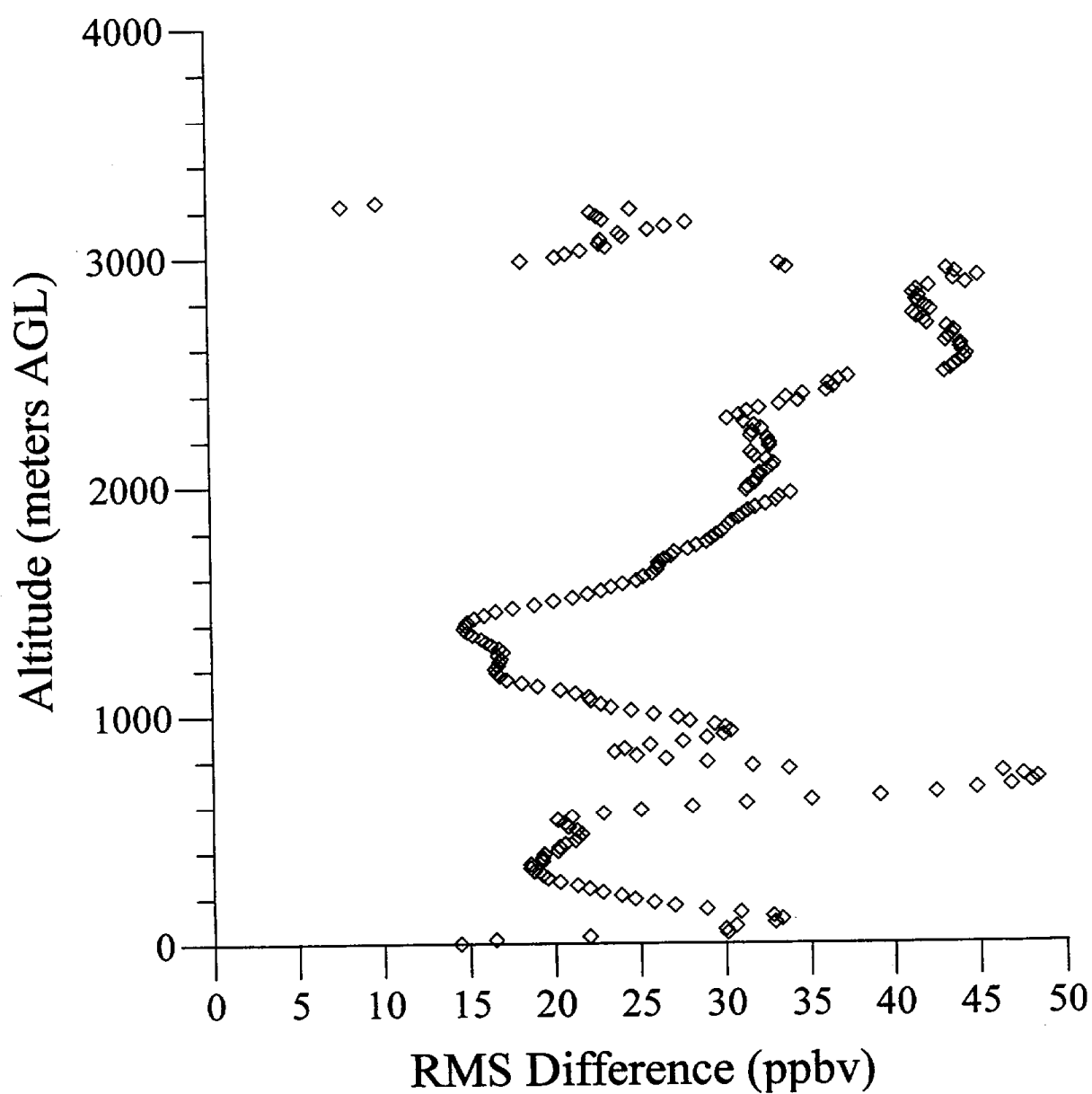


Figure 16: Plot of the RMS difference between the lidar and aircraft ozone concentrations within 7 nm of the lidar site.



## Lidar - Aircraft Bias and Aircraft Ozone Concentration

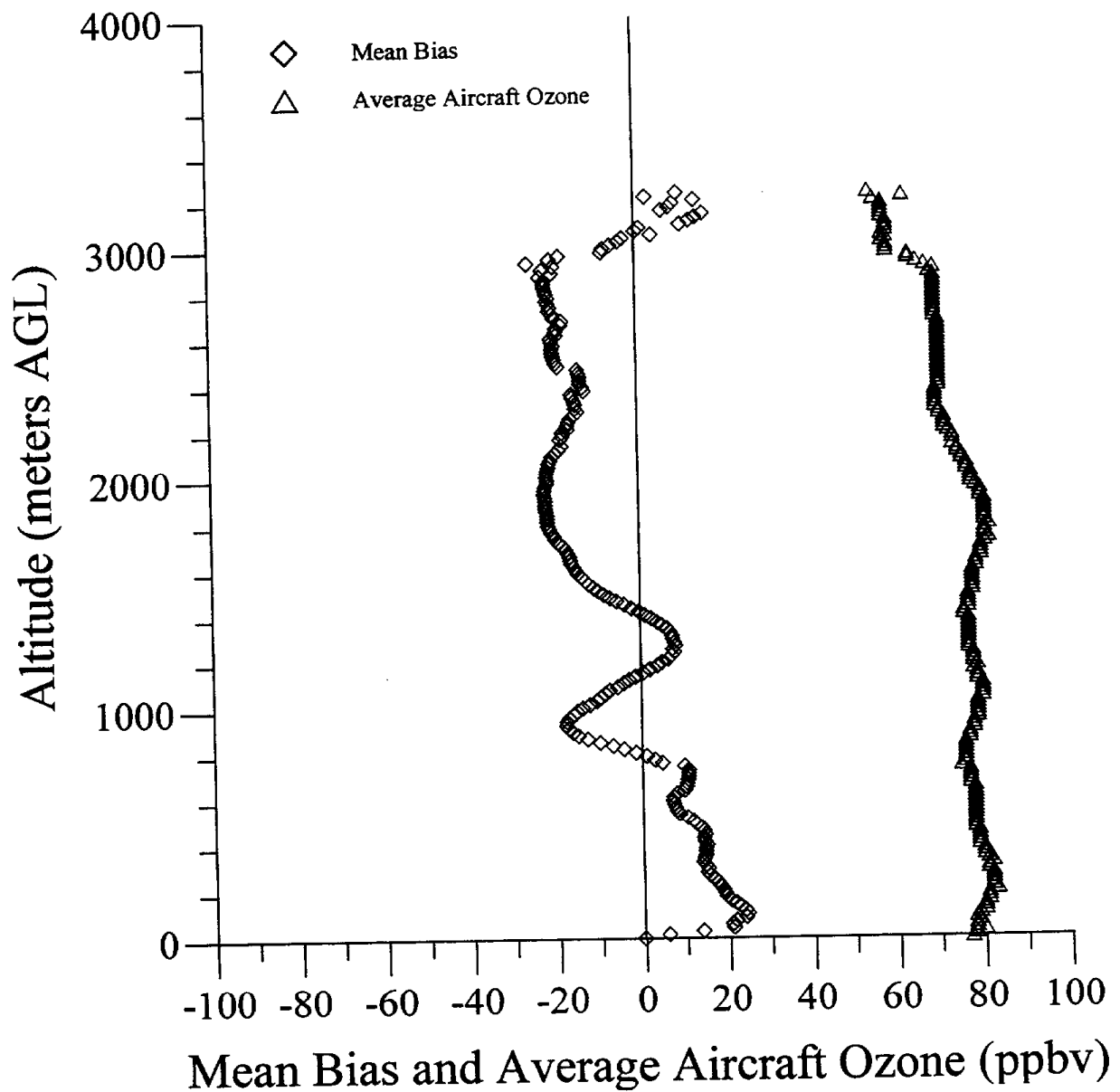
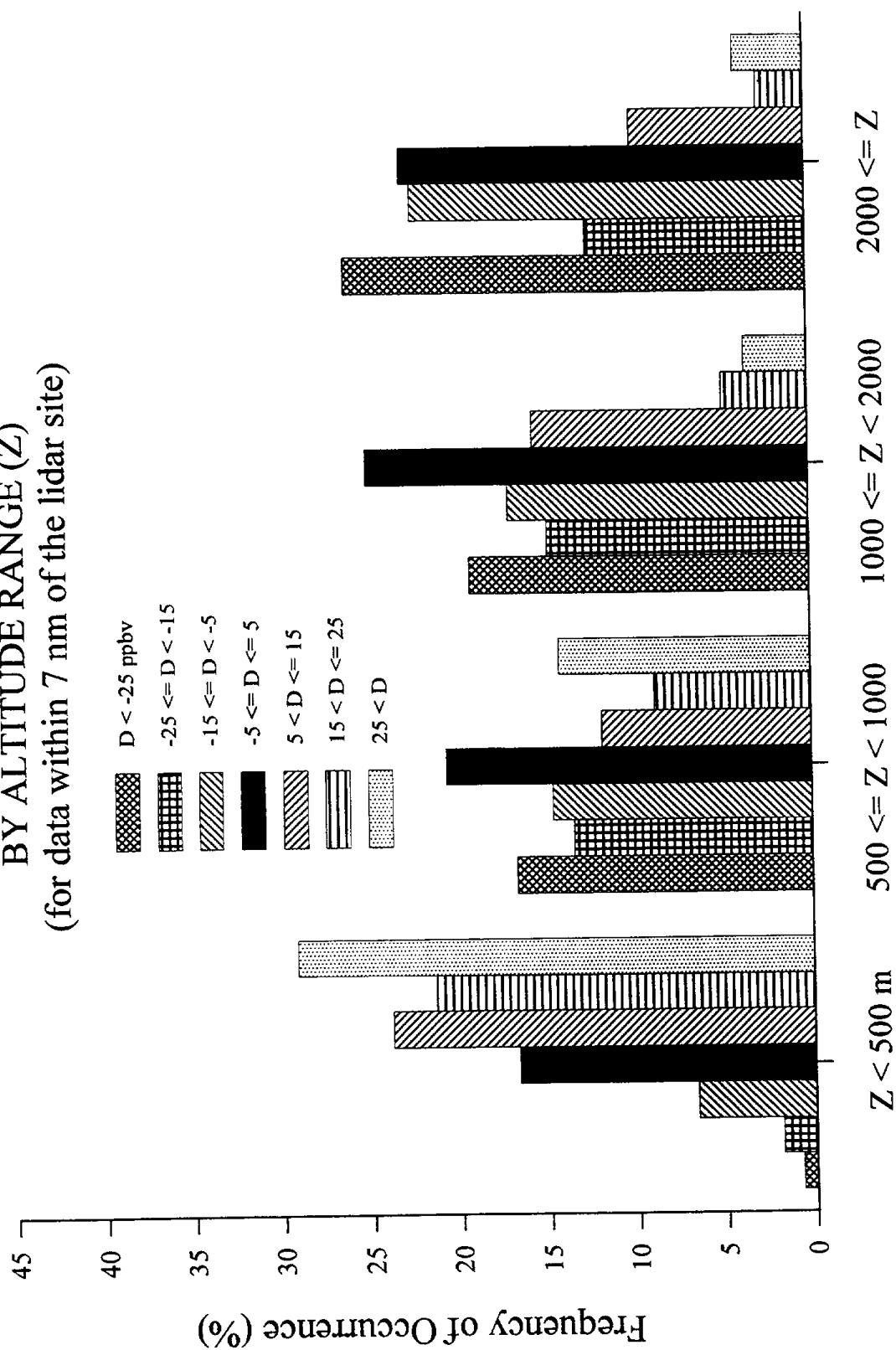


Figure 17: Plot of the mean bias between the lidar and aircraft ozone concentrations and of average aircraft ozone concentrations at a given altitude for aircraft flight within 7 nm of the lidar site.

**FIGURE 18**  
**LIDAR - AIRCRAFT OZONE DIFFERENCES (D)**  
**BY ALTITUDE RANGE (Z)**  
**(for data within 7 nm of the lidar site)**



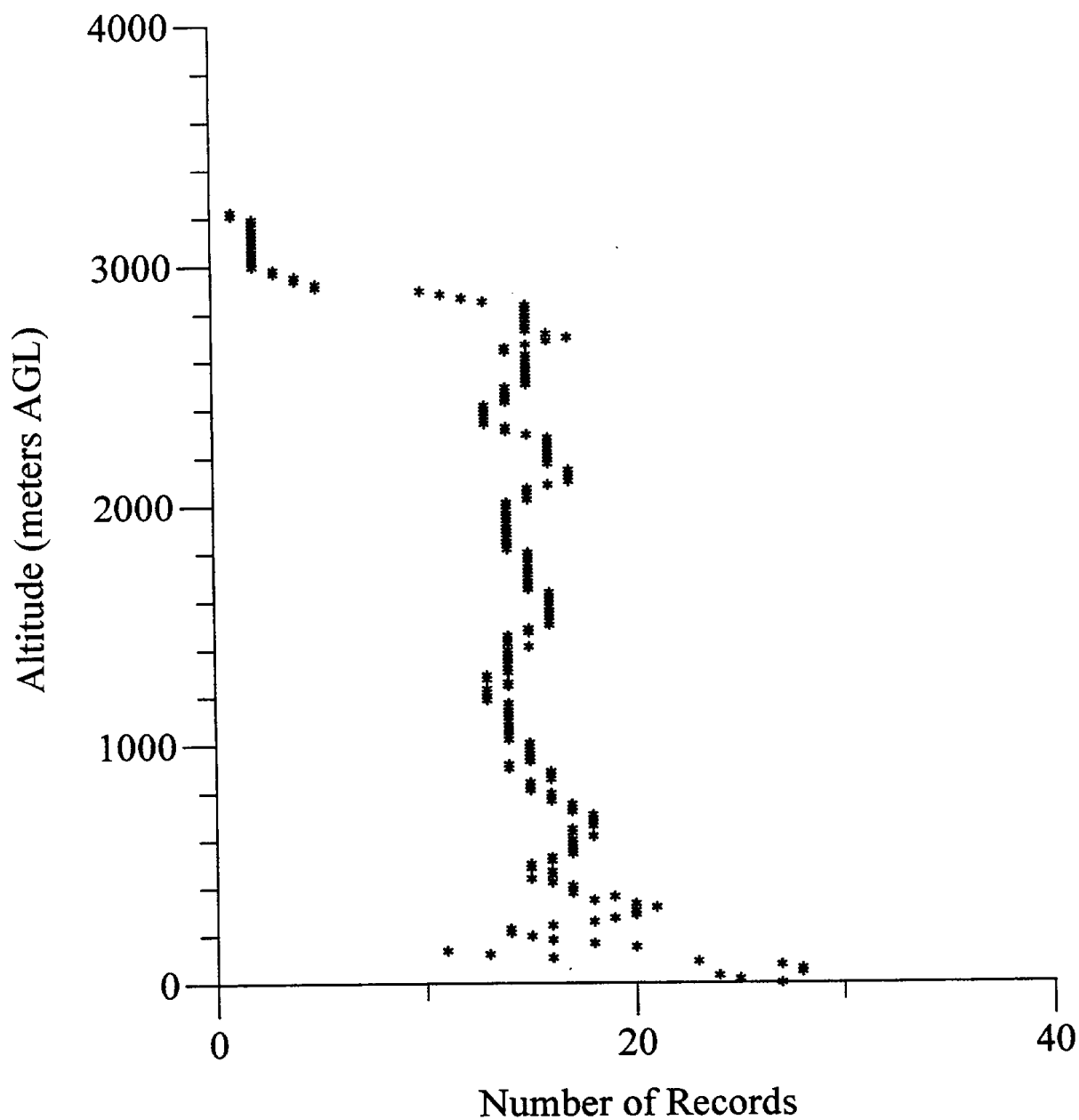


Figure 19: Plot of the number of records of both aircraft and lidar ozone data available at each altitude within 0.75 nm of the lidar site.

## Lidar - Aircraft Ozone RMS Difference

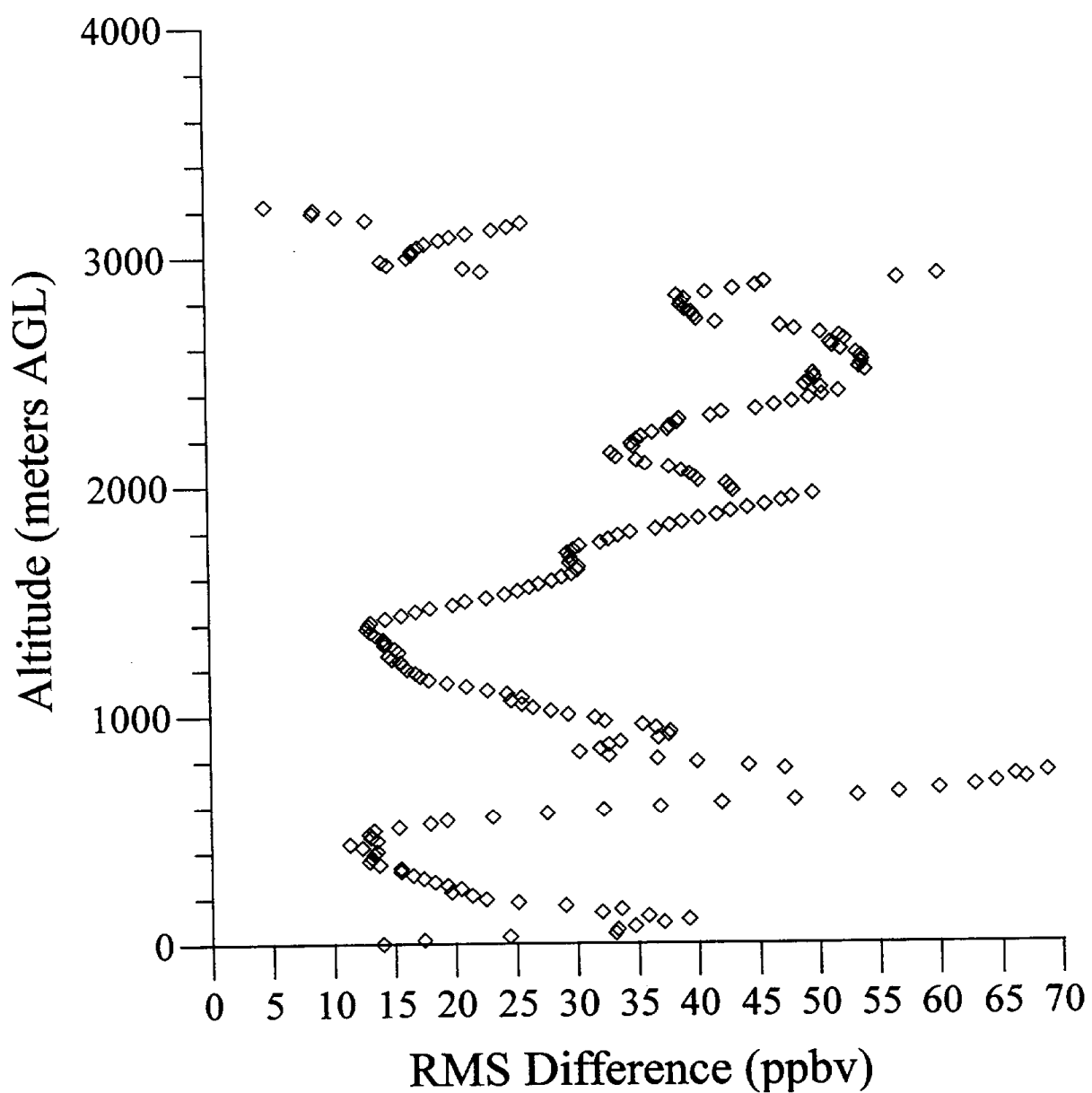


Figure 20: Plot of the RMS difference between the lidar and aircraft ozone concentrations for data within 0.75 nm of the lidar site.

## Lidar - Aircraft Bias and Aircraft Ozone Concentration

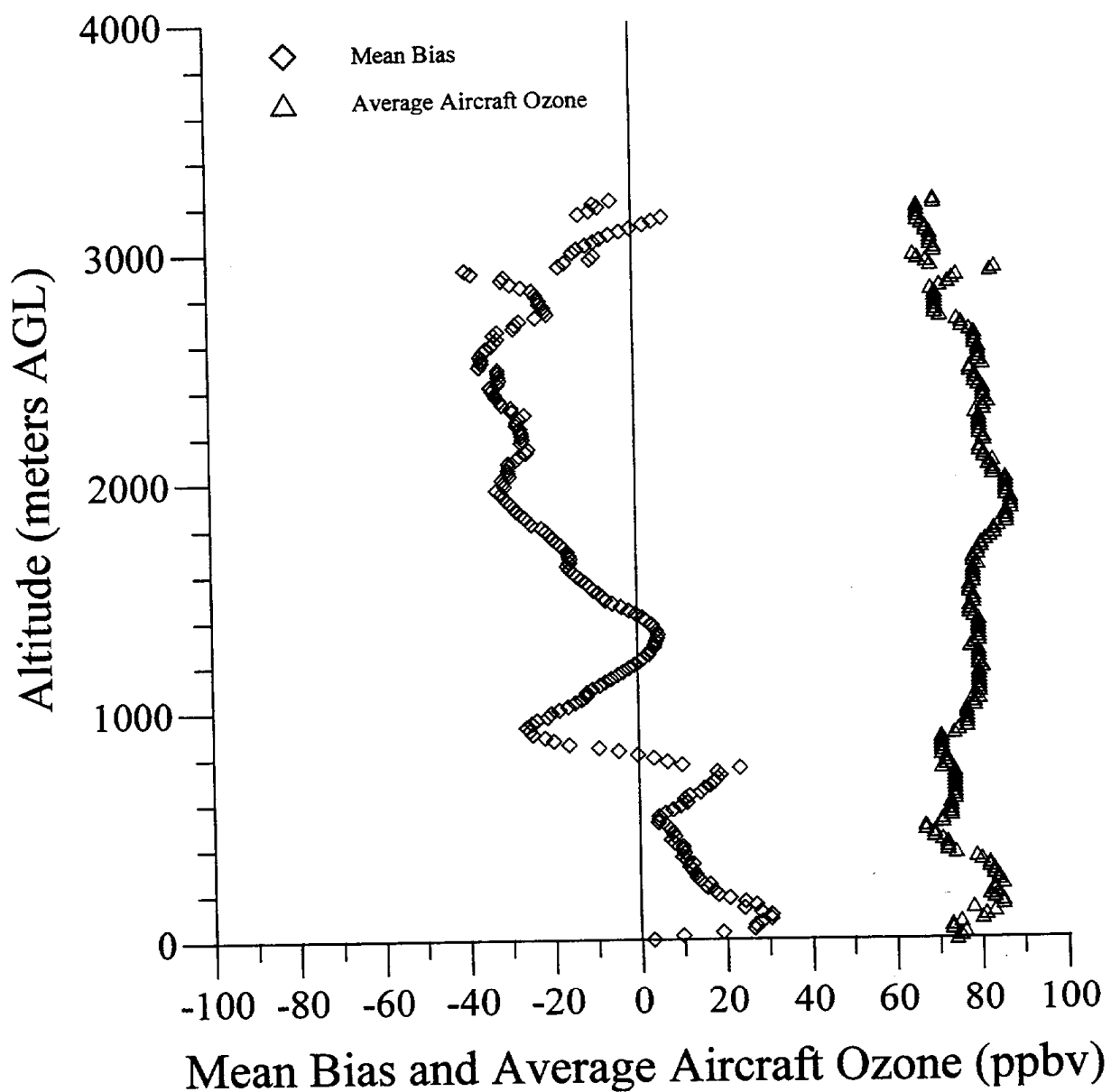
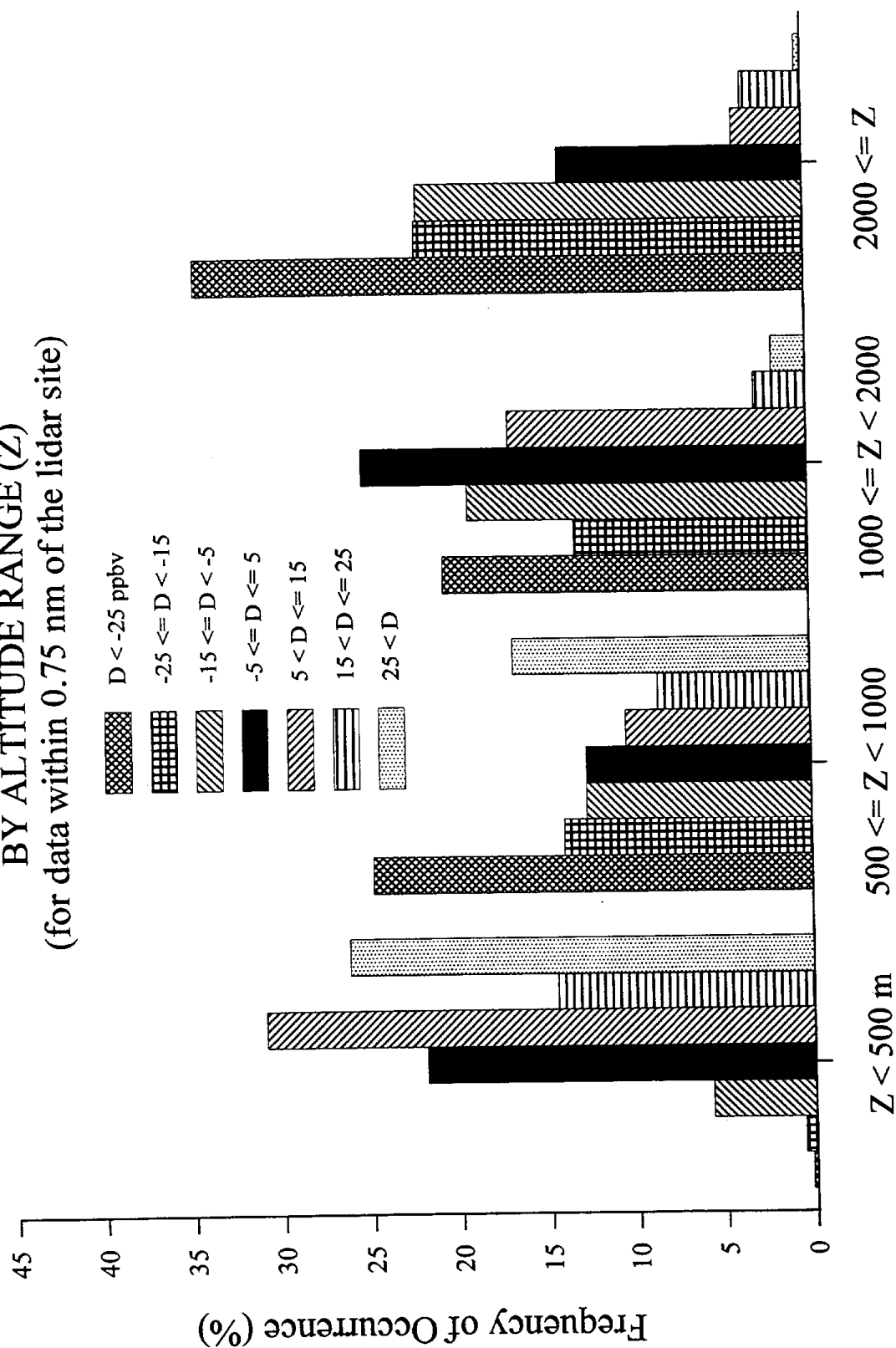


Figure 21: Plot of the mean bias between the lidar and aircraft ozone concentrations and of average aircraft ozone concentrations at a given altitude for aircraft flight within 0.75 nm of the lidar site.

FIGURE 22  
 LIDAR - AIRCRAFT OZONE DIFFERENCES (D)  
 BY ALTITUDE RANGE (Z)  
 (for data within 0.75 nm of the lidar site)



DATE: 08-03-95    TIME: 17:20 - 18:04    FILE #'s 01 & 02

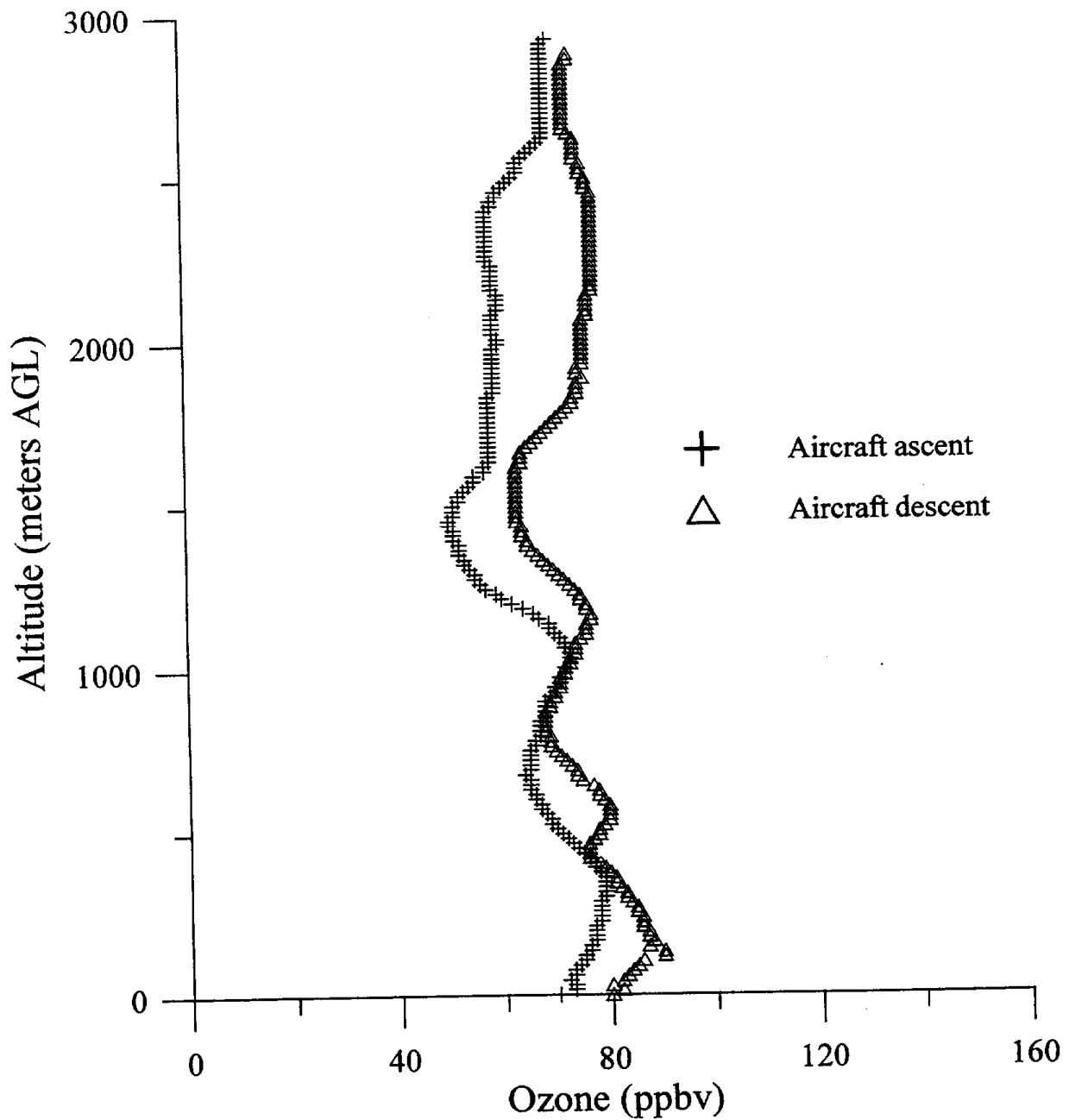


Figure 23: Plot of aircraft observed ozone concentrations during an ascent and descent on 08-03-95 from 17:20 to 18:04 UTC (09:20 to 10:04 PST)  
Note: The soundings shown here were both flown in box patterns.

DATE: 08-04-95    TIME: 18:01 to 18:48    FILE #'s 13 & 14

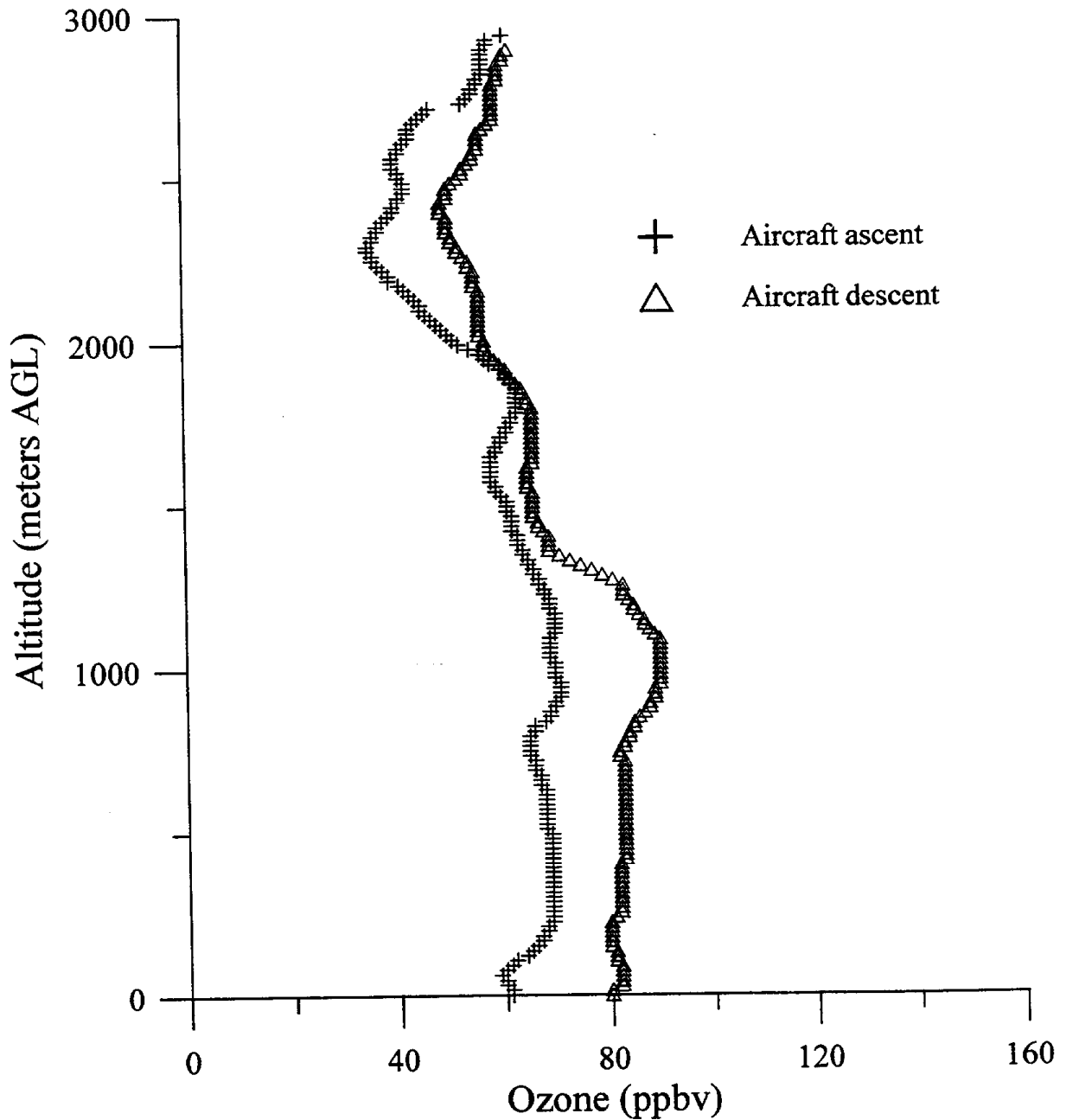


Figure 24: Plot of aircraft observed ozone concentrations during an ascent and descent on 08-04-95 from 18:01 to 18:48 UTC (10:01 to 10:48 PST)  
Note: The soundings shown here were both flown in box patterns.



DATE: 08-08-95    TIME: 22:08 to 22:58    FILE #'s 41 & 42

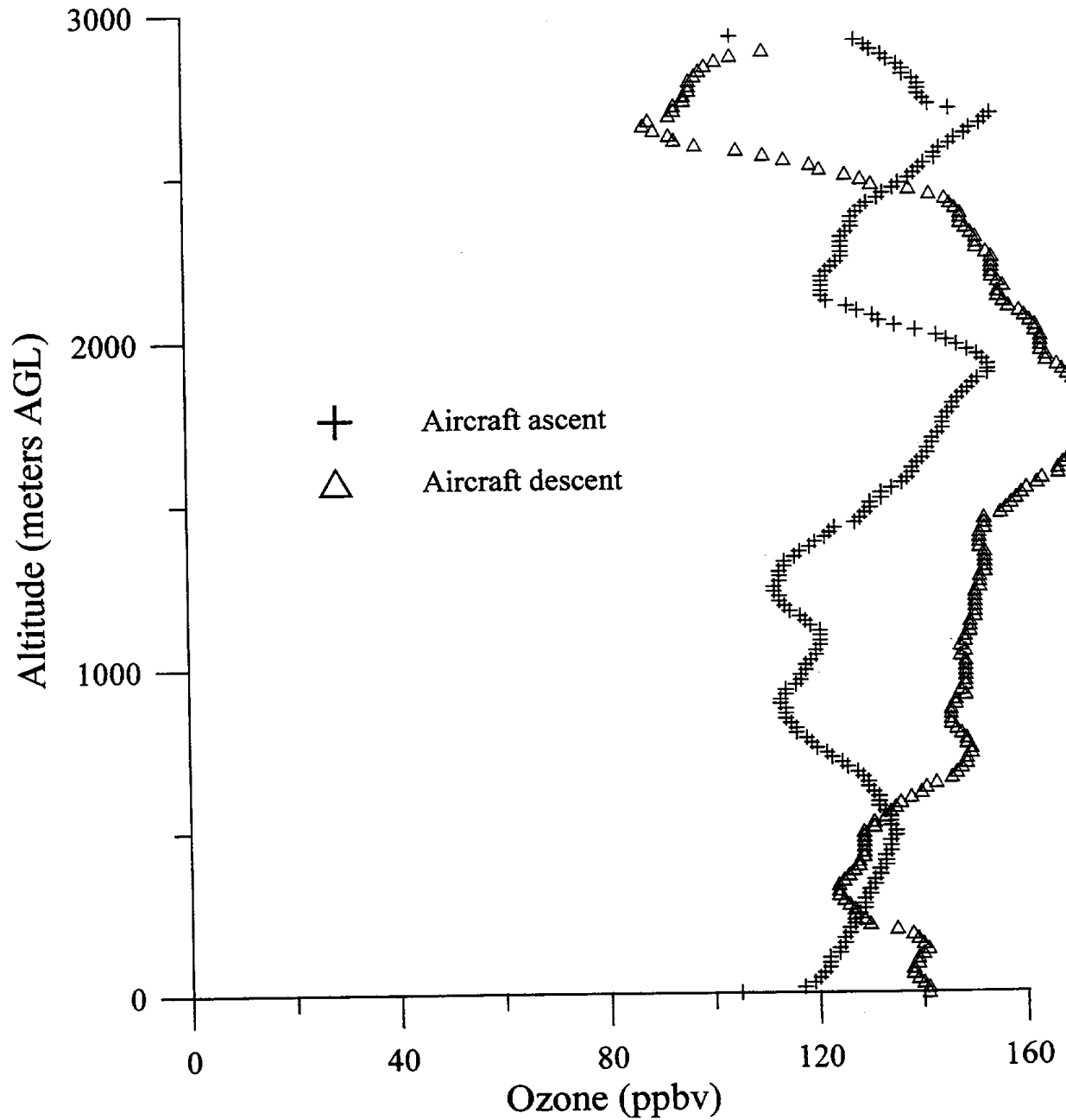


Figure 25: Plot of aircraft observed ozone concentrations during a box pattern ascent and a descending spiral on 08-08-95 from 22:08 to 22:58 UTC (14:08 to 14:58 PST).

DATE: 08-10-95    TIME: 14:01 to 14:46    FILE #'s 11 & 12

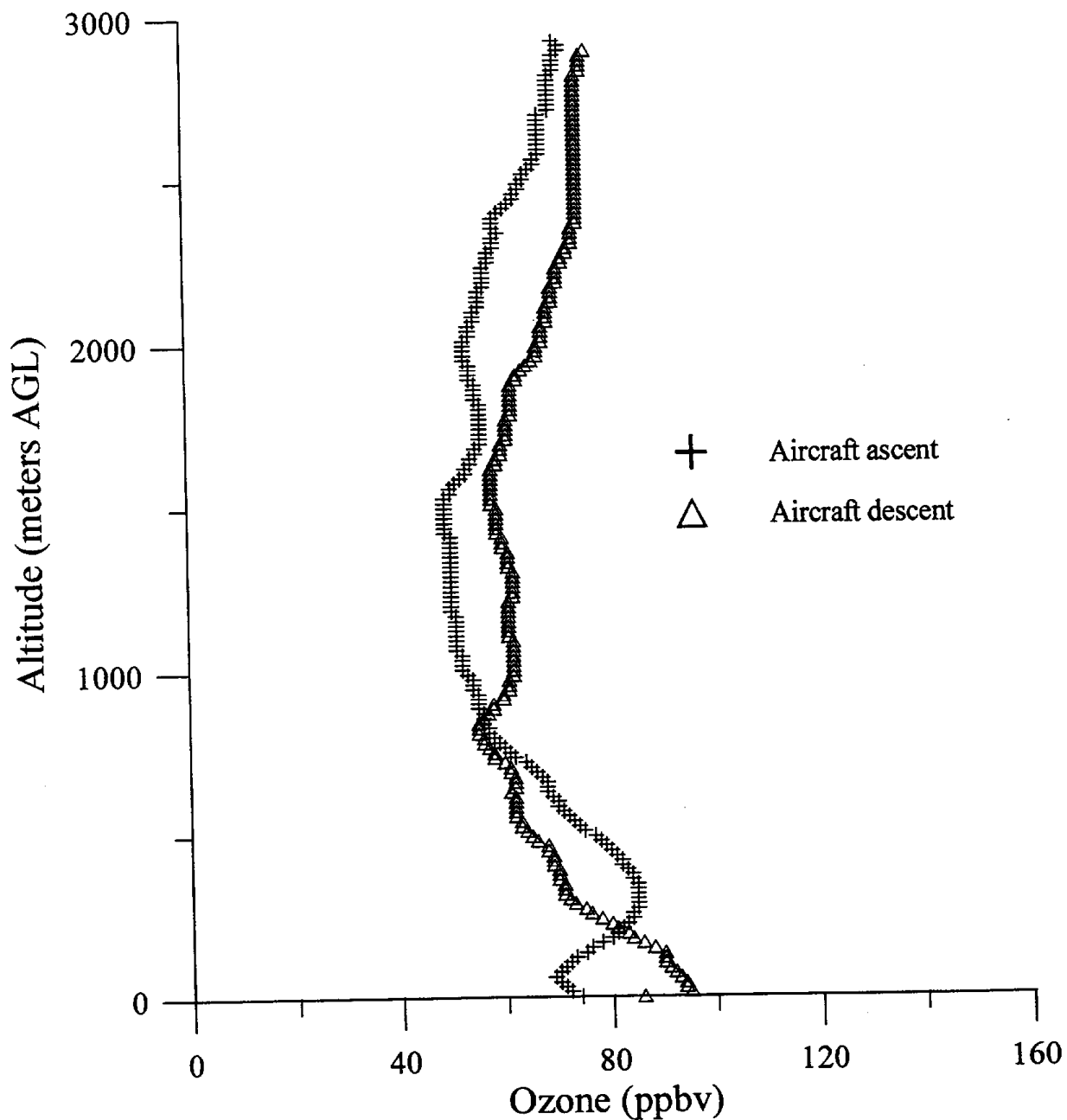


Figure 26: Plot of aircraft observed ozone concentrations during a box pattern ascent and a descending spiral on 08-10-95 from 14:01 to 14:46 UTC (06:01 to 06:46 PST).

DATE: 08-11-95    TIME: 13:59 to 14:43    FILE #'s 11 & 12

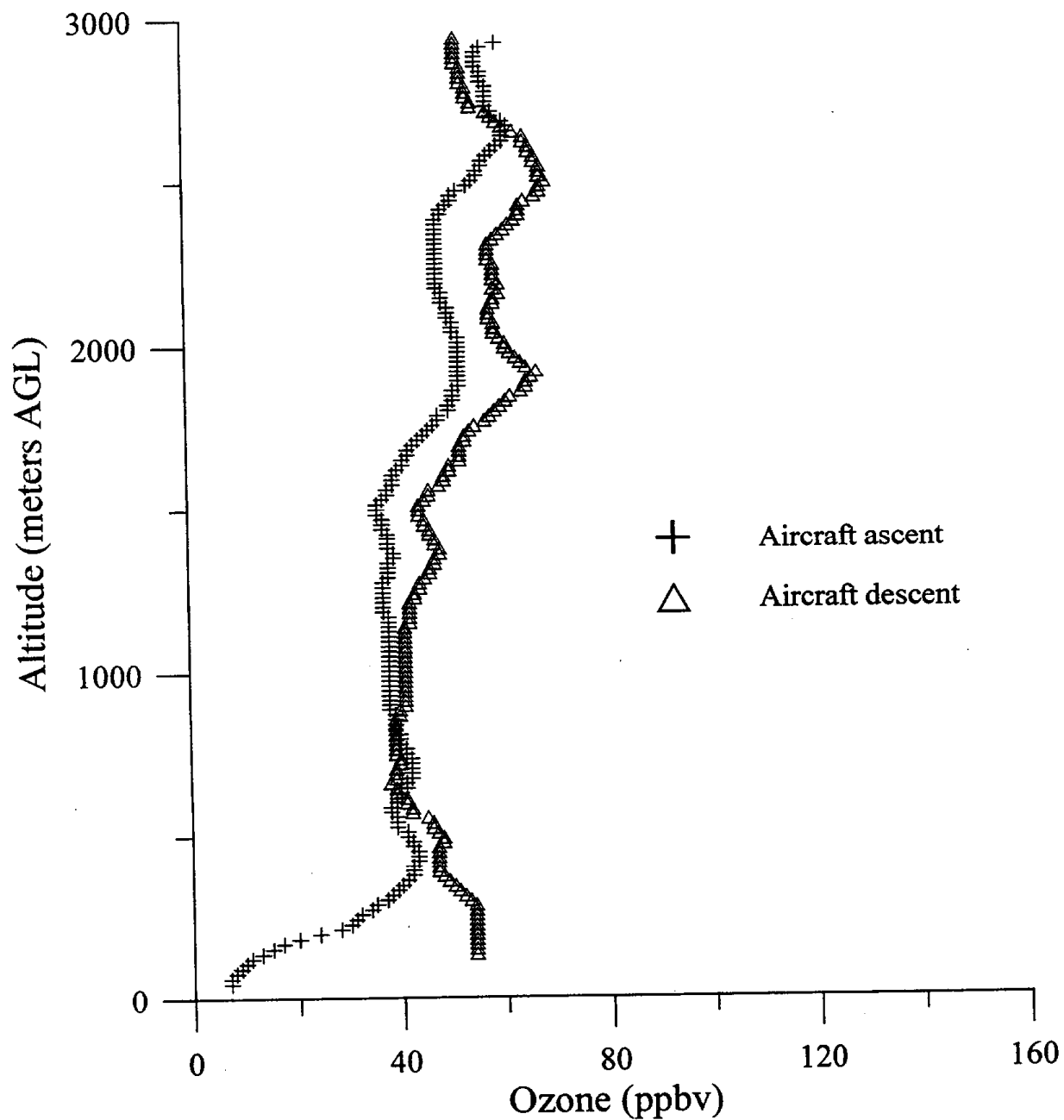


Figure 27: Plot of aircraft observed ozone concentrations during a box pattern ascent and a descending spiral on 08-04-95 from 13:59 to 14:43 UTC (05:59 to 06:43 PST).

DATE: 08-12-95    TIME: 01:57 to 02:42    FILE #'s 01 & 02

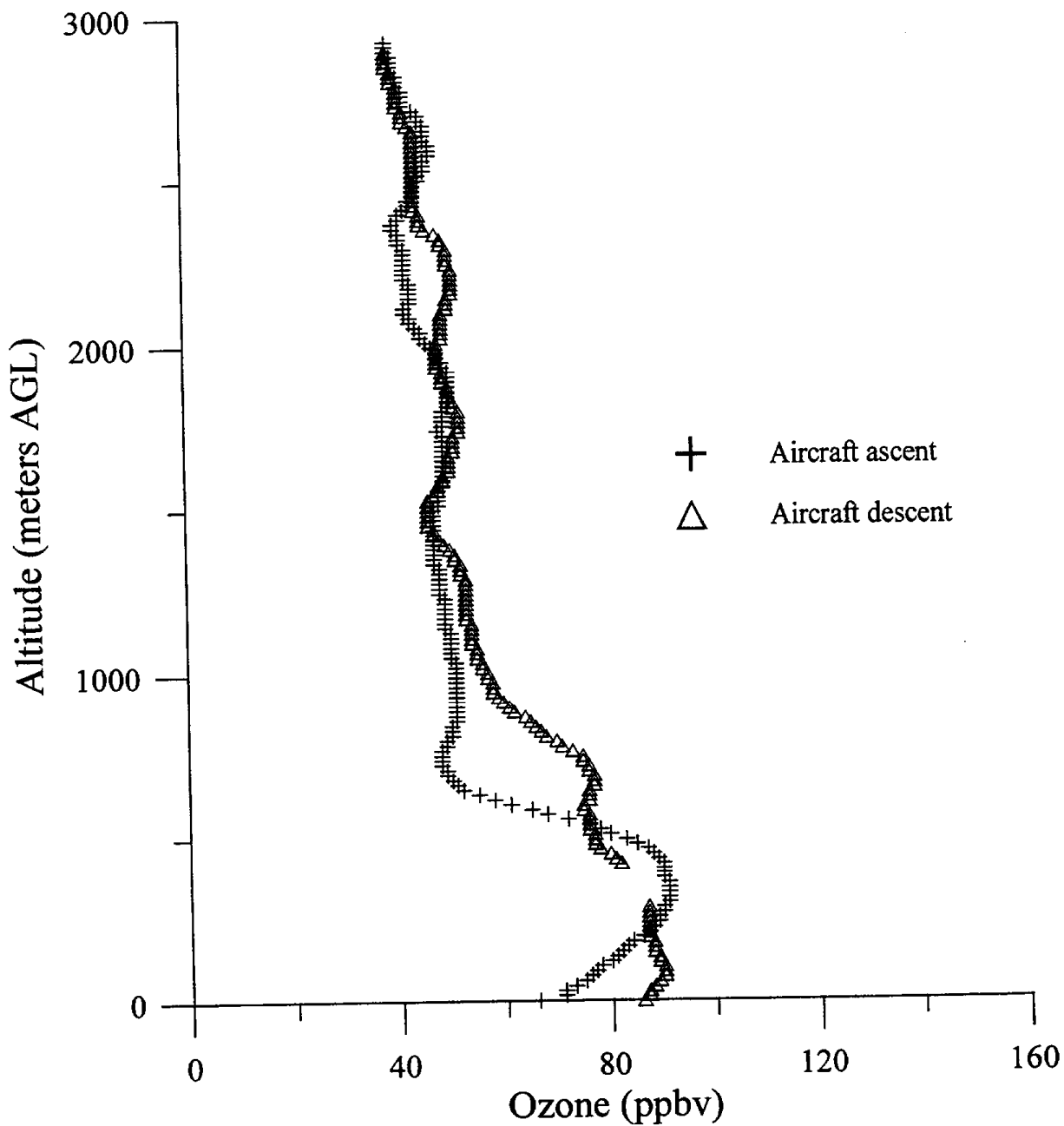


Figure 28: Plot of aircraft observed ozone concentrations during a box pattern ascent and a descending spiral on 08-12-95 from 01:57 to 02:42 UTC (08-11-95, 17:57 to 18:42 PST).

# Lidar - Aircraft Bias and Aircraft Ozone Concentration 13:00 to 16:00 UTC (05:00 to 08:00 PST)

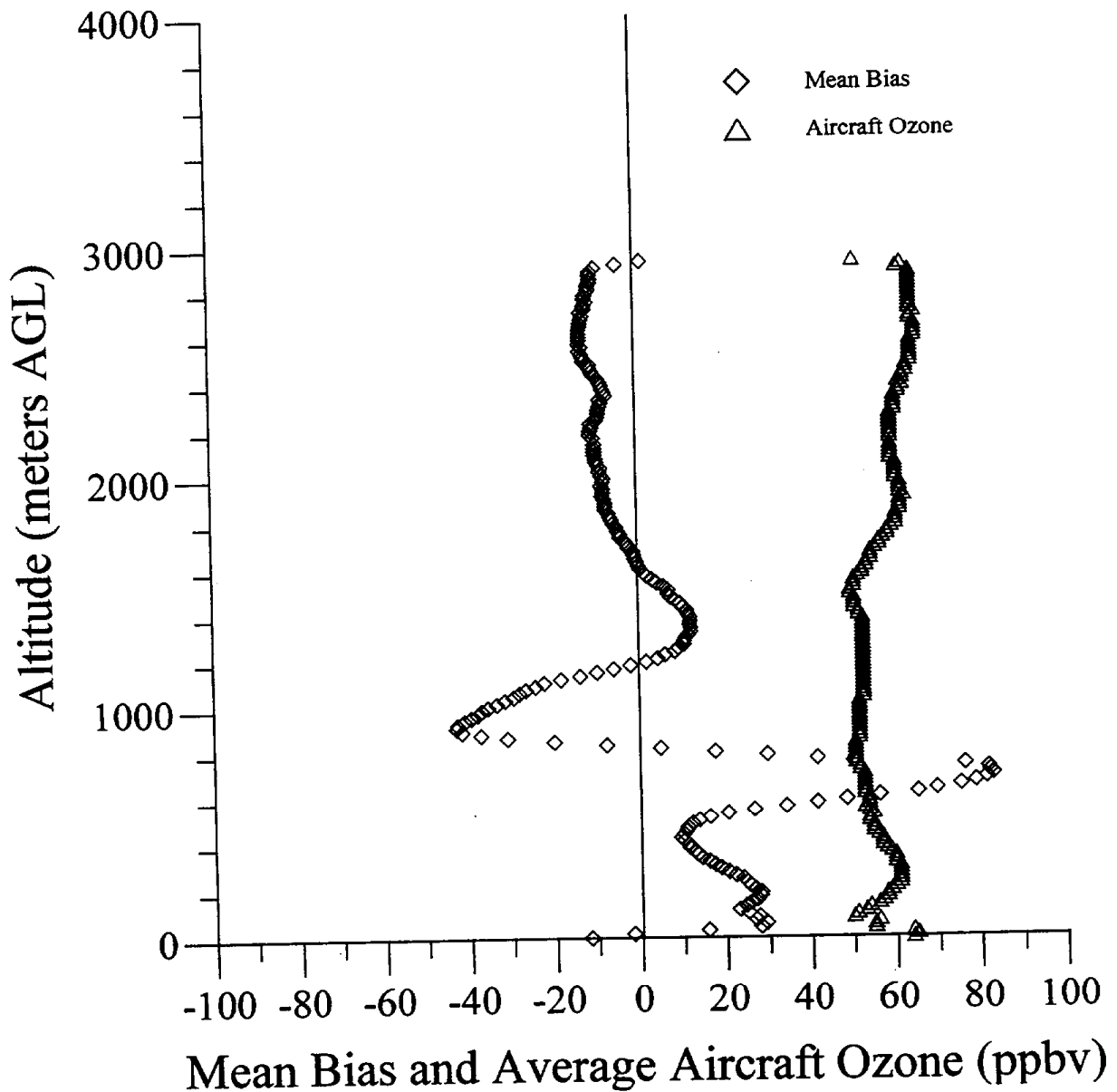


Figure 29: Plot of the mean bias between the lidar and aircraft ozone concentrations and of average aircraft ozone concentrations at a given altitude for aircraft flight within 7 nm of the lidar site and between 13:00 and 16:00 UTC (05:00 and 08:00 PST).

# Lidar - Aircraft Bias and Aircraft Ozone Concentration 17:00 to 20:00 UTC (09:00 to 12:00 PST)

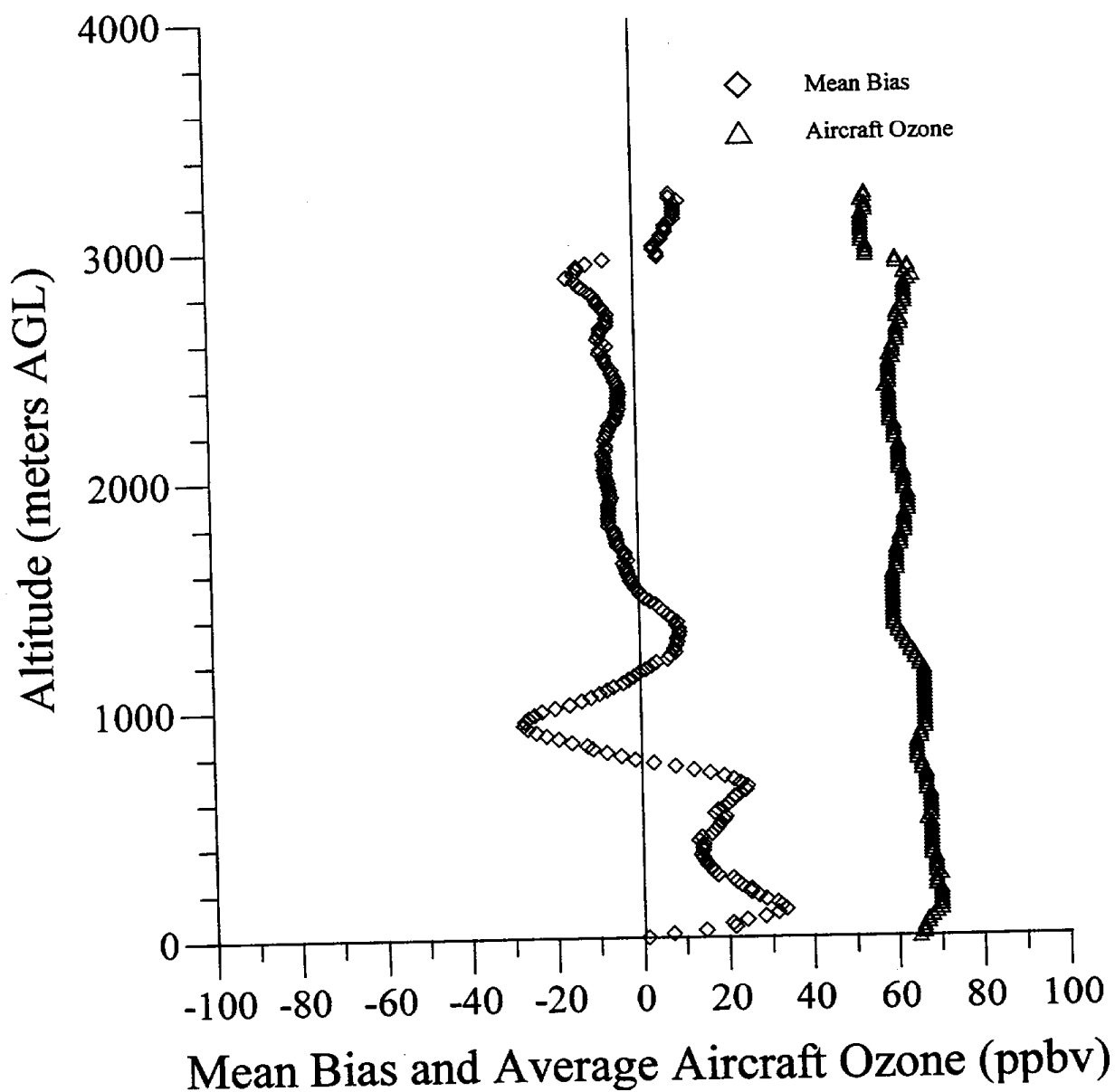


Figure 30: Plot of the mean bias between the lidar and aircraft ozone concentrations and of average aircraft ozone concentrations at a given altitude for aircraft flight within 7 nm of the lidar site and between 17:00 and 20:00 UTC (09:00 and 12:00 PST).

Lidar - Aircraft Bias and Aircraft Ozone Concentration  
21:00 to 23:59 UTC (13:00 to 15:59 PST)

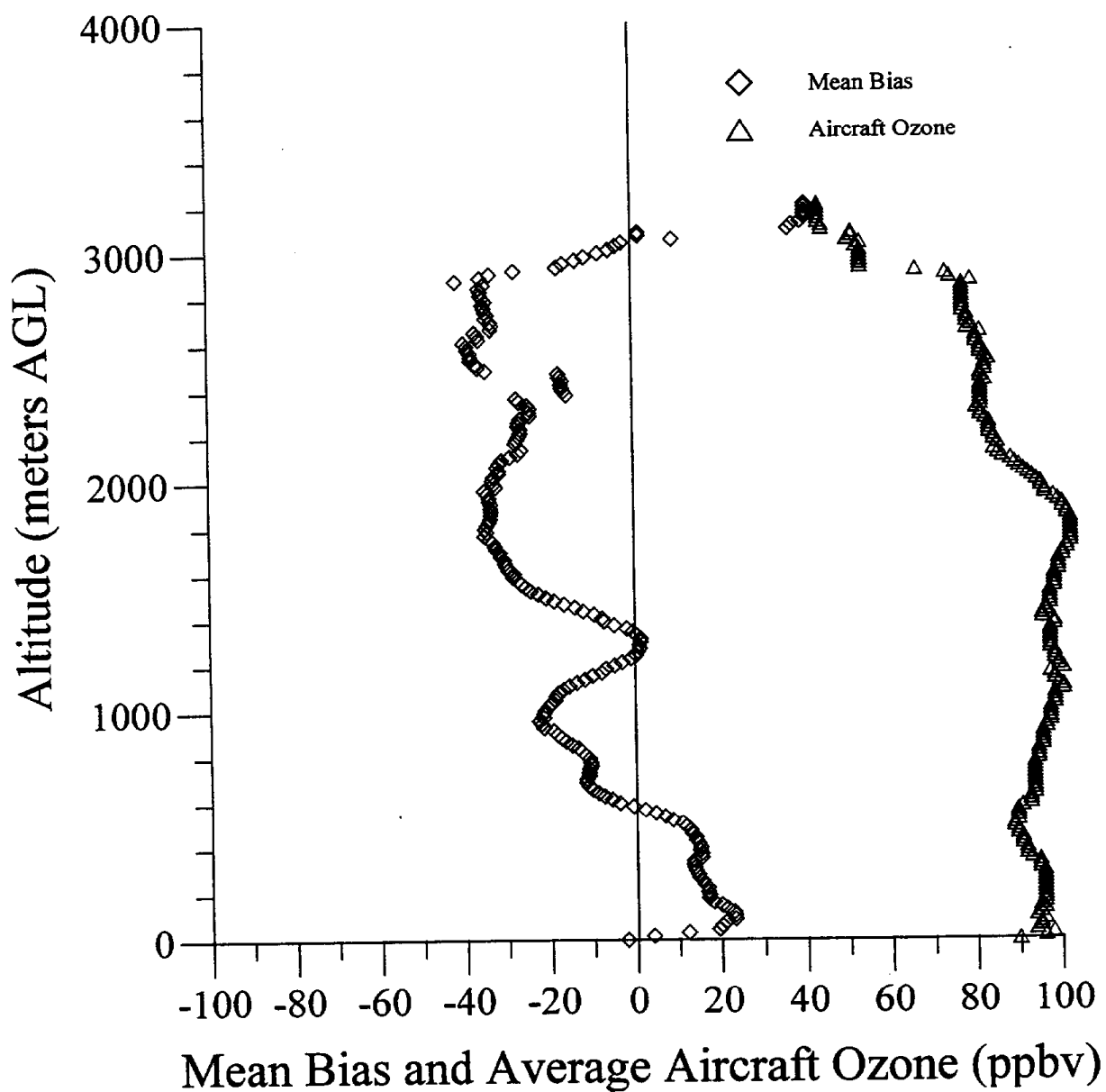


Figure 31: Plot of the mean bias between the lidar and aircraft ozone concentrations and of average aircraft ozone concentrations at a given altitude for aircraft flight within 7 nm of the lidar site and between 21:00 and 23:59 UTC (13:00 and 15:59 PST).

# Lidar - Aircraft Bias and Aircraft Ozone Concentration 01:00 to 04:00 UTC (17:00 to 20:00 PST)

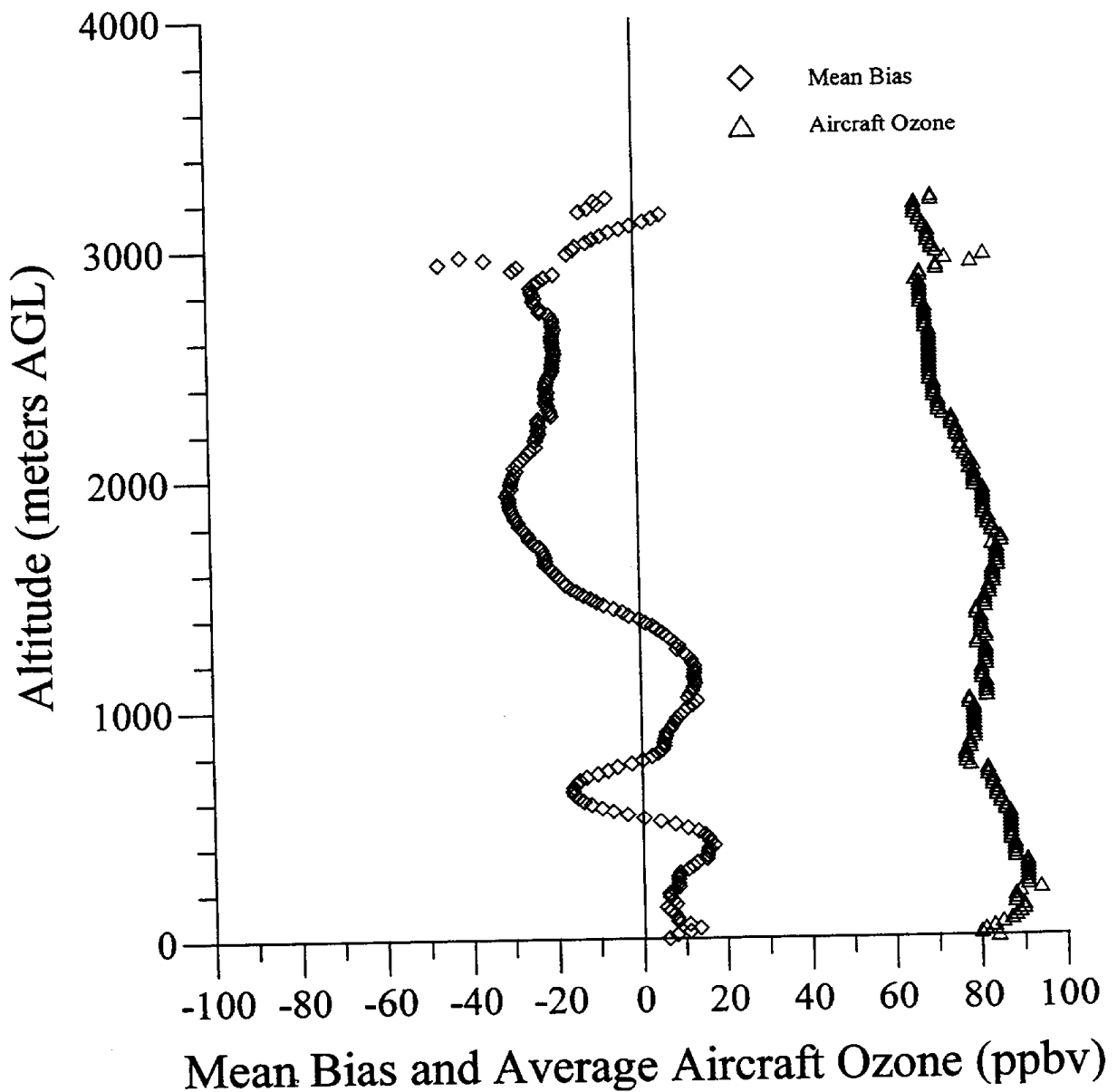


Figure 32: Plot of the mean bias between the lidar and aircraft ozone concentrations and of average aircraft ozone concentrations at a given altitude for aircraft flight within 7 nm of the lidar site and between 01:00 and 04:00 UTC (17:00 and 20:00 PST).



Lidar - Aircraft Ozone RMS Difference  
For 13:00 to 16:00 UTC (05:00 to 08:00 PST)

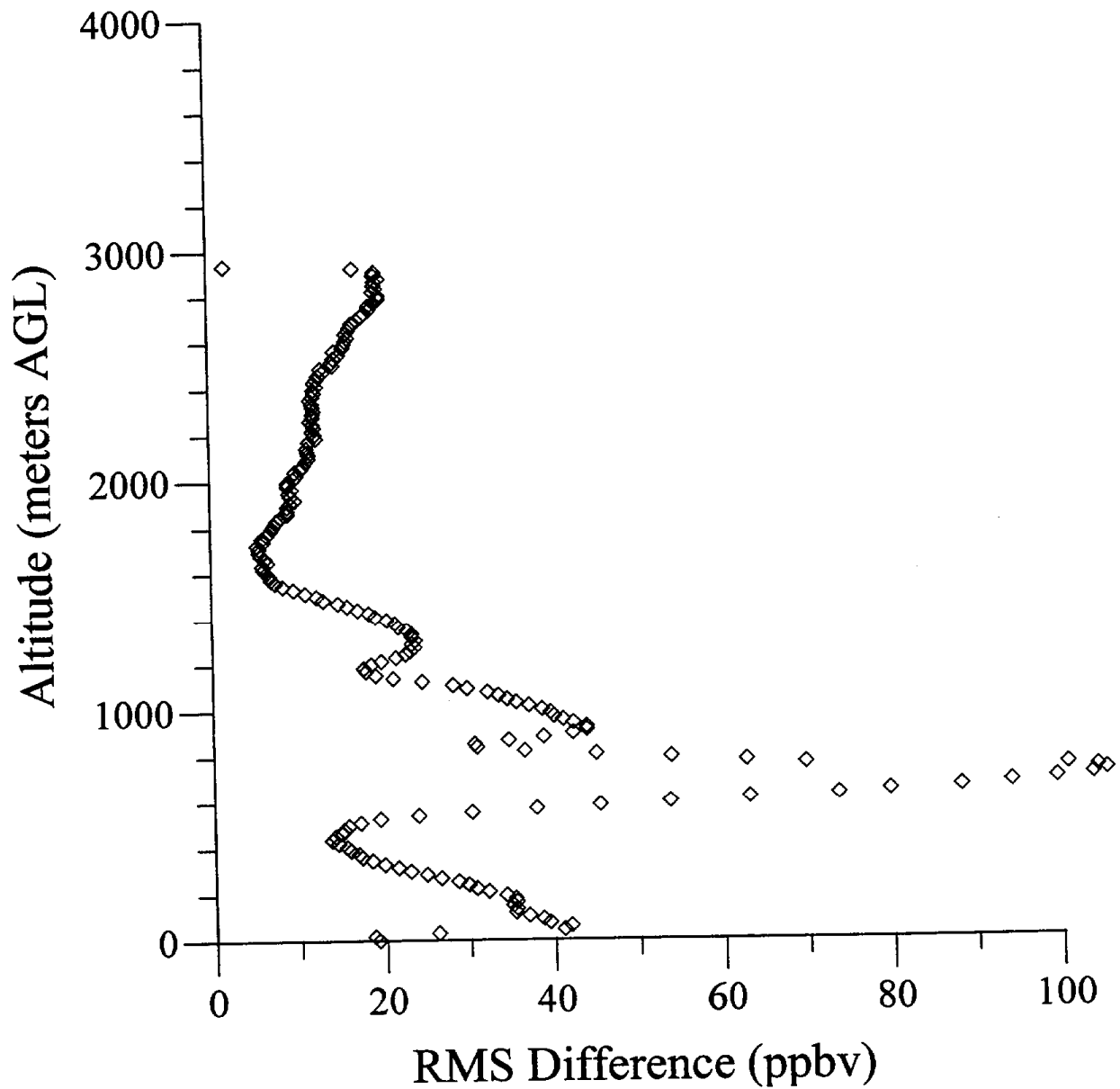
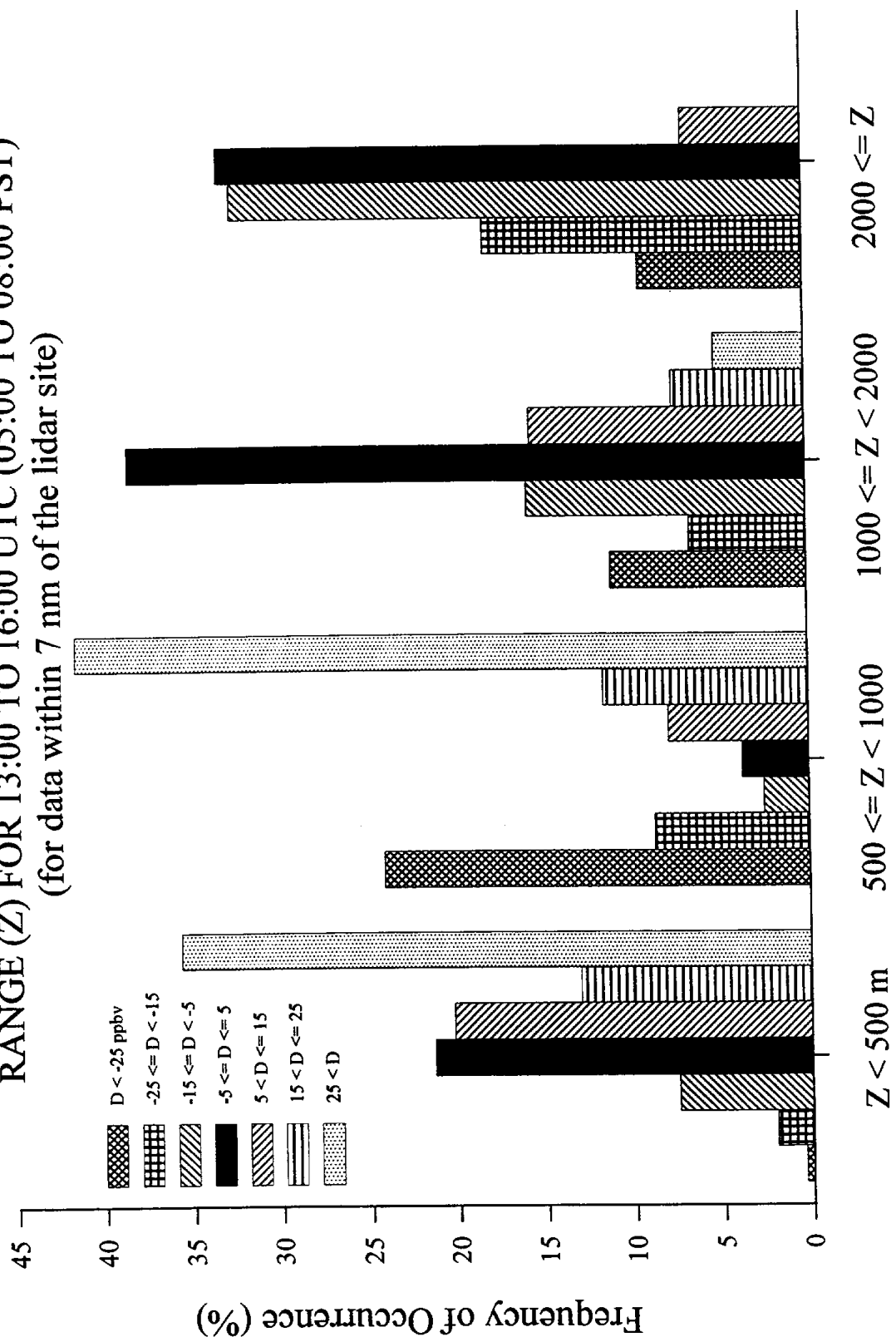


Figure 33: Plot of the RMS difference between the lidar and aircraft ozone concentrations within 7 nm of the lidar site and between 13:00 and 16:00 UTC (05:00 and 08:00 PST).

FIGURE 34  
 LIDAR - AIRCRAFT OZONE DIFFERENCES (D) BY ALTITUDE  
 RANGE (Z) FOR 13:00 TO 16:00 UTC (05:00 TO 08:00 PST)  
 (for data within 7 nm of the lidar site)



Lidar - Aircraft Ozone RMS Difference  
For 21:00 to 23:59 UTC (13:00 to 15:59 PST)

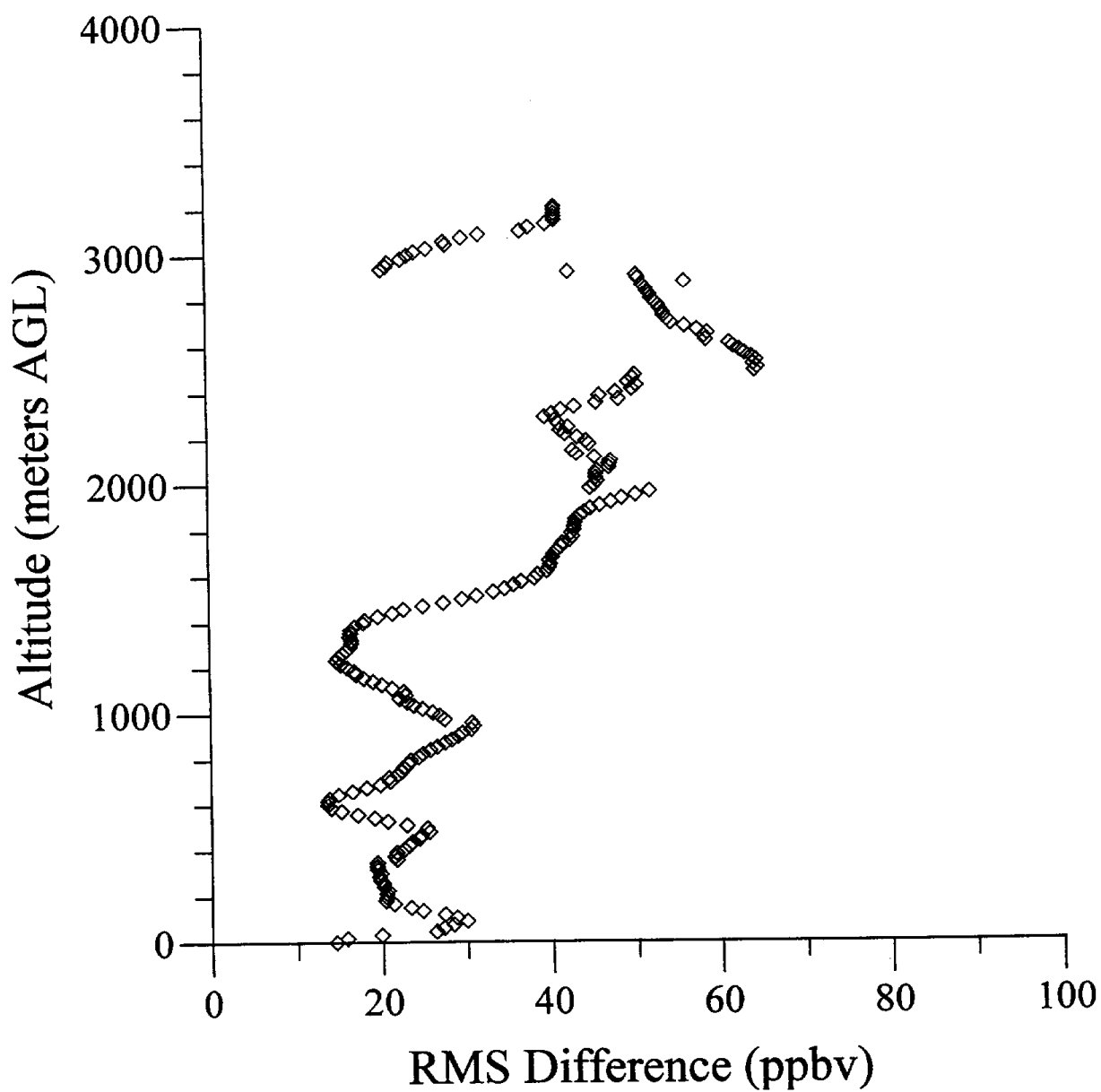

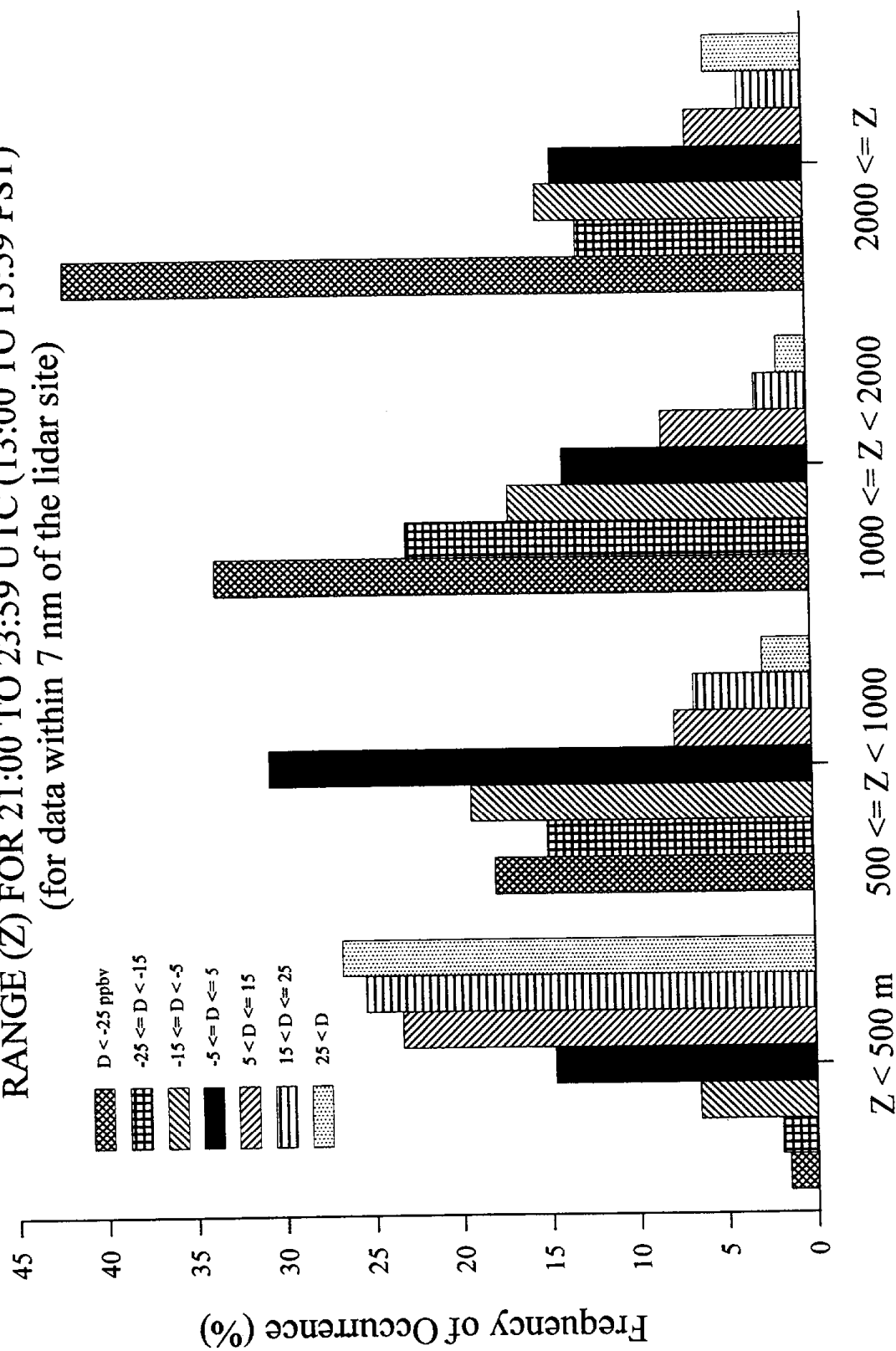


Figure 35: Plot of the RMS difference between the lidar and aircraft ozone concentrations within 7 nm of the lidar site and between 21:00 and 23:59 UTC (13:00 and 15:59 PST).

FIGURE 36

LIDAR - AIRCRAFT OZONE DIFFERENCES (D) BY ALTITUDE  
RANGE (Z) FOR 21:00 TO 23:59 UTC (13:00 TO 15:59 PST)  
(for data within 7 nm of the lidar site) 



## Lidar - Aircraft Bias and Temperature

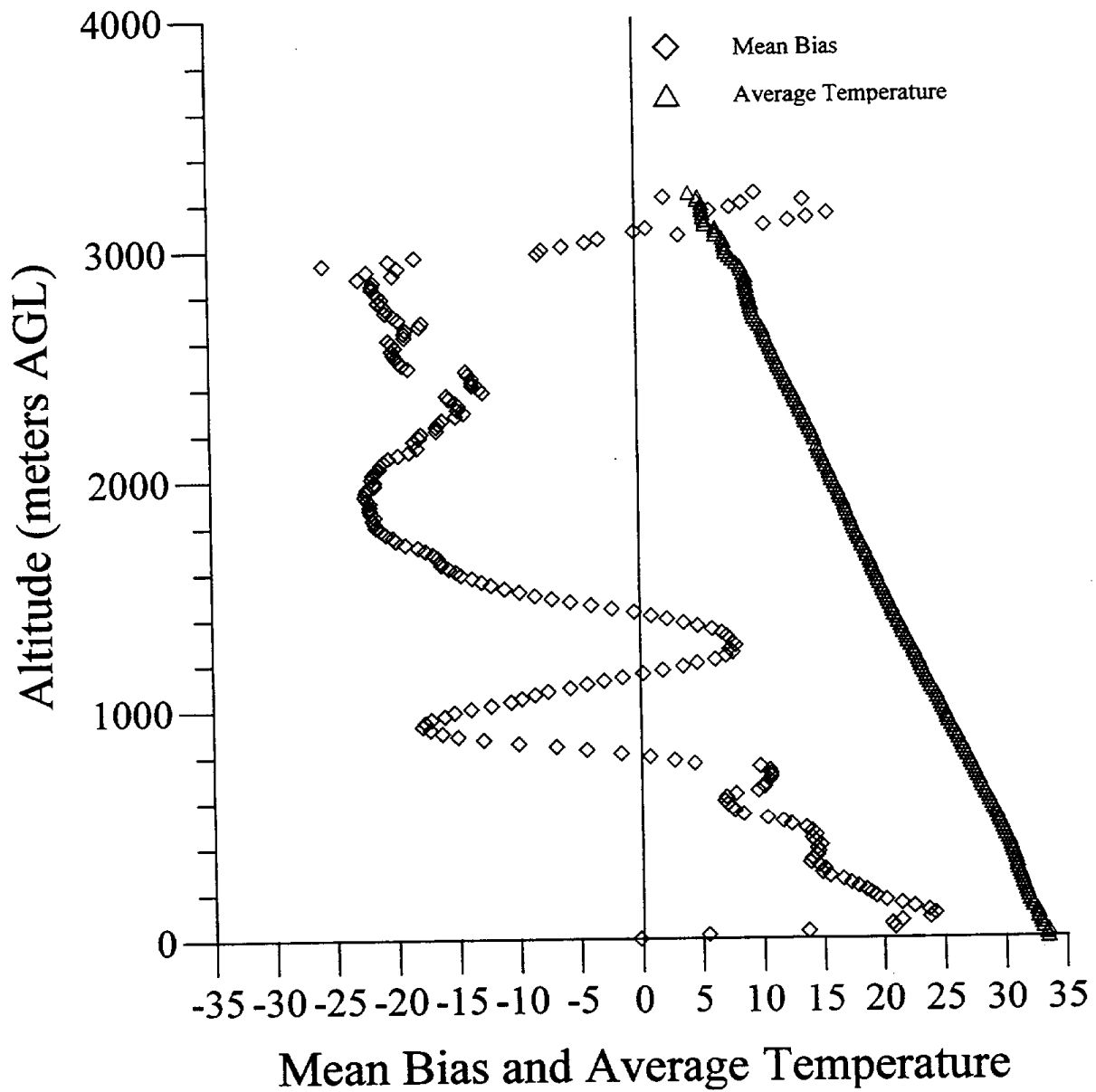


Figure 37: Plot of the mean bias between the lidar and aircraft ozone concentrations (ppbv) and of average temperature (degrees C) at a given altitude within 7 nm of the lidar site.

## Lidar - Aircraft Bias and Relative Humidity

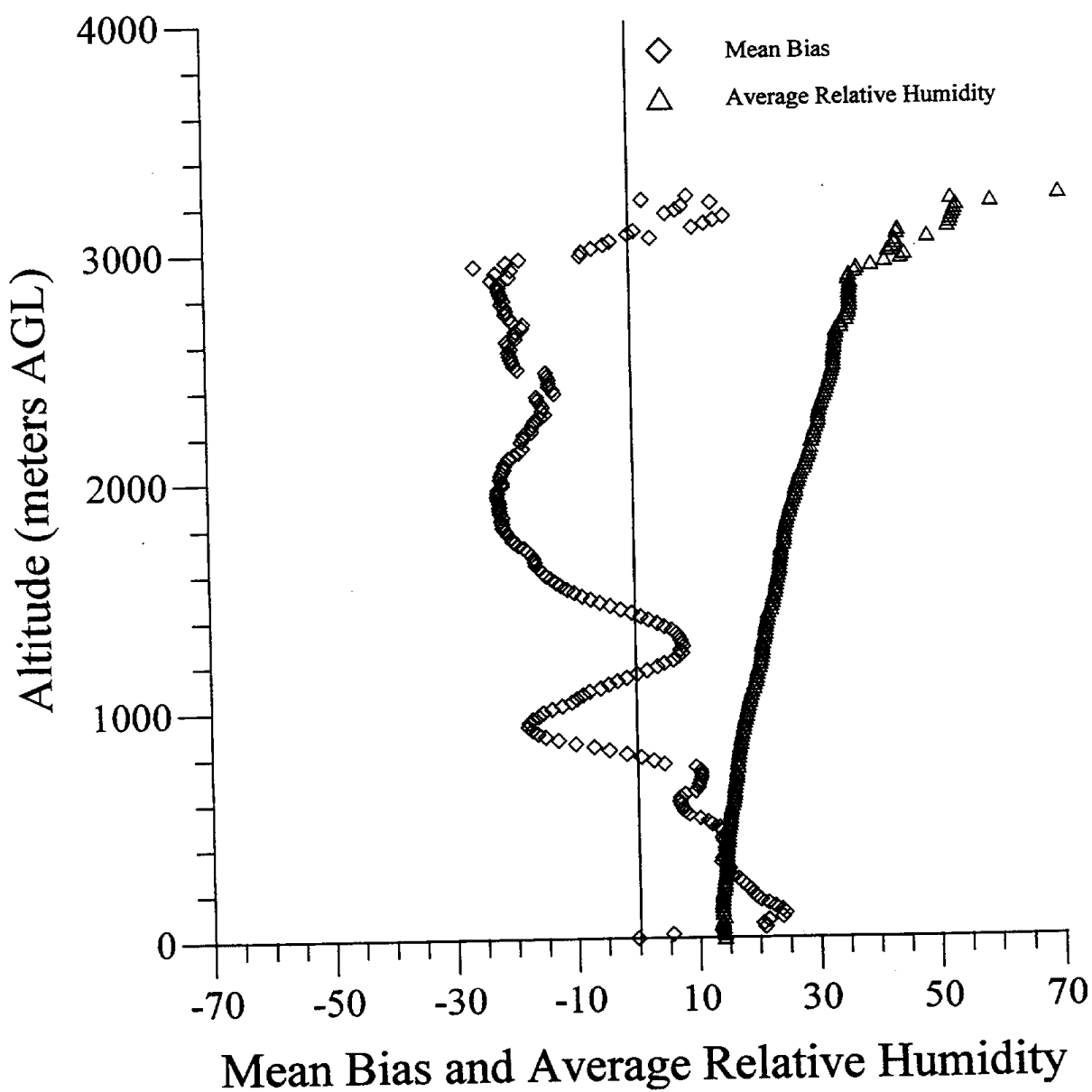


Figure 38: Plot of the mean bias between the lidar and aircraft ozone concentrations (ppbv) and of average relative humidity (percent) at a given altitude within 7 nm of the lidar site.

## Lidar - Aircraft Bias and Particles > 0.3 microns

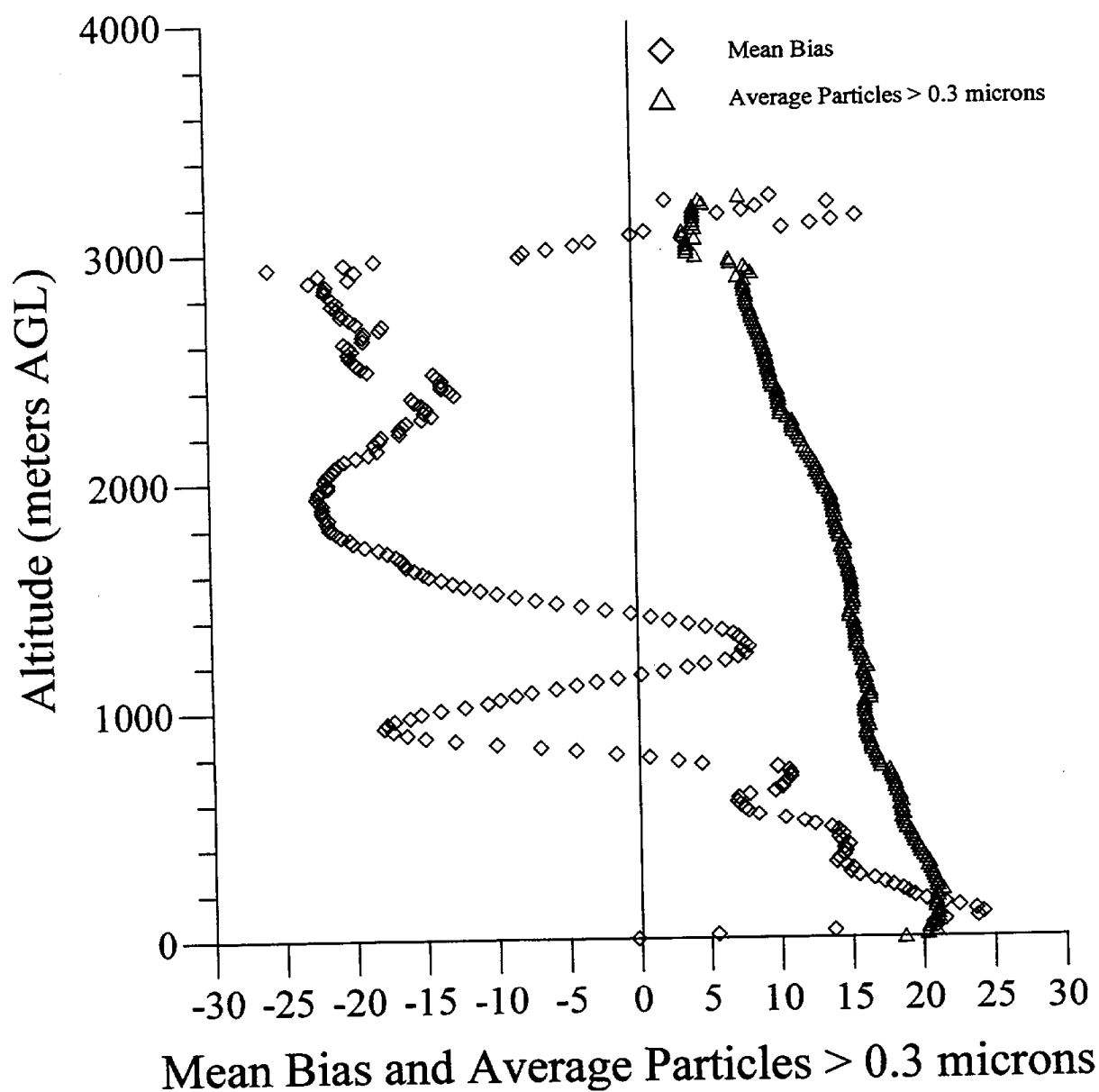


Figure 39: Plot of the mean bias between the lidar and aircraft ozone concentrations (ppbv) and of particle count (millions) greater than 0.3 microns at a given altitude within 7 nm of the lidar site.

## Lidar - Aircraft Bias and Particles > 3.0 microns

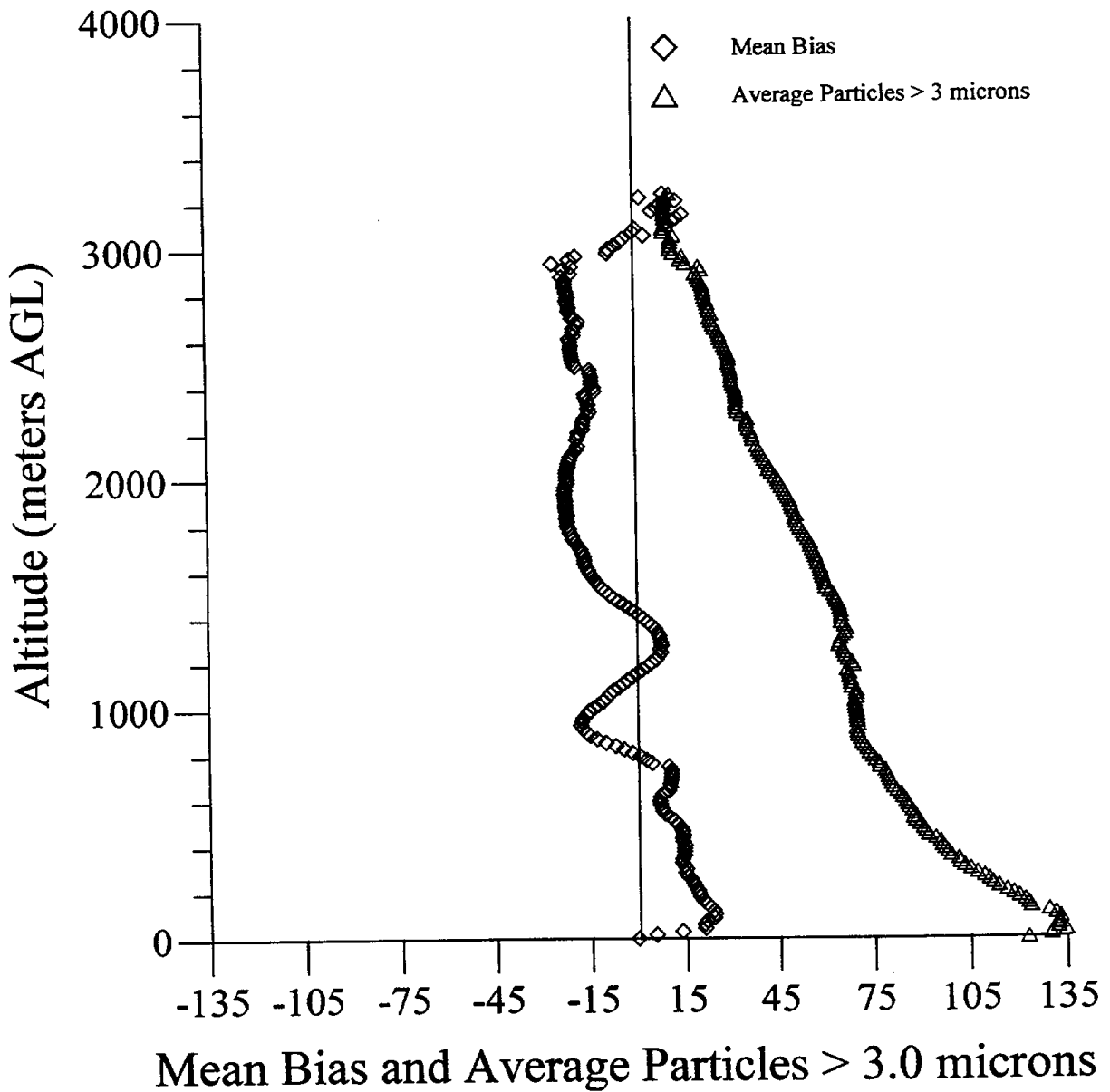


Figure 40: Plot of the mean bias between the lidar and aircraft ozone concentrations (ppbv) and of particle count (thousands) greater than 3.0 microns at a given altitude within 7 nm of the lidar site.



# Lidar - Aircraft Bias and Temperature For 13:00 to 16:00 UTC (05:00 to 08:00 PST)

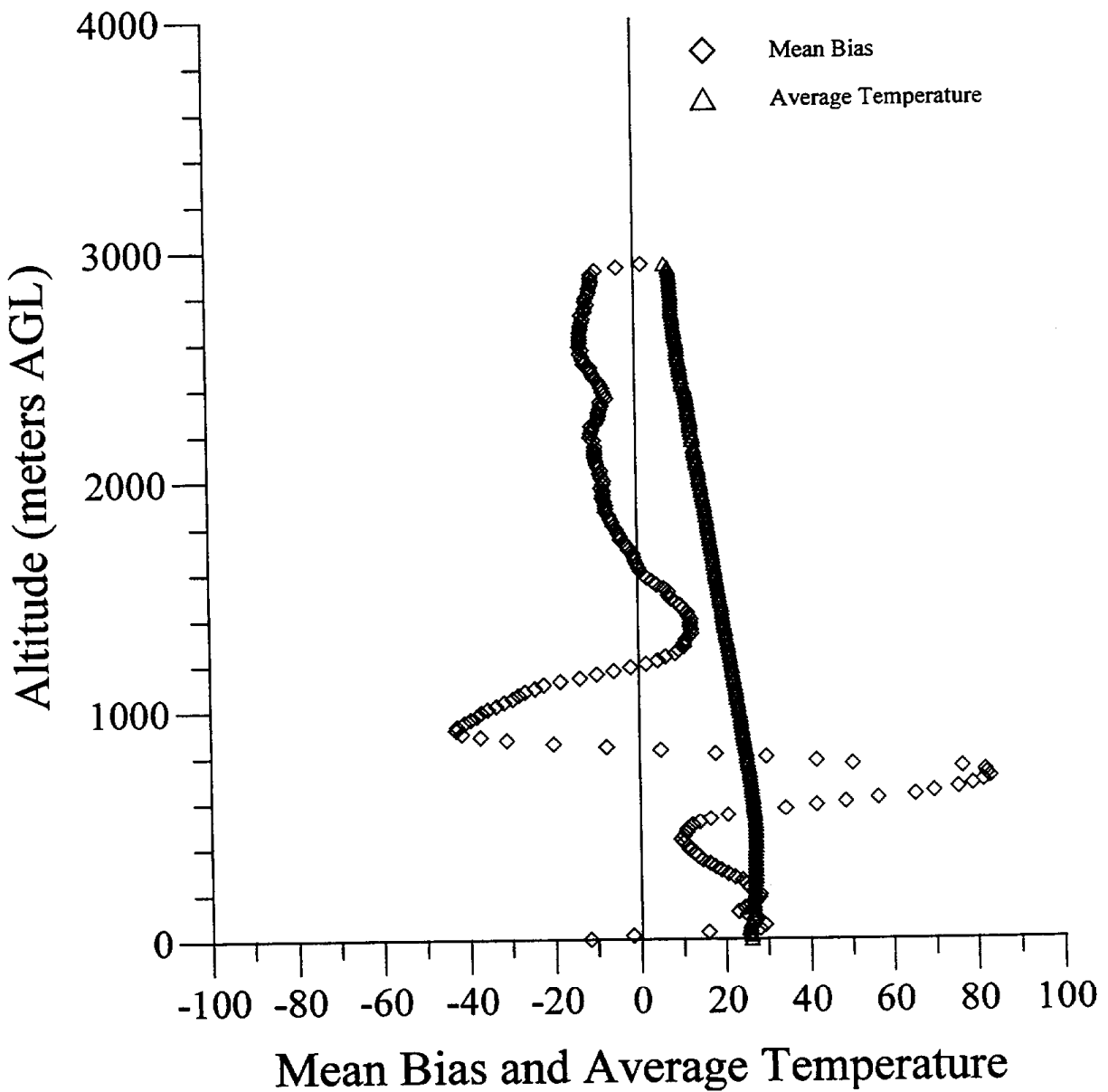


Figure 41: Plot of the mean bias between the lidar and aircraft ozone concentrations (ppbv) and of average temperature (degrees C) at a given altitude within 7 nm of the lidar site and between 13:00 and 16:00 UTC (05:00 and 08:00 PST).

# Lidar - Aircraft Bias and Relative Humidity For 13:00 to 16:00 UTC (05:00 to 08:00 PST)

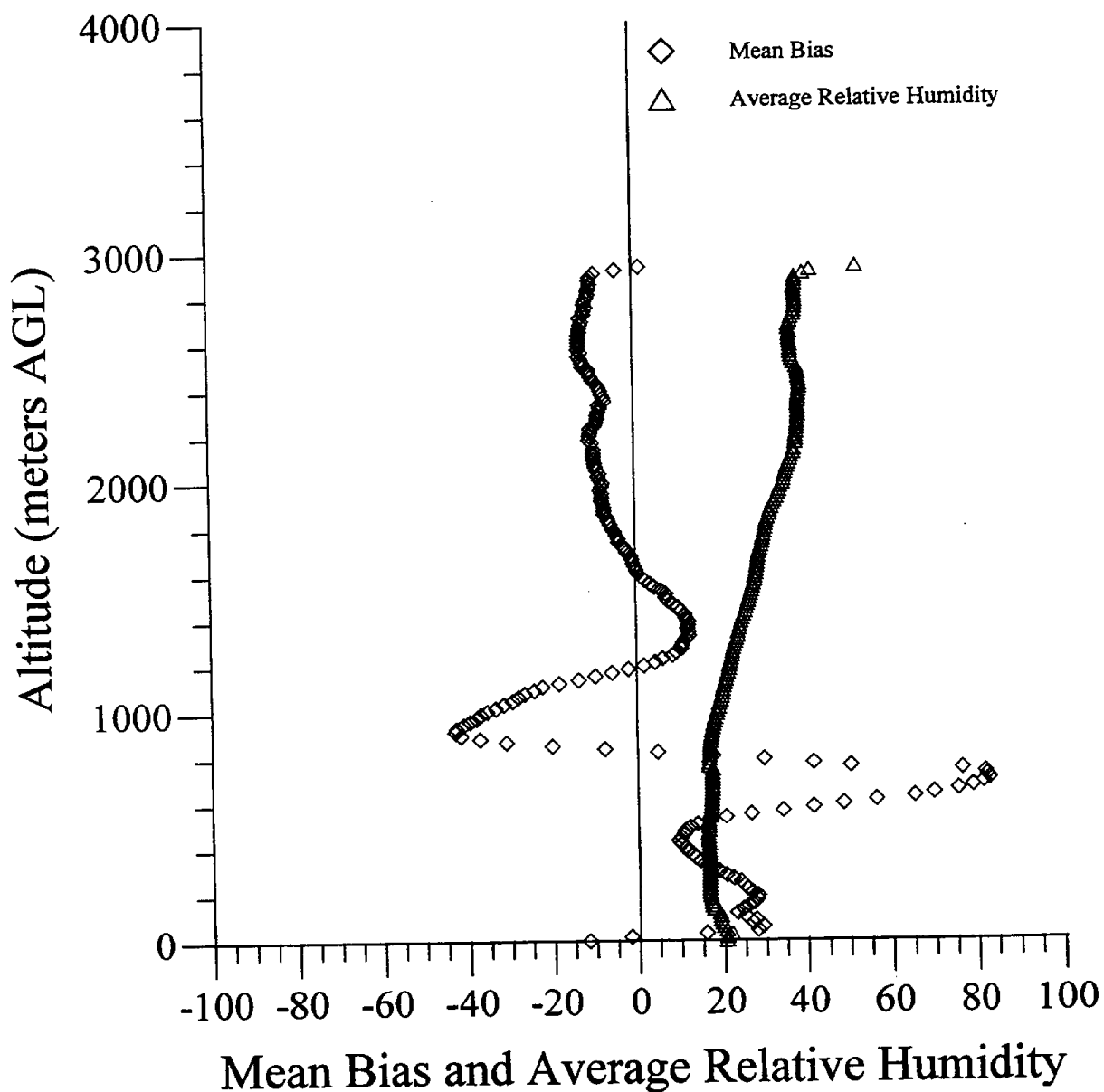


Figure 42: Plot of the mean bias between the lidar and aircraft ozone concentrations (ppbv) and of average relative humidity (percent) at a given altitude within 7 nm of the lidar site and between 13:00 and 16:00 UTC (05:00 and 08:00 PST).

Lidar - Aircraft Bias and Particles > 0.3 microns  
For 13:00 to 16:00 UTC (05:00 to 08:00 PST)

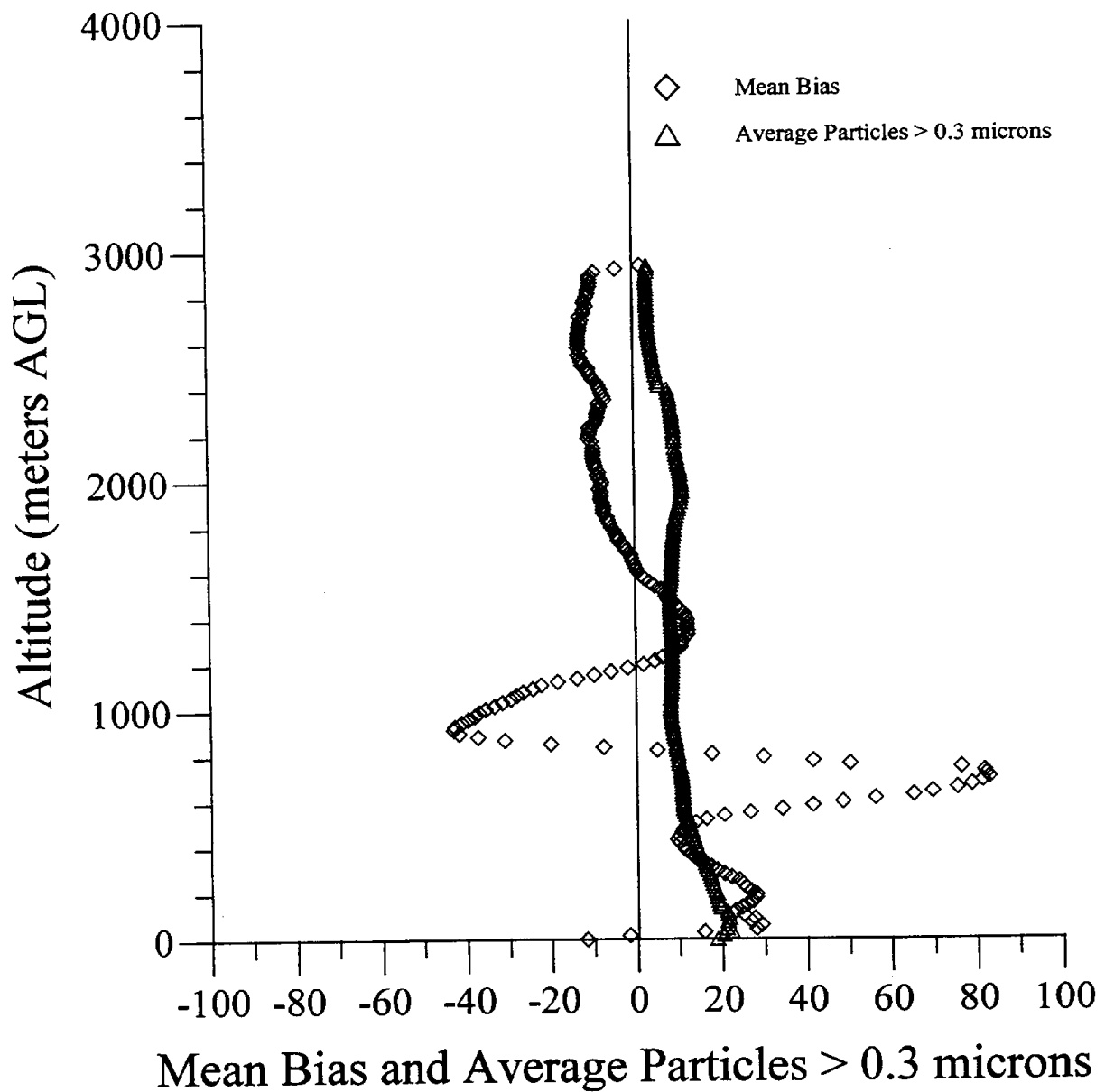


Figure 43: Plot of the mean bias between the lidar and aircraft ozone concentrations (ppbv) and of particle count (millions) greater than 0.3 microns at a given altitude within 7 nm of the lidar site and between 13:00 and 16:00 UTC (05:00 and 08:00 PST).

Lidar - Aircraft Bias and Particles > 3.0 microns  
For 13:00 to 16:00 UTC (05:00 to 08:00 PST)

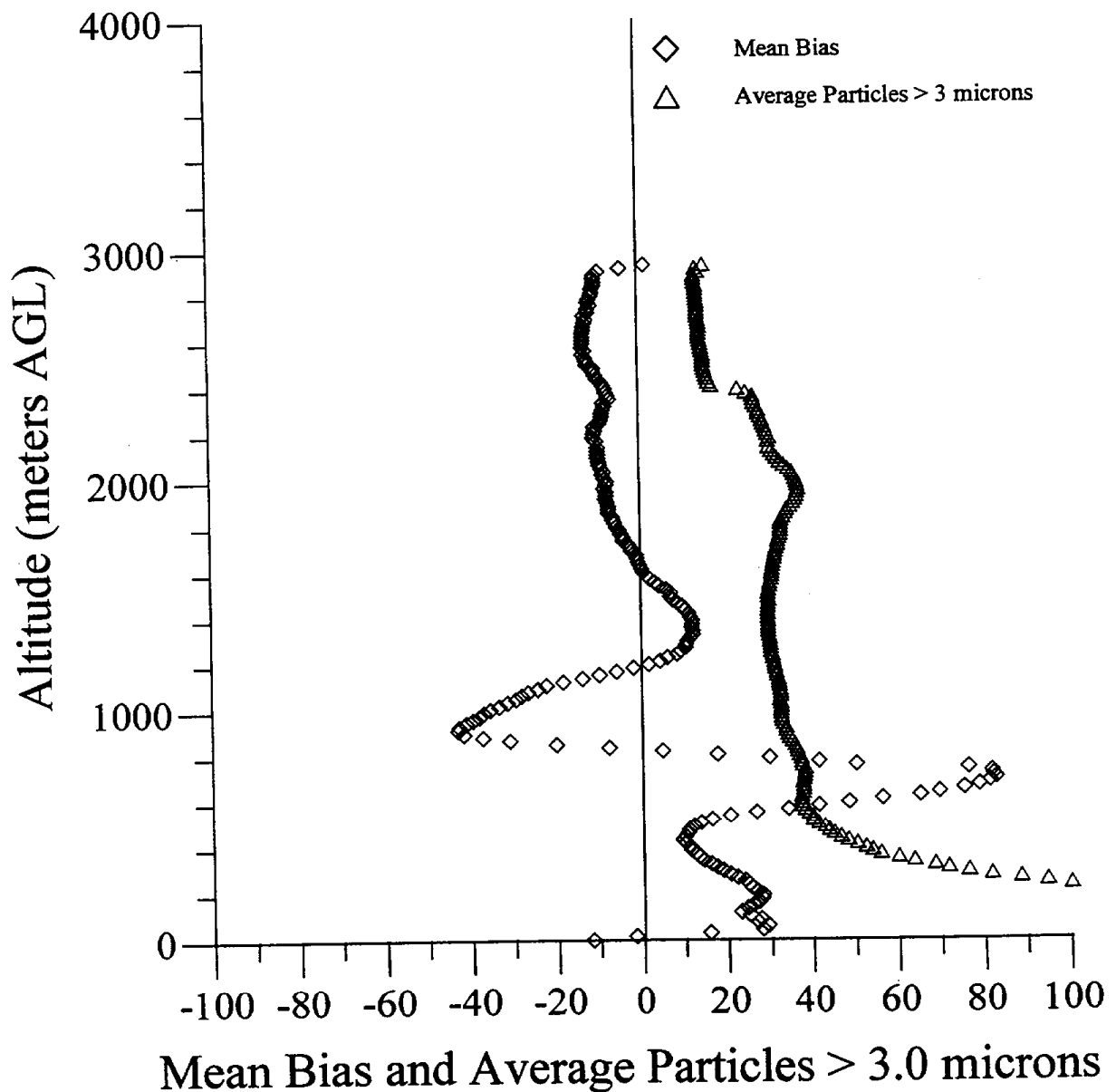


Figure 44: Plot of the mean bias between the lidar and aircraft ozone concentrations (ppbv) and of particle count (thousands) greater than 3.0 microns at a given altitude within 7 nm of the lidar site and between 13:00 and 16:00 UTC (05:00 AND 08:00 PST).

# Lidar - Aircraft Bias and Temperature For 21:00 to 23:59 UTC (13:00 to 15:59 PST)

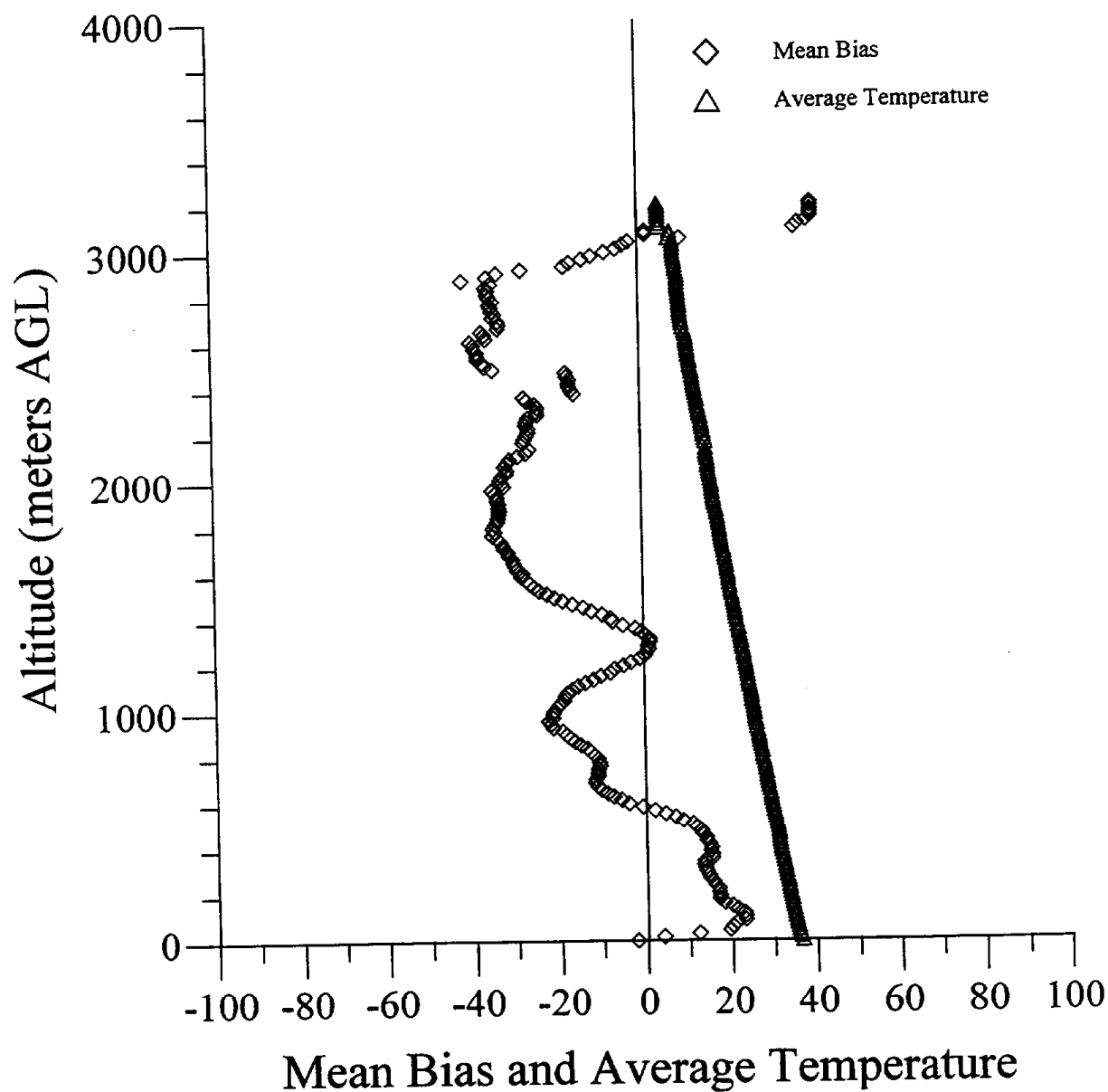


Figure 45: Plot of the mean bias between the lidar and aircraft ozone concentrations (ppbv) and of average temperature (degrees C) at a given altitude within 7 nm of the lidar site and between 21:00 and 23:59 UTC (13:00 and 15:59 PST).

Lidar - Aircraft Bias and Relative Humidity  
For 21:00 to 23:59 UTC (13:00 to 15:59 PST)

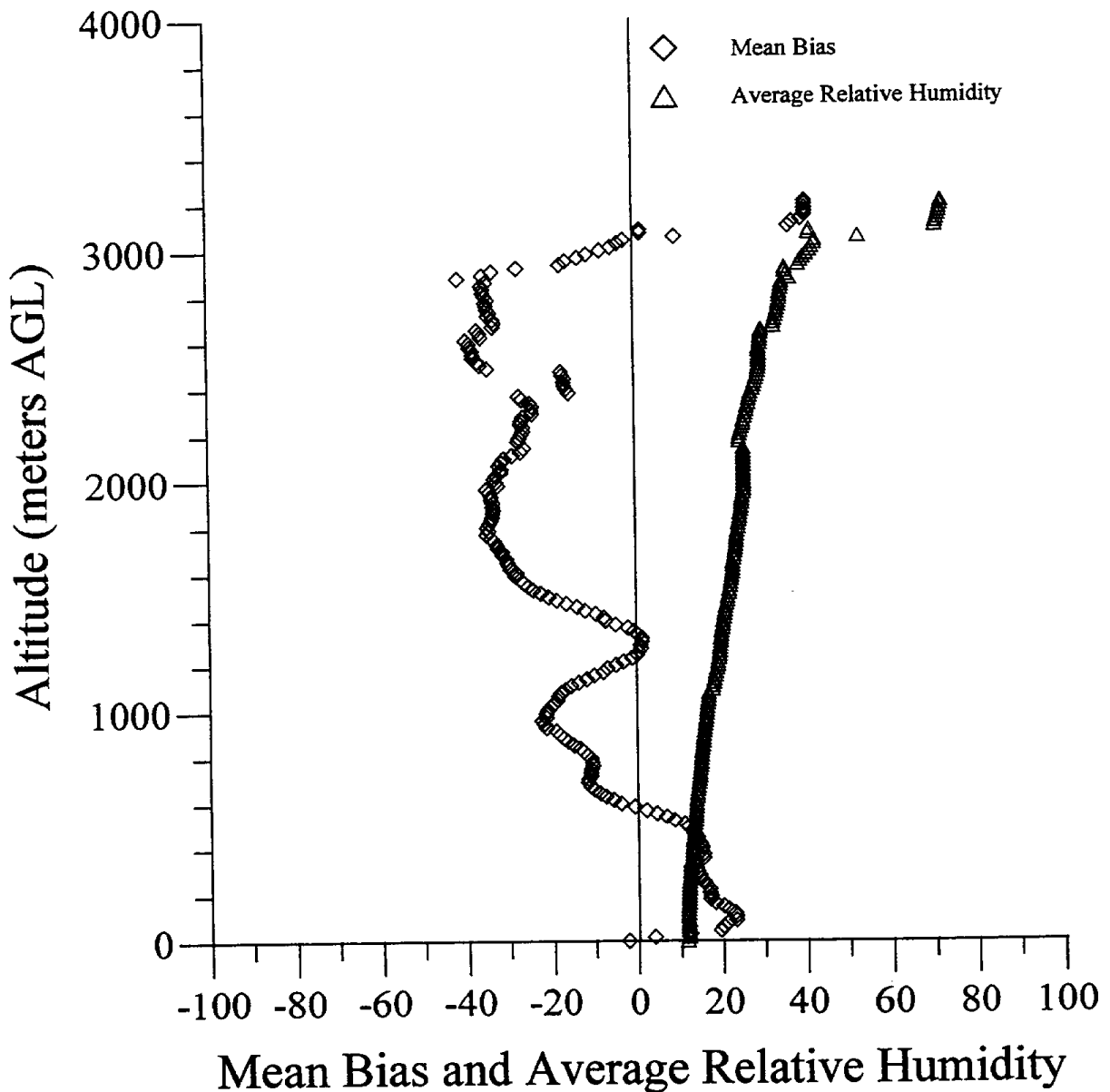


Figure 46: Plot of the mean bias between the lidar and aircraft ozone concentrations (ppbv) and of average relative humidity (percent) at a given altitude within 7 nm of the lidar site and between 21:00 and 23:59 UTC (13:00 and 15:59 PST).

# Lidar - Aircraft Bias and Particles > 0.3 microns For 21:00 to 23:59 UTC (13:00 to 15:59 PST)

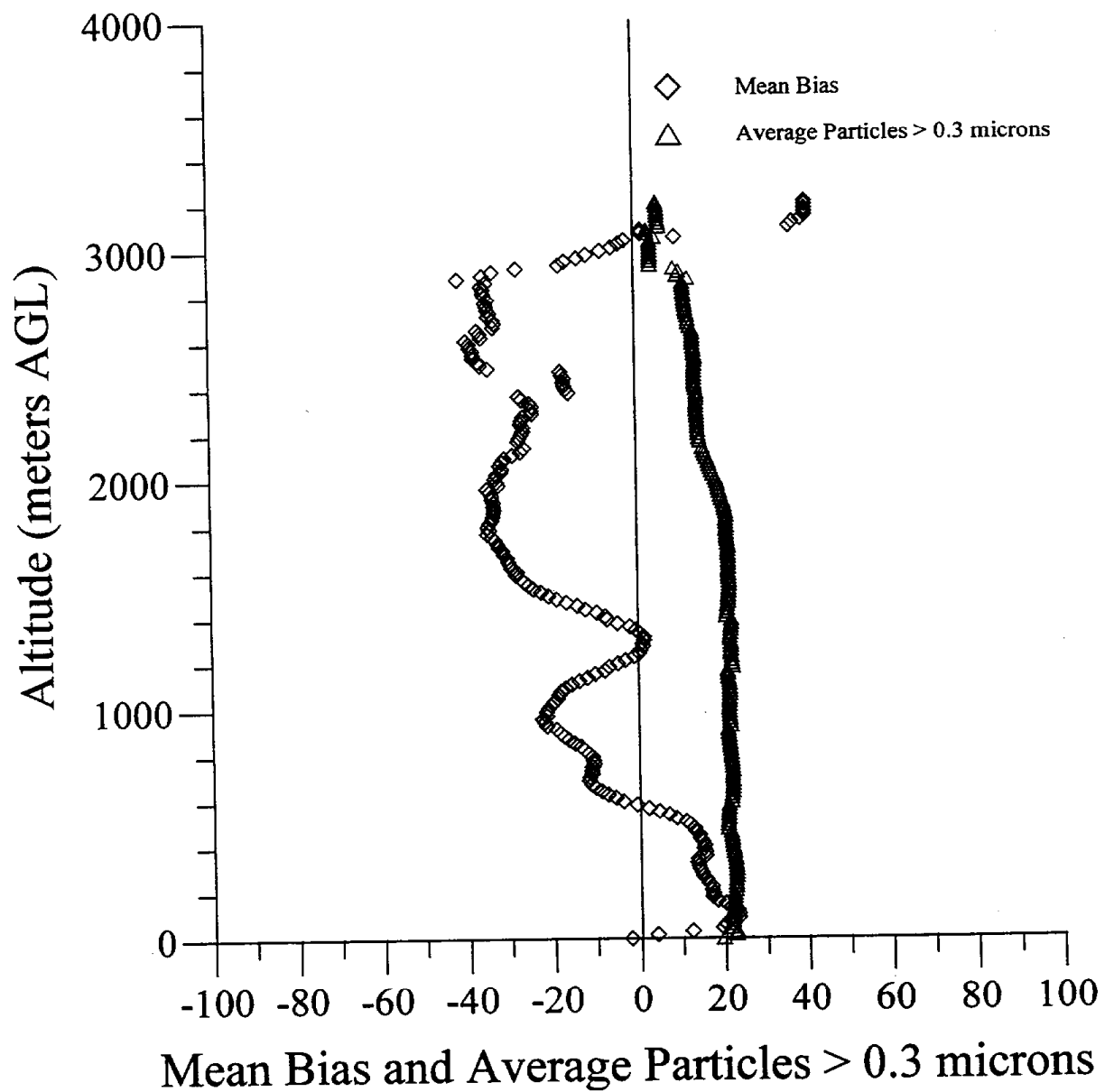


Figure 47: Plot of the mean bias between the lidar and aircraft ozone concentrations (ppbv) and of particle count (millions) greater than 0.3 microns at a given altitude within 7 nm of the lidar site and between 21:00 and 23:59 UTC (13:00 and 15:59 PST).

# Lidar - Aircraft Bias and Particles > 3.0 microns For 21:00 to 23:59 UTC (13:00 to 15:59 PST)

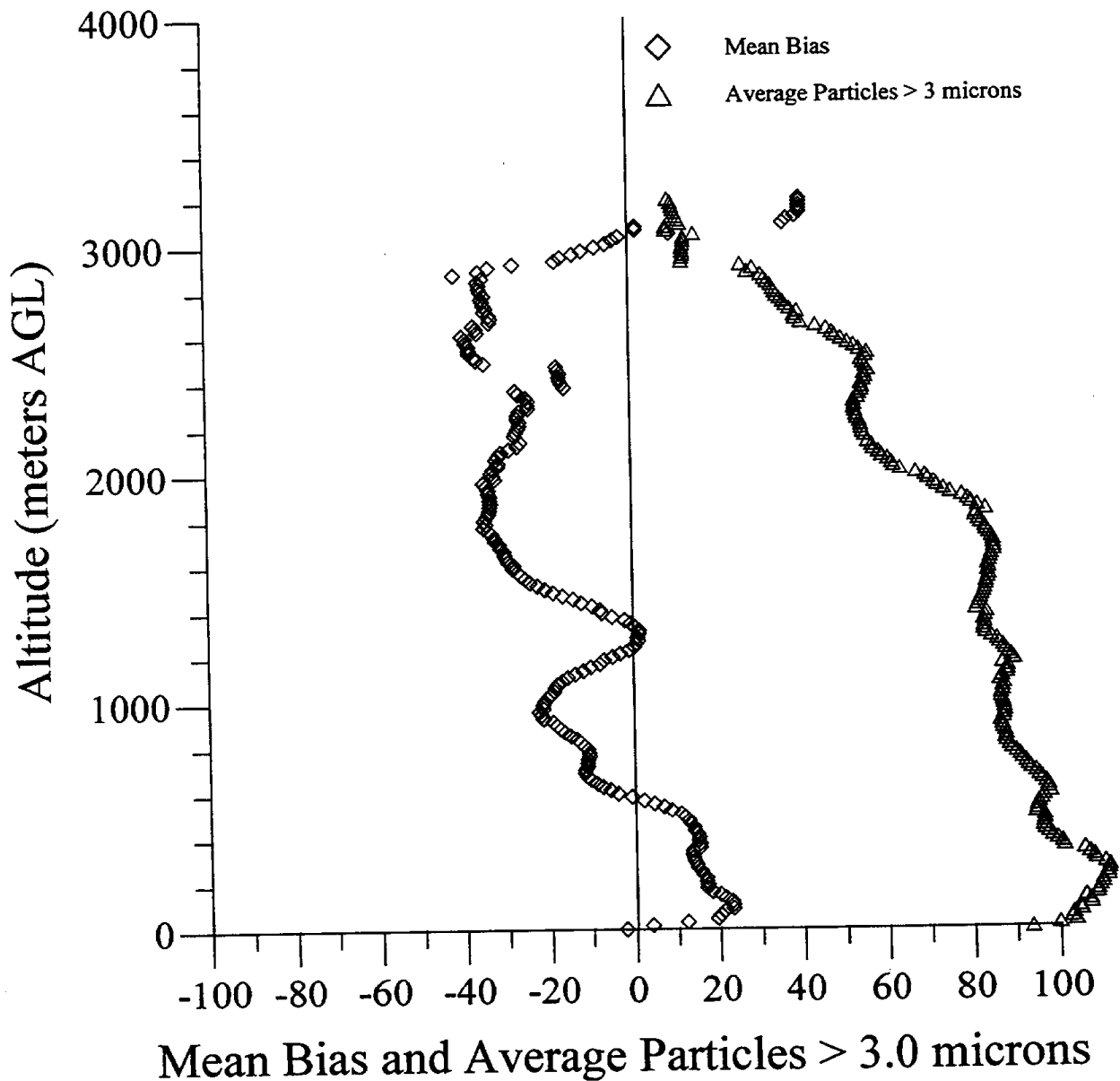


Figure 48: Plot of the mean bias between the lidar and aircraft ozone concentrations (ppbv) and of particle count (thousands) greater than 3.0 microns at a given altitude within 7 nm of the lidar site and between 21:00 and 23:59 UTC (13:00 and 15:59 PST).





